ALMA MATER STUDIORUM
UNIVERSITÀ DI BOLOGNA

DOTTORATO DI RICERCA IN

SCIENZE VETERINARIE

Ciclo 38

Settore Concorsuale: 07/H1 - ANATOMIA E FISIOLOGIA VETERINARIA

Settore Scientifico Disciplinare: VET/02 - FISIOLOGIA VETERINARIA

MITOCHONDRIAL FUNCTION AND REPRODUCTIVE INNOVATION IN MAMMALIAN MODELS

Presentata da: Ilaria Troisio

Coordinatore Dottorato

Carolina Castagnetti

Supervisore

Nadia Govoni

Co-supervisore

Maria Laura Bacci

Esame finale anno 2026

Abstract

Mitochondria are among the most crucial cellular organelles involved in various physiological and pathological processes. After decades of simplistic descriptions portraying them merely as the cell's energy hubs, it has now become evident that the tight relationship between ATP production and oxidative stress caused by reactive oxygen species (ROS) plays a far more complex and dynamic role. This relationship is particularly significant in high-energy demanding cells, such as spermatozoa and cardiomyocytes, which are the focus of this thesis.

The aim of this work is to highlight the interrelations between physiological aspects that might appear distant. Rather than presenting a linear sequence of experiments exploring a single specific topic, this thesis builds a conceptual bridge between findings and observations that can integrate different aspects of cellular function.

Two animal models are considered: the pig and the roe deer. The pig represents a fundamental model in reproductive research, both for its global relevance in livestock studies and for its suitability in investigating cytotoxicity and maternal inheritance phenomena. The roe deer, on the other hand, offers unique insights into seasonal reproduction, as its males display distinctive reproductive patterns. The study of this species allows for the collection of data across different seasons, effectively mirroring the entire reproductive lifespan seen in other species.

In conclusion, this thesis aims to be an example of an integrative approach that connects different levels of biological organization and fosters a broader understanding of mitochondrial function in diverse physiological contexts.

Summary

Introduction 1

The Mitochondrion: Structure, Genome, and Evolving Functions 2

The Role of Mitochondria and Oxidative Stress in Sperm Function 5

Boar semen: Structure, Metabolism and Cryopreservation's vulnerability .. 11

Boar Semen Preservation in One Health perspective 15

Paternal Mitochondria Fate and Mitophagy Post-Fertilization 17

Mitochondrial Sheath Stabilization and Destabilization Along the Male–Female Reproductive Tract 18

The Porcine Cell-free System 21

A Learning Journey Abroad 24

Seasonal spermatogenesis and oxidative balance in the roe deer 26

Peculiarity of the species 27

Oxidative Stress: From Literature Insights to Experimental Results 28

The Porcine Model in Cardiovascular Research 29

Ischemia–Reperfusion Injury: A Major Challenge in Transplantation 30

Mitochondria-Targeted Therapeutic Strategies: From Literature Insights to Experimental Results 32

Aim of the study 36

Experimental Section 38

Boar Semen Preservation 39

Roe deer as model for photoperiod spermatogenesis regulation 61

Porcine model in DCD transplantation research 75

Conclusion 93

References 96

Additional paper 113

Non-Invasive Hormonal Analysis in Apennine wolf 114

Introduction

The Mitochondrion: Structure, Genome, and Evolving Functions

"A cell without mitochondria is regarded as a biological curiosity, a ship without engine". This was a statement of Siekevitz in his iconic publication in 1957 (Siekevitz, 1957) in which introduces the now-famous epithet *"Powerhouse of the cell",* highlighting the pivotal mitochondria's role in cellular energy production in eukaryotic cells (Annesley & Fisher, 2019; Nunnari & Suomalainen, 2012). Despite the rudimentary technique Fig.1, the author was able to identify key features of the mitochondrion establishing fundamental concepts cornerstones of mitochondrial biology still today. The resulting picture that emerges makes mitochondrion the central hub of cellular energy metabolism. Hover, beyond the overt functionality already recognized, such as ATP production (Mitchell, 2011; Mitchell & Moyle, 1967), recent works highlighted that ROS (Reactive Oxygen Species) traditionally considered merely a dysfunctional sub products (Beckman & Ames, 1998) also play important regulatory roles in mitochondria, acting as fundamental mediators in adaptive cellular processes, another pivotal functions of mitochondria, essential for life, since ROS act as fundamental mediators in adaptive processes (Palma et al., 2024). ROS are chemical species such as superoxide (O_2^-), hydrogen peroxide (H_2O_2), and the hydroxyl radical (OH) highly reactive to oxygen. It is largely demonstrated that they can damage lipids, proteins, and DNA, but at low concentrations, they play physiological roles, for example in cell signalling and sperm maturation (Rj, 2017).

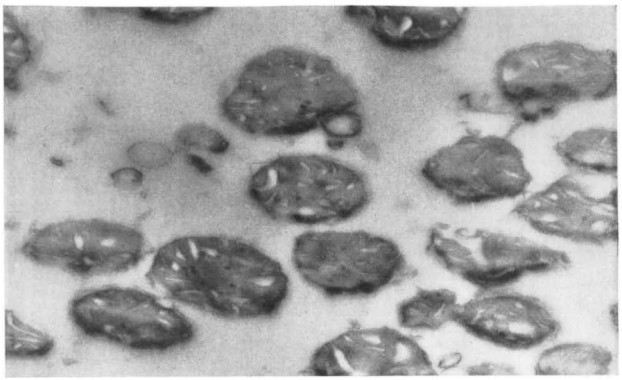

Figure 1 *Normal mitochondria observed in electron micrographs, isolated from cells and suspended in a sucrose solution. From Siekevitz (1957); magnification 44,000X.*

A wide range of physiological processes such as sperm motility (Foutouhi & Meyers, 2022), tissue differentiation (Palma et al., 2024), and conversely, pathological conditions, including metabolic disorders, cardiovascular diseases (Bugger & Pfeil, 2020) and reproductive impairments (Wang et al., 2025) are influenced by mitochondrial activities and dysfunction. Some of these aspects will be discussed and explored in the following sections of this thesis.

To better understand mitochondrial functions in physiological and pathological contexts it is important to shed a light on its structure (Fig. 2) and on its own genome, the most distinctive features of this organelle. Mitochondria are delimited by a double membrane: the outer one permeable to small molecules through porins, and the inner membrane, selective and folded into cristae to increase the surface available for metabolic reactions (Kühlbrandt, 2015). The matrix, instead, contains enzymes of the tricarboxylic acid cycle, as well as mitochondrial DNA and ribosomes (van der Bliek et al., 2017).

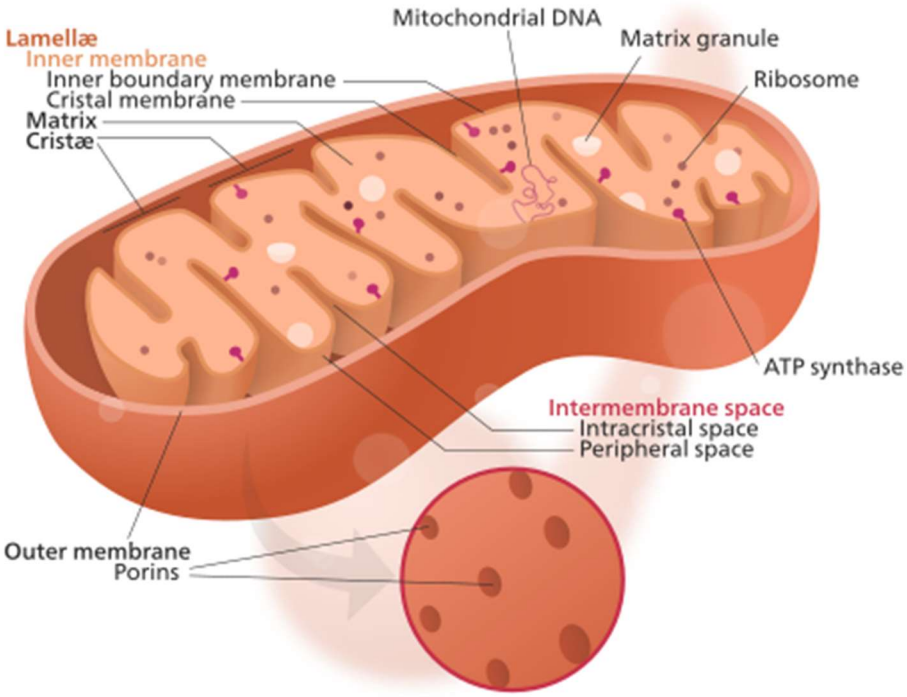

Figure 2 *Diagram of mitochondrial structure. From Mitochondrion structure's, Kelvinsong; modified by Sowlos, CC BY-SA 3.0. Available at https://commons.wikimedia.org/wiki/File:Mitochondrion_structure.svg*

The peculiar dual membrane and the presence of their own genome support the endosymbiotic theory (Sagan, 1967), according to which mitochondria originated from aerobic bacteria engulfed by ancestral eukaryotic cells, establishing a symbiotic relationship fundamental for survival in an oxygen-rich atmosphere (Mills et al., 2022). Mitochondria are central for cellular respiration: pyruvate is converted into acetyl-CoA in the matrix and enters the citric acid cycle, producing NADH and $FADH_2$, which provide electrons into the electron transport chain (ETC) (van der Bliek et al., 2017). The transfer of electrons to oxygen generates a proton gradient that drives ATP synthesis by oxidative phosphorylation. Moreover, the ETC is also the main site of ROS (Reactive Oxygen Species) production, this is partially the reason explaining

the vulnerability to mutations of mtDNA (Atici et al., 2023). In fact, the mtDNA mutation rate is 10-20 higher than nuclear genome, given by closeness with the site of ROS production and to the absence of histones (Annesley & Fisher, 2019). The first total sequencing of the human mitochondrial genome has been done by (Anderson et al., 1981). The authors revealed a circular DNA molecule of approximately 16.5 kb containing 37 genes: 13 of them encoding for essential protein subunits of the oxidative phosphorylation, 22 genes encode transfer RNAs (tRNAs) ensuring the correct mitochondrial mRNAs decoding and 2 genes involved in ribosomal RNSs (rRNAs) encoding (12S and 16S rRNAs), structural components of ribosomes, necessary for protein synthesis within the organelle. These functional genes highlight the organelle's autonomous protein synthesis machinery, reaffirming its partial independency from the nuclear genome of cells. Given this central role, mitochondria are not uniformly distributed across cell types, but rather adapt their morphology, abundance, and spatial arrangement according to specific energetic demands (Siekevitz, 1957).

This plasticity becomes particularly evident in highly energy-dependent systems such as reproductive cells (Abruzzese et al., 2024), where mitochondria sustain the intense motility and metabolic activity required for fertilization (Abruzzese et al., 2024; Gadella, 2017). In fact, conversely to the primitive spermatozoa with external fertilization (inferior vertebrates), the one of animals, such as mammals, with internal fertilization, appear to present structural and physiological characteristics (Abruzzese et al., 2024), allowing them to cover long distances to reach the site of fertilization, especially the ampulla where fertilize the just-ovulated egg (Gadella, 2017; Li & Winuthayanon, 2017; Coy et al., 2012; Brüssow et al., 2008).

The delicate balance between mitochondrial energy production and oxidative stress, which determines sperm performance and fertilization success, mirrors a more general paradigm of mitochondrial susceptibility. Similar redox-dependent mechanisms emerge in other highly metabolic systems, including the heart, where mitochondrial dysfunction plays a decisive role in ischemia-reperfusion injury, particularly relevant in the context of DCD transplantation (Akande et al., 2020; Wyss et al., 2019), theme that will be discussed later in this thesis.

The Role of Mitochondria and Oxidative Stress in Sperm Function

The key modification of mammalian spermatozoa is given from the elongation of the midpiece, where mitochondria are tightly packed in a helical sheath to sustain the fertilization capacity of the spermatozoa (Foutouhi & Meyers, 2022). See Fig. 3 for a comparative schematic representation of the sperm midpiece across different species, adapted from (Leung et al., 2021)**.** Moreover, a recent study conducted on more than 1000 vertebrate species highlighted that the length of the midpiece has evolved more than 3 times faster than the head and 1.4 faster than flagellum, confirming that it is the one that is subject to the most selective pressure (Kahrl et al., 2022). The midpiece consists of 50-80 mitochondria helically arranged and end-to-end inside mitochondrial sheath (MS), that develops around proximal region of spermatozoa tail. This region contains the axoneme with the classical 9 + 2 microtubule arrangement, surrounded by 9 external dense fibres (ODF), that are important to give further mechanical support to movement in the viscous environment of female reproductive tract (Foutouhi & Meyers, 2022).

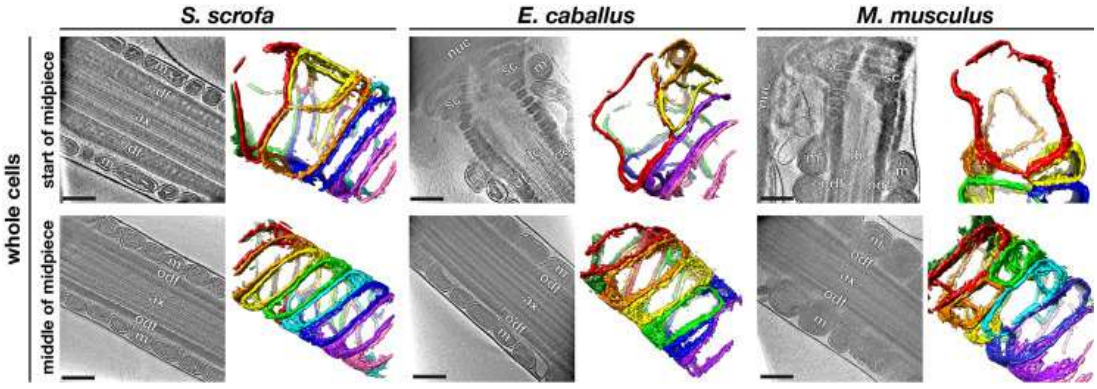

Figure 3 *Whole-cell view of sperm midpieces from pig, horse, and mouse, showing the helical arrangement of mitochondria within the mitochondrial sheath (MS), axoneme (9+2 microtubules), and outer dense fibres (ODF). Only the whole-cell sections are shown; lamellae and zoomed subregions, presented in original imagine, have been omitted for clarity. Adapted from (Leung et al., 2021)*

The great presence of mitochondria organized in such of specialized structure is linked with the massive energy production that spermatozoa must sustain during the pathway to reach the oocytes, especially for the *"hyperactivation"* (Foutouhi & Meyers, 2022). There are two possible pathways for ATP production in mammals' spermatozoa, that are: glycolysis that occurs in the principal piece of the flagellum, given by the presence of glycolytic enzymes anchored to fibrous sheath, and oxidative phosphorylation, capable to produce 16 times ATP produced in glycolysis, but, on the other hand, responsible for extensive production of ROS (Abruzzese et al., 2024). It is important

to consider that the varying degrees of reliance on distinct metabolic pathways for energy production is species specific, and consequently, so it is the amount of ROS generated (Abruzzese et al., 2024; O'Brien et al., 2021). A consideration about the amount of these molecules production is necessary, because the oxygen reactive species are considered as *"two-edged sword"* especially in the field of reproduction (Aitken & Drevet, 2020). In fact, ROS, besides being sub-products of phosphorylation, are strictly involved in the substantial process of capacitation (B. Zhang et al., 2021; Aitken & Drevet, 2020).

Capacitation refers to a final maturational process that spermatozoa undergo after the ejaculation, enabling them to fertilize an oocyte (Abruzzese et al., 2024; Gadella, 2017) and occurs in the female reproductive tract (Gadella, 2017). Once initiated, capacitation can only be delayed but not halted or revered, as it ultimately leads to the physiological exhaustion of the spermatozoon's lifespan (Balbach et al., 2023). Capacitation involves the reorganization of the plasma membrane and membrane lipids (Abruzzese et al., 2024; Gadella et al., 2008), a precondition for acrosome reaction (Rodriguez-Martinez et al., 2024; Gadella et al., 2008). This dynamic and complex process directly influences sperm functionality, motility and longevity.

During capacitation, spermatozoa acquire hyperactivation, which alters the symmetry of the flagellar beat. Previously, the beat was symmetric, low in amplitude, and progressive. After hyperactivation, the flagellar movement becomes asymmetric, faster, and exhibits an irregular trajectory (Balbach et al., 2023). Propulsive forces generated by hyperactivation are necessary to overcome obstacles in the female reproductive tract, such as the cumulus oophorous and the zona pellucida (Balbach et al., 2023). Hyperactivation is sustained by increased ATP production supported also by phosphorylation (Abruzzese et al., 2024; Gadella, 2017), which also leads to the generation of reactive oxygen species (ROS) that, in excess, can compromise sperm functionality and structure (B. Zhang et al., 2021).

In fact, the key to success for the correct development of the sperm capacitation mostly lies in the right balance between the ROS production and the antioxidant defence system, including enzymes such as superoxide dismutase (SOD), catalase, and glutathione peroxidase, as well as non-enzymatic molecules such as vitamins and coenzyme Q10 (Pezo et al., 2021). Physiologically, ROS such as superoxide (O_2^-) and

hydrogen peroxide (H_2O_2) act as signalling mediators (Awda et al., 2009; Pezo et al., 2021). They can trigger what can be termed as *"ROS-induced signalling cascade"*, which activates downstream signalling pathways (Abruzzese et al., 2024; B. Zhang et al., 2021) that culminates in the phosphorylation of tyrosine residues (Awda et al., 2009; Gadella, 2017) on specific flagellar proteins directly involved in the sperm motility regulation (Abruzzese et al., 2024; Gadella, 2017). So that it is promoted the hyperactivation and capacitation, through dynamics of flagellar movement modifications (Awda et al., 2009). Moreover, ROS are involved also in the cholesterol peroxidation (Gadella, 2017). Cholesterol, housed inside the spermatozoon's membrane, is pivotal for the stabilization of the entire structure, conferring rigidity to the membrane (Gadella, 2017; Gadella et al., 2008), whereas, during capacitation, the oxidation and the efflux of cholesterol from the membrane increases its lateral fluidity, allowing the entry of ions such as Ca^{2+} and HCO_3^-(Gadella, 2017; Gadella et al., 2008), which are essential for flagellar hyperactivation (Abruzzese et al., 2024) and, subsequently, for the acrosome reaction and fusion with the oocyte (Gadella, 2017).

These redox-dependent signalling cascades not only regulate motility, but also set the stage for subsequent structural rearrangements within the sperm head, influencing the reorganization of membrane and protein domains, typical of capacitation events (Abruzzese et al., 2024; Pezo et al., 2021; Ded et al., 2019; Gadella, 2017; Awda et al., 2009).

Mature spermatozoa are unable to renew their surface, as protein synthesis is permanently halted during the final stages of maturation (Gadella, 2017). At this point, they lose ribosomes and the Golgi apparatus, becoming highly specialized cells entirely dependent on pre-existing proteins (Abruzzese et al., 2024; Gadella, 2017; Belmonte et al., 2005). The membrane recycling also ceases, so spermatozoa cannot effectively renew the membrane surface (Gadella, 2017; Belmonte et al., 2005). Consequently, the cell relies on extensive proteome remodelling, achieved through the lateral rearrangement of existing components (Zigo et al., 2024; Gadella, 2017).

Key molecules, such as SNARE proteins (Soluble -ethylmaleimide sensitive factor for attachment receptor) and zona pellucida-binding proteins, that are previously distributed across the surface above the acrosome, migrate to the apical ridge of the head (Gadella, 2017; Gadella et al., 2008; Belmonte et al., 2005). This redistribution,

regulated by the ubiquitin-proteasome system (UPS) (Zigo et al., 2024), and simplified by the aggregation of lipid microdomains called *"lipid rafts"* (composed mostly of cholesterol and sphingomyelin and formed after the cholesterol efflux) (Gadella, 2017; Gadella et al., 2008; Rodriguez-Martinez et al., 2024) ensures that the sperm head is properly primed for the acrosome reaction and successful fusion with the oocyte (Belmonte et al., 2005), during the acrosome reaction, the final step enabling oocyte penetration (Gadella, 2017).

The acrosome reaction is a process whose physiological trigger of this event is species-specific (Gadella, 2017; Hirohashi & Yanagimachi, 2018; Rodriguez-Martinez et al., 2024). In swine it occurs upon contact with the oocyte's zona pellucida, when the outer acrosomal membrane of the sperm fuses with its plasma membrane (Belmonte et al., 2005; Ded et al., 2019). This fusion results in the release of proteolytic enzymes housed within the acrosome (Belmonte et al., 2005; Gadella et al., 2008; Jakop et al., 2022). The acrosome is a large secretory vesicle capping the anterior portion of the sperm nucleus, delimited by an inner and an outer acrosomal membrane (Belmonte et al., 2005; Gadella et al., 2008) and containing a matrix rich in hydrolytic and proteolytic enzymes essential for oocyte penetration (Jakop et al., 2022). During the acrosome reaction, multiple fusion points are formed between the sperm plasma membrane and the outer acrosomal membrane, mainly in the apical ridge and pre-equatorial regions (Belmonte et al., 2005; Gadella, 2017; Gadella et al., 2008). This membrane fusion, driven by calcium influx and mediated by preassembled SNARE protein complexes, leads to vesiculation and release of acrosomal enzymes that locally digest the zona pellucida, allowing the sperm to advance toward the oolemma and ultimately fertilize the oocyte (Gadella, 2017; Gadella et al., 2008).

One of the techniques that could be involved in the study of the biochemical processes leading to the acrosome reaction, such as lipid and protein redistribution and membrane fusion, is the fluorescence microscopy, as proposed by (Ded et al., 2019) of which it is reported an imagine used by the authors as a visual reference to classify spermatozoa into three distinct functional states: Non-capacitated (NC) → Capacitated (C) → Acrosome-Reacted (AR), based on the specific fluorescence pattern detected by each stain, that are:

- Chlortetracycline (CTC) to reveal intracellular calcium redistribution in the sperm head (A1–A3)
- Anti-acrosin antibody (ACR.2) to detect acrosomal matrix rearrangement (B1–B3)
- anti-phosphotyrosine (pY) antibody (anti-pY) to detect tyrosine-phosphorylated proteins associated with capacitation (C1–C3)

Fig. 4 provides a clear visual representation of the dynamic changes and movements of key molecular players during capacitation, highlighting the complexity of this process at each segment of the sperm head.

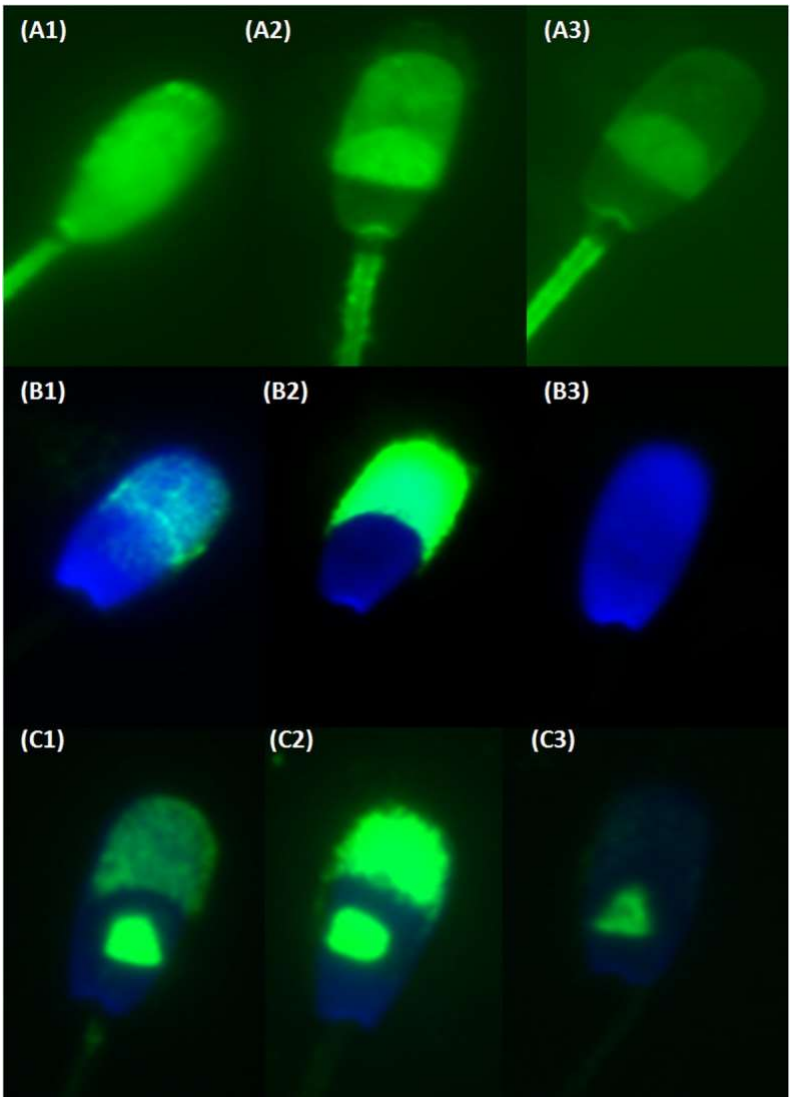

Figure 4 *Dynamic changes in sperm during capacitation. Fluorescent patterns show the repositioning of ions (CTC), acrosomal proteins (ACR.2), protein phosphorylation (anti-pY), from Non-capacitated (NC) → Capacitated (C) → Acrosome-Reacted (AR), visually illustrating key structural rearrangements in the head (Ded et al., 2019)*

Regarding calcium distribution: in NC sperm head fluorescence is bright and dispersed across the entire sperm head (A1). Upon capacitation (C) fluorescence becomes concentrated in the equatorial segment, while a non-fluorescent band appears in the post-acrosomal region (A2). In reacted acrosome spermatozoon instead, the fluorescence signal is extremely reduced across the head and with low positive reduced signal in equatorial segment only (A3).

The ACR.2 staining shows moderate, uniform fluorescence in the acrosomal region of NC sperm (B1). Following capacitation, acrosomal matrix rearrangement is evident, with intense fluorescence in the acrosome (B2). After the acrosome reaction fluorescence is completely absent due to enzymatic release (B3).

Finally, anti-pY staining reveals moderate phosphorylation in the acrosomal region of NC sperm, with a clear triangular segment visible inside the head (C1). During capacitation phosphorylation and protein repositioning increase, producing strong fluorescence in the head, especially in the triangular segment (C2). In AR sperm phosphorylation in the acrosomal region is drastically reduced, still detectable only in the triangular segment (C3).

Overall, the fluorescence patterns observed are consistent with the expected molecular changes occurring during capacitation, providing a detailed visual overview of this dynamic process in support of what detailed described in this section.

Although these essential functionalities played by ROS, when their production exceeds the antioxidant buffering capacity, this leads to oxidative stress (Abruzzese et al., 2024; Pezo et al., 2021) that can compromise sperm viability and motility (Awda et al., 2009; B. Zhang et al., 2021). As already mentioned before, each animal species exhibits distinct levels of reliance on specific metabolic pathways to produce energy and, therefore different susceptibility to oxidative stress (Abruzzese et al., 2024; O'Brien et al., 2021). In this thesis will be treated two different species and one of them is swine that will be largely explore. Boar is among the best-studied in this context, as boar spermatozoa presents enormous difficulties in cryopreservation (Awda et al., 2009; Pezo et al., 2021; B. Zhang et al., 2021). The biochemical and lipidic structure, along with high mitochondrial reliance imply the creation of instable oxidative environments as soon as the entire system undergoes shocks, as could be represented by cryopreservation (Pezo et al., 2021; B. Zhang et al., 2021).

In the next paragraphs will be deepen the structure and physiology of boar semen, because it will be one of the themes of this thesis, especially for what concerns the complicate boar semen preservation and the fascinating theme of mitophagy of paternal mitochondria. Apparently, both arguments could appear distant one from each other, instead are linked more than expected, and oxidative stress generated by mitochondrial energy metabolism appears to represent the key connecting mechanism.

Boar semen: Structure, Metabolism and Cryopreservation's vulnerability

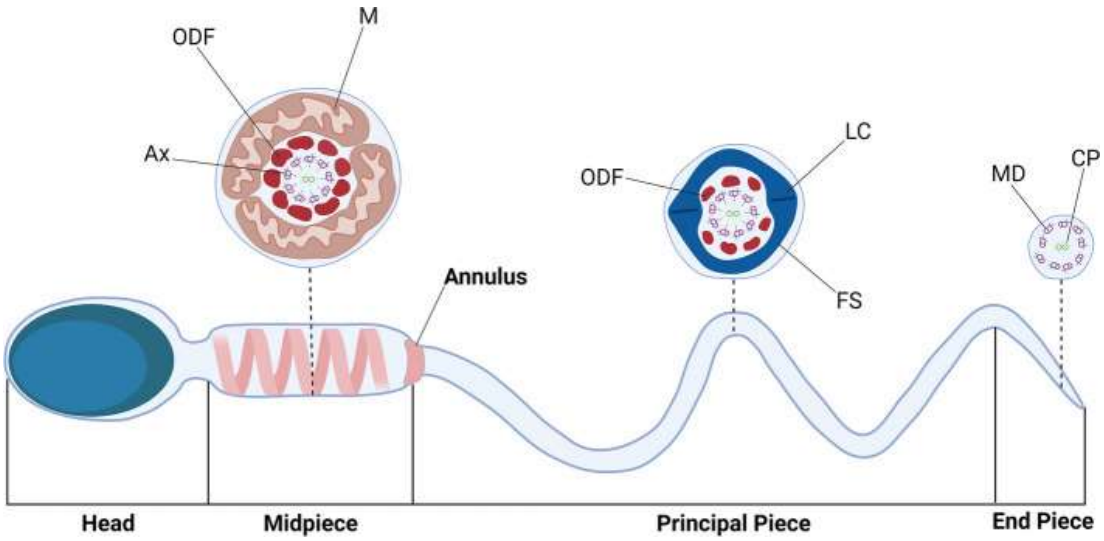

Figure 5 *Graphical cross-sections of spermatozoa segments, adapted from (Whitfield, 2024). It is reported the flagellum's structure, including the axoneme, mitochondrial sheath, and fibrous sheath, highlighting the organization of microtubules and associated proteins*

Spermatozoa are germinal cells highly specialized (male gametes) with the specific purpose of delivery genomic haploid male material in the oocytes (Abruzzese et al., 2024; Gadella, 2017). So, the structure reflects these specific functions (Fig.5), which are supported by motility and energy production (Abruzzese et al., 2024).

One of the key points for accomplish the task of fertilization is the compartmentalization of the structure from anatomical point of view (Gadella et al., 2008), and boar spermatozoa provide an excellent model for the study of this specialization.

The functional units of the boar spermatozoa are two: head and flagellum. The last, in its turn is subdivided into three other specific regions: Midpiece, Principal piece, End

piece (Rodriguez-Martinez et al., 2024). The peculiarity referred to these three different structures for what concerns swine are discussed more in details hereunder.

- **Midpiece**: crucial for energy production, since it contains mitochondria (Abruzzese et al., 2024; Gadella, 2017), with an average number of 80 per cell, one of the species-specific characteristics (Rodriguez-Martinez et al., 2024). Although boar spermatozoa are generally considered predominantly glycolytic (Abruzzese et al., 2024), during the specific process of capacitation, when is required a particular high energetic demand, a metabolic switch occurs, enhancing mitochondrial oxidative phosphorylation (Abruzzese et al., 2024) to supply the ATP required to sustain motility (Abruzzese et al., 2024; Gadella, 2017).
- **Principal piece:** in this area takes place glycolysis, here there is a cytoskeletal structure known as fibrous sheath, which acts as a scaffold for glycolytic enzymes to guarantee a localized production and availability of ATP along the flagellum (Abruzzese et al., 2024; Gadella, 2017; Rodriguez-Martinez et al., 2024). The compartmentalization, given by the fibrous sheath, may act to compensate for a potentially lower efficiency in transferring ATP produced by the mitochondria to the distal regions of the flagellum (Abruzzese et al., 2024). The glycolysis activity does not switch off during the capacitation and continues to provide localized energy directly where ATPase and other motility-related proteins operate (Abruzzese et al., 2024; Gadella, 2017).
- **End piece:** distal area of flagellum, thin and completely naked, without any energy functions recognized (Rodriguez-Martinez et al., 2024). Its anatomical disposition appears to be coherent as its role is intrinsically linked to motility, being the terminal portion of the flagellum, responsible for generating propulsive movement (Gadella, 2017).

Although the flagellum appears to be the protagonist for what concerns the energy production in spermatozoa, glycolysis takes place in the head too (Abruzzese et al., 2024). Nevertheless, numerous structural and functional adaptations contribute to the high degree of specialization observed in this compartment.

- **Head:** in the head of spermatozoa lies the essential function of the cell, since here it is housed the nucleus (Abruzzese et al., 2024; Gadella, 2017). The head

represents 1/10 of the entire length of the boar spermatozoa. Anatomically it appears as an oval, slightly dorsoventrally flattened shape *(racket like)* (Rodriguez-Martinez et al., 2024), with a length approximately 8.01-8.03 µm and width 4.3-4.5 µm (Banaszewska & Andraszek, 2021; Gadella, 2017). In the main body of the head resides the nucleus exhibiting a highly condensed chromatin structure to protect the haploid male genome contained in it (Rodriguez-Martinez et al., 2024; Gadella, 2017). Anteriorly, the nucleus is capped by the acrosome: a large secretory vesicle (Gadella, 2017), which contains hydrolytic enzymes necessary for the penetration of zona pellucida during acrosome reaction (Jakop et al., 2022; Gadella, 2017).

The acrosome forms during spermiogenesis by progressive fusion of small vesicles derived from the Golgi apparatus, which condense on the nuclear surface (Rodriguez-Martinez et al., 2024; Gadella, 2017; Belmonte et al., 2005). Once spermiogenesis is completed, the Golgi apparatus is disassembled, as the mature spermatozoon ceases de novo protein synthesis. so no longer requires an active secretory system (Gadella, 2017).

Acrosome is surrounded by two membranes: outer acrosomal membrane and inner acrosomal membrane, while the entire spermatozoon is delimited by a membrane that presents structural domains as described in drawings reported in Fig. 6 (Downing Meisner et al., 2005), highly specialized especially for what concerns the head (Rodriguez-Martinez et al., 2024; Gadella et al., 2008). The membrane here is organized in subdomains that perform distinct functions as the sperm approaches the oocyte (Gadella et al., 2008). There are 4 different regions: Apical ridge, Pre-equatorial ridge, Equatorial segment and Post-equatorial region (Rodriguez-Martinez et al., 2024; Gadella, 2017; Gadella et al., 2008)

- **Apical ridge**: the first to be involved in the zona pellucida recognition, at the end of the capacitation (Gadella, 2017).
- **Pre-equatorial region**: covering the apical area of acrosome, where will take place the fusion with acrosome to start the acrosomal reaction (Gadella et al., 2008).
- **Equatorial segment:** involved in the fusion with oocyte plasma membrane letting finally the entrance of male genetic material inside the oocyte (Gadella et al., 2008).

- **Post-equatorial region:** no direct involvement in fertilization, but it may contribute indirectly to the organization of interactions occurring in the anterior region (Gadella, 2017).

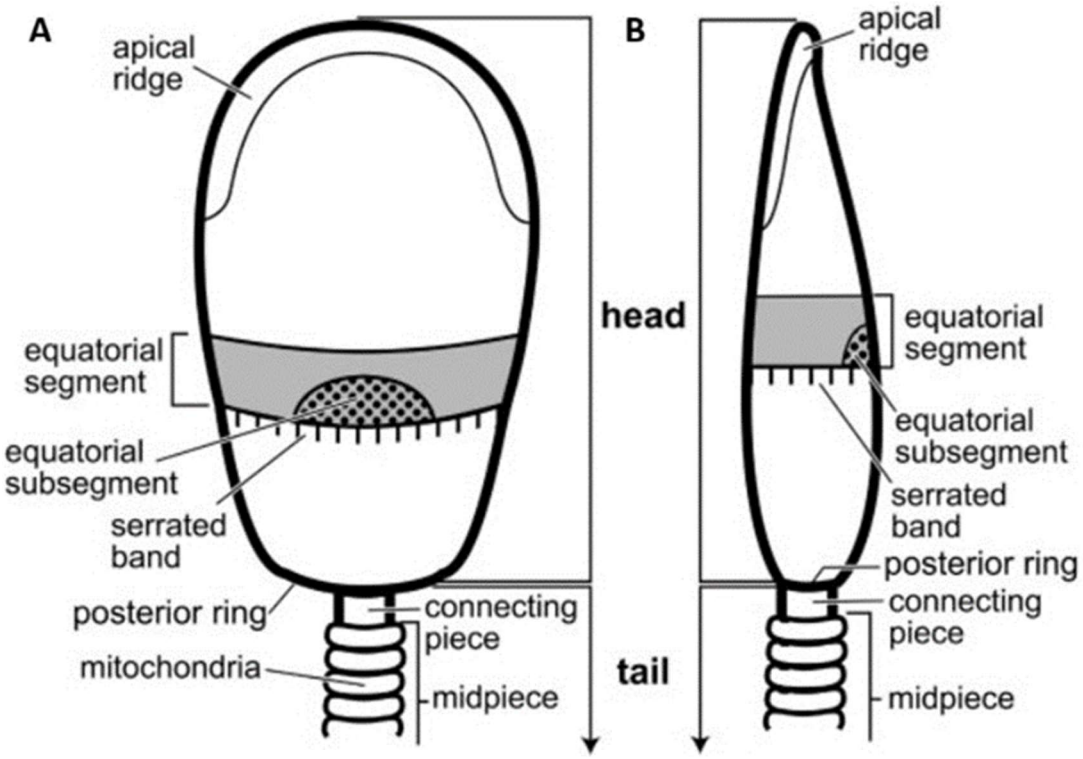

Figure 6 *Drawings of a mammalian sperm head with plasma membrane (surrounded the entire sperm cell) A: flat side. B: Lateral side, adapted from (Downing Meisner et al., 2005)*

Flagellum is completely covered by membrane too (Rodriguez-Martinez et al., 2024; Downing Meisner et al., 2005). Conversely to what happens for the head, in the flagellum there is a segregation of domains, helping the creation of compartmentalization barriers along all the structure, given by specialized junctional protein ring structures (Whitfield, 2024; Gadella et al., 2008):

- **Distal ring:** between the head and midpiece (Whitfield, 2024; Gadella, 2017).
- **Annular Ring:** between midpiece and tail (Gadella, 2017; Downing Meisner et al., 2005);

The composition of plasmatic membrane is what mostly define susceptibility of boar semen to low temperature (Abruzzese et al., 2024). To understand the reason why it is worth investigating the lipidic composition of the membrane further. Spermatic membrane is rich in polyunsaturated fat acids (PUFA) (Jakop et al., 2022; Pezo et al., 2021), but on the other hand presents less cholesterol compared to other mammalians species (Abruzzese et al., 2024; Pezo et al., 2021; Gadella, 2017). This means that

whilst this unique composition could be positive for the fluidity necessary during the pathway to reach the oocyte (Jakop et al., 2022; Gadella et al., 2008), on the other side, exposes the cell to extraordinary lipidic peroxidation (Jakop et al., 2022; Awda et al., 2009). This, added to the compromised antioxidant defence system, lead to an increasement of oxidative stress damages (B. Zhang et al., 2021; Awda et al., 2009), rendering boar semen one of the most challenging mammalian sperm samples to preserve and cryostore effectively among conventional livestock species (Rodriguez-Martinez et al., 2024; Pezo et al., 2021; B. Zhang et al., 2021; Awda et al., 2009).

Boar Semen Preservation in One Health perspective

In the following section some aspects related to boar semen preservation will be discussed in more detail, to introduce one of the peer-reviewed contributions published during the PhD of this candidate. Considering that about 95% of livestock inseminations are performed through Artificial Insemination (AI), particularly in the swine sector where this percentage accounts for approximately 99% of all artificial inseminations performed worldwide (Pezo et al., 2019). One of the most critical challenges concerns the preservation of semen quality, since the maintenance of sperm motility, viability, and acrosomal integrity is fundamental for the success of fertilization (Ngo et al., 2023; Althouse & Lu, 2005). It had been demonstrated that sperm viability decreases by 6.4% for every 1.0 $\log_{10}$ increasement in total bacterial count (Ngo et al., 2023). In Fig. 7 are summarized the most important consequences given by bacterial contamination of boar semen, such as: damage to the acrosome, decreased mitochondrial membrane potential, cryoresistance, sperm motility, and integrity of the sperm membrane, and increased ROS and apoptosis. The diagram is adapted from (Contreras et al., 2022).

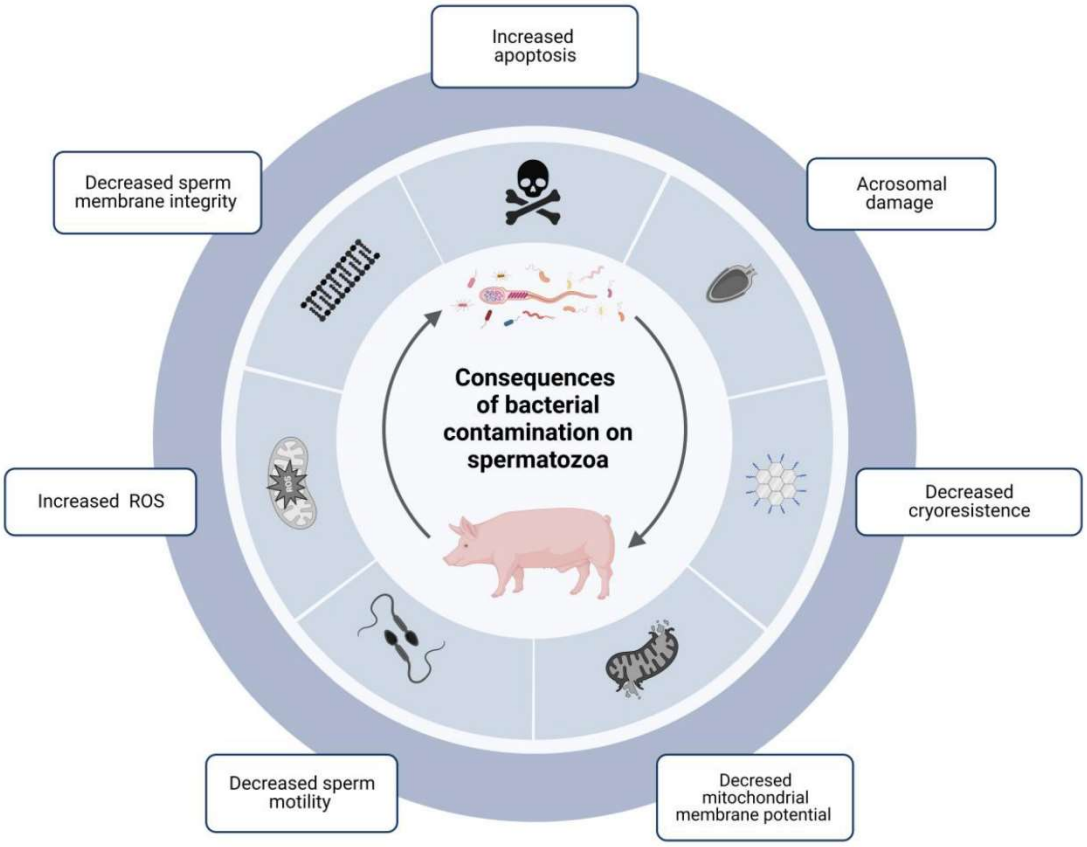

***Figure** 7 Diagram reported effects of bacterial contaminations in boar sperm and quality parameters during storage. Highlighting significant consequences on the quality and functionality parameters of spermatozoa, adapted from (Contreras et al., 2022).*

Over the past fifty years, the preventive use of antibiotics has represented what appeared to be the only feasible strategy for controlling bacterial contamination (Ros-Santaella et al., 2024). The most common added in semen extenders is gentamicin (Schulze et al., 2015; Althouse & Lu, 2005). However, this approach has raised serious concerns related to antimicrobial resistance (AMR), a global issue that affects the animal, plant, and human domains within the One Health perspective (Ros-Santaella et al., 2024). Antimicrobial resistance has already been demonstrated towards antibiotics most commonly widespread suggesting losing of the antimicrobial potential of gentamicin (Ngo et al., 2023; Althouse & Lu, 2005).

This problem is particularly relevant for boar semen, which can be conveniently preserved only in liquid phase at 16–18 °C for no longer than five days (Pezo et al., 2019), since, as previously discussed, its specific lipid composition and limited antioxidant protection against ROS make it highly prone to quality deterioration during storage (B. Zhang et al., 2021; Pezo et al., 2019).

To address both the need for microbial control and the growing AMR crisis, research has focused on antibiotic alternatives, including Antimicrobial Peptides and Proteins (AMPPs) (Ros-Santaella et al., 2024; Elmi, Prosperi, et al., 2019), among which lysozyme appears to be promising (Ros-Santaella et al., 2024) and natural compounds such as Essential Oils (EOs) (Elmi, Ventrella, et al., 2019; Elmi et al., 2017). Essential oils are well known for their antibacterial and antioxidant properties. However, before their antimicrobial potential can be effectively exploited, it is crucial to evaluate their cytotoxicity on spermatozoa, since EOs are known to exert strong toxic effects on various cell types, including sperm cells, with effects that are often concentration dependent.

This topic was addressed in (Troisio et al., 2024) the first peer-reviewed publication arising from this PhD research, that is reported in the experimental section.

Paternal Mitochondria Fate and Mitophagy Post-Fertilization

So far, it has been described that preserving sperm functionality is crucial for the successful achievement of fertilization (Sutovsky & Song, 2017). Particularly, the preservation of motility is largely linked to the health of the mitochondrial sheath (Vahedi Raad et al., 2024; Song et al., 2021). However, immediately after fertilization, the fate of paternal mitochondria is tightly regulated (Zuidema & Sutovsky, 2020). They will be selectively degraded in the process known as mitophagy, which ensures the exclusive maternal inheritance of mitochondrial DNA in the embryo (Zuidema & Sutovsky, 2020). The study of this fascinating event was the fulcrum of my research during the period abroad of 6 months at Utrecht University under the supervision of Professor Bart Gadella, where I was involved in the development of a feasible system to investigate this process and to understand why and exactly how it occurs.

As previously discussed, the paternal mtDNA is particularly subject to oxidative stress because of its peculiar sensitivity (Pezo et al., 2021) due to the absence of histones (Annesley & Fisher, 2019) and a simple repair mechanism that cannot face the intense damages given by oxidative stress (Awda et al., 2009) due to the high mitochondrial activity required during hyperactivation (Song et al., 2021; Zuidema & Sutovsky, 2020).

This is probably the most relevant reason why in the first embryonic development phase the Mitophagy (the event of selective degradation of paternal mitochondria) occurs (Zuidema & Sutovsky, 2020; Sutovsky & Song, 2017). The maternal inheritance of mitochondrial DNA (mtDNA) is a fundamental principle in animal and human development, also known as the *"Mitochondrial Eve"* paradigm (Zuidema et al., 2023; Zuidema & Sutovsky, 2020; Sutovsky & Song, 2017). This event is strictly linked with the embryo healthy development, since heteroplasmy (having two different types of mitochondrial DNA within a single individual) is often associated with reduced fitness, and, in some cases, is responsible for the development of severe mitochondrial diseases (Zuidema et al., 2023; Zuidema & Sutovsky, 2020; Aparicio et al., 2016). Recently it has been demonstrated that in many mammals' species, this active elimination is carried out through the synergistic action of the ubiquitin–proteasome system (UPS) and the oocyte's autophagic machinery (Zuidema et al., 2023).

Although the maternal inheritance is widespread among almost all mammalian species, only one of them emerges as the most suitable model for the study of the mechanisms involved in and it is the domestic pig (Zuidema & Sutovsky, 2020). This is primarily due to the early occurrence of complete degradation of mitochondrial sheath that occurs before the first embryonic division (Zuidema et al., 2023; Sutovsky & Song, 2017). So, it is possible to isolate and analyse the mitophagy process, with the use of selective proteosome inhibitor such as lactacystin and MG132, without interfering with subsequent embryo cleavage in which the UPS is strictly involved too, as metaphase-anaphase transition (Zuidema et al., 2023). So that, conducting this study in other species such as rodents, ruminants and primates, where mitophagy occurs at 2-4 cells state, it is impossible without compromising cell division (Zuidema et al., 2023; Zuidema & Sutovsky, 2020).

Mitochondrial Sheath Stabilization and Destabilization Along the Male–Female Reproductive Tract

As previously mentioned, sperm mitochondria are organized within a structure known as *"mitochondrial sheath",* where they are helically arranged around the axoneme and outer dense fibres (Zuidema et al., 2023; Zuidema & Sutovsky, 2020; Gadella, 2017). It is important to emphasize that this mitochondrial organization is further stabilized

by a compact protein aggregate, which provides mechanical protection to the entire sheath (Song et al., 2016). The stabilization, destabilization and mitophagy of the mitochondrial sheath occurring during the journey of spermatozoon toward oocyte, as described in porcine model, graphically reported in Fig. 8, according hypothesis proposed by (Zuidema & Sutovsky, 2020). In the following description, the events are presented according to this theoretical model. Starting from the mitochondrial sheath's stabilization, this is ensured by disulphide bridges (S–S) and zinc cross-links, both of which confer remarkable rigidity and structural integrity to the mitochondrial sheath until fertilization occurs (Zuidema & Sutovsky, 2020; Song & Sutovsky, 2019).

1. **Disulphide Bonds (S-S)**: The MS is stabilised by the disulphide bond cross-linking of its structural, cysteine-rich proteins (Song et al., 2021; Zuidema & Sutovsky, 2020; Sutovsky & Song, 2017). This stabilizing cross-linking conceals the ubiquitin tags on the sperm mitochondria, already present since the maturation in the epididymis (Zuidema & Sutovsky, 2020). In fact, prohibitin is the first protein to be ubiquitinated during spermatogenesis (Sutovsky & Song, 2017), so the fate of paternal mitochondria is already sealed till their early development in male reproductive tract, well before the damages to which they are prone in the female reproductive tract.
2. **Zinc Bridges:** Furthermore, the structure is stabilized by the potential formation of zinc bridges (Zuidema & Sutovsky, 2020; Sutovsky & Song, 2017). These bridges may form when spermatozoa intermix with zinc-rich seminal plasma at ejaculation (Kerns et al., 2018).

This twofold protective stabilization must be actively reversed within the zygote to expose the ubiquitinated proteins for subsequent recognition and degradation by the ooplasm factors (SQSTM1, VCP) (Zuidema et al., 2023; Zuidema & Sutovsky, 2020).

A first phase of destabilization occurs before the fertilization during capacitation with zinc ion efflux leading to partial destabilization of the mitochondrial sheath (MS) and activation of mitochondrial enzymes previously inhibited by zinc, preparing the sperm for hyperactivation and fertilization (Zuidema & Sutovsky, 2020; Kerns et al., 2018). Instead, after the entrance of spermatozoa inside the oocyte, takes place the reduction of S-S bonds given by glutathione (GSH), a reducing tripeptide synthesized by the oocyte (Song & Sutovsky, 2019). This reduction continues the destabilization of the

mitochondrial sheath and, mostly important, exposes the ubiquitin tags hidden during spermatogenesis (Song et al., 2021; Zuidema & Sutovsky, 2020).

Once this cross-linking removal takes place, with the exposition of ubiquitin tags, the organelle is ready for the recognition and degradation into the oocyte (Zuidema & Sutovsky, 2020; Song et al., 2016).

The mechanisms that are involved in paternal mitochondrial degradation involve two principal systems once spermatozoon is inside the oocyte (fertilization-triggered event) (Zuidema et al., 2023; Zuidema & Sutovsky, 2020):

1. **The Ubiquitin-Proteosome system (UPS) and VCP**: The ubiquitin-proteosome system is a universal system responsible for selective protein degradation (Sutovsky & Song, 2017). Ubiquitination acts as a tag that directs proteins proteosome for selective degradation (Zuidema et al., 2023). Sperm mitochondria are ubiquitinated as early as within the male reproductive tract (Song et al., 2016), during their development, and continue to undergo ubiquitination throughout their journey in the female reproductive tract (Song et al., 2021). VCP (Valosin-Containing Protein) is a ubiquitinated protein dislocase that extracts ubiquitinated proteins and presents them to the 26S proteosome for degradation (Sutovsky & Song, 2017), thereby destabilizing the membrane and priming the entire organelle for complete destruction (Zuidema & Sutovsky, 2020).
2. **Autophagy and SQSTM1:** the UPS converges with lysosomal proteolysis during autophagy (Sutovsky & Song, 2017). Protein aggregates are completely degraded, and it is possible to recognize key autophagic protein in superior mammalian species that is: SQSTM1 (Sequestosome 1, also known as p62) (Zuidema et al., 2023; Sutovsky & Song, 2017), is an oocyte-derived ubiquitin binding pro-autophagic receptor, acting as an early adaptor that recognizes ubiquitinated male mitochondria proteins (Zuidema et al., 2023; Sutovsky & Song, 2017; Song et al., 2016), exclusively associates with the sperm mitochondria after fertilization (Song et al., 2021, 2016), channelling them towards the autophagic machinery for subsequent degradation (Sutovsky & Song, 2017).

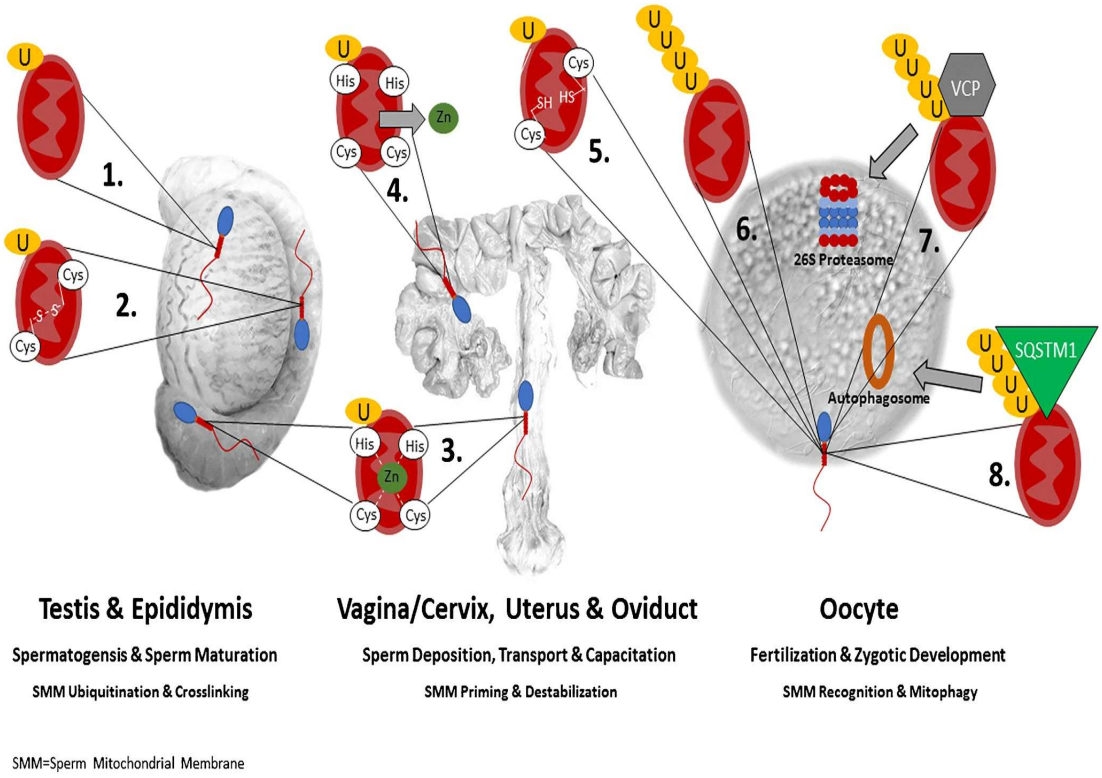

Figure 8 *Graphical summarize of proposed mechanism of porcine post-fertilization mitophagy, following a chronological series of event, starting from development inside male reproductive tract, up to the entrance of spermatozoon inside the oocyte. The ubiquitination starts inside male reproductive tract. The drawing shows the stabilization attempts with disulphide bonds S-S and zinc bridges, the destabilization outside and inside the oocyte and the final process of mitophagy with UPS and autophagosome, highlighted roles played by VCP and SQSTM1(Zuidema & Sutovsky, 2020).*

The Porcine Cell-free System

In the field of maternal mitochondrial inheritance, which ensures the clonal propagation of mitochondrial genes through the maternal lineage (Zuidema et al., 2023; Zuidema & Sutovsky, 2020), Dr. Peter Sutovsky and his research team are recognized as undisputed authorities. The authorship of a system known as *porcine cell-free system* is attributed to Dr. Sutovsky's group (Zuidema & Sutovsky, 2020). This system was developed to overcome the limitations of in vivo studies, such as *in-vitro* fertilization (IVF) and intracytoplasmic sperm injection (ICSI) (Zuidema et al., 2023). In these conventional protocols researchers can co-incubate oocyte extracts with only a single spermatozoa per oocyte. In contrast, the cell-free system allows for the co-incubation of hundreds or even thousands of spermatozoa with oocytes extractions in a single trial (Zuidema et al., 2023). This system has been shown to reproduce the *early fertilization proteomic interactions* mimicking structural remodelling that spermatozoa undergo inside the oocyte, such as the reduction of disulphide bonds (S-S) (Zuidema et al., 2023).

Specifically, the system foresees the preparation of male and female gametes for the subsequent co-incubation. The subsequent steps for gametes preparation and consequently co-incubation are summarized here below in according to (Song e Sutovsky 2019), where the Methodology is explained in details.

1. Preparation of the Female Component (Oocyte Extract)

- Collection and maturation: Porcine oocytes are collected from ovaries and matured in vitro to the Metaphase II (MII) stage.
- Denudation: the cumulus cells are chemically removed from mature MII oocytes using hyaluronidase, and the zona pellucida (ZP) is removed using pronase.
- Extraction and energization: the ZP-free are transferred in an extraction buffer containing an energy-regenerating system, including ATP (2 mM) and GTP (2 mM), along with phosphocreatine and creatine kinase, necessary to mimic the active, early post-fertilization ooplasm. To disrupt the cellular membranes, the oocytes are subjected to three rounds of flash freezing followed by thawing in liquid nitrogen.
- Collection of Content: The frozen-thawed material is crushed by subsequent high-speed centrifugation to collect the supernatant, which constitutes the oocyte extract.

2. Preparation of the Male Component (Sperm Priming)

For what concerns the male gametes, spermatozoa are prepared through a sequential chemical treatment called priming, necessary for mimicking the structural changes typical of mitophagy in vivo:

- Labelling and Washing: Spermatozoa are pre-labelled with the mitochondrial probe Mito Tracker Red CMXRos.
- Demembranation/Permeabilization: Spermatozoa are demembranated using L-α-lysophosphatidylcholine (lysolecithin). This mimics the removal of the plasma membrane during sperm-oolemma fusion.
- Chemical Destabilization: The spermatozoa are then incubated with Dithiothreitol (DTT), a disulphide bond (S-S) reducing agent. This is the

critical step to destabilize the structural sperm proteins (such as the mitochondrial sheath, which is hardened by S-S cross-linking) and expose the ubiquitin tags that initiate mitophagy, mimicking the action of ooplasmic glutathione.

3. Co-Incubation and Analysis

The primed spermatozoa are ready for the co-incubation with oocyte extract, at a concentration of approximately 1 x 10^4 spermatozoa per 10 µL of oocyte extract. The co-incubation typically occurs over periods such as 4 hours and 24 hours to capture temporal differences in degradation events.

The subsequent analyses are performed primarily on the spermatozoa after co-incubation, revealing interactions and degradation events:

Mass Spectrometry (MALDI-TOF) was used to conduct a quantitative investigation of the proteome, comparing the abundance of proteins in control (*primed*) spermatozoa versus those exposed to the extract. The key findings of this analysis were the reveal of a total amount of 185 proteins that showed statistically significant differences in abundance (increase, decrease, or new association) between the control and cell-free-treated spermatozoa, making them possible candidates for mitophagy co-factors

Western Blotting (WB) and Immunocytochemistry (ICC) were used, instead, to confirm the presence and characterize the localization patterns of key candidate proteins (such as MVP, PSMG2, PSMA3, FUNDC2, SAMM50, and BAG5), of which role is known in the context of autophagy or cellular proteolysis (in somatic cells or gametes) (Zuidema et al., 2023). The aim was to verify whether their known roles also extended to spermatid mitophagy, a species-specific process. In this result it is included also the visualization of the binding of oocyte-derived SQSTM1 to the sperm mitochondrial sheath.

The research conducted by Sutovsky and colleagues represented the starting point of my study during the period abroad. Their work paved the way for investigating the role of several proteins that they identified as active protagonists in the complex and highly regulated process of mitophagy.

A Learning Journey Abroad

The first step of my study was to find the most suitable solution to replace Sutovsky's work, following their procedures and to verify whether it was replicable in other laboratories. Our work was conducted in collaboration among three different universities (Utrecht University, Pisa University, and Bologna University). The collaboration among these three institutions enabled the study to be successfully replicated in a relatively short time, incorporating only minor modifications. Here below Fig. 9 is reported the workflow of the project carried out during the period abroad.

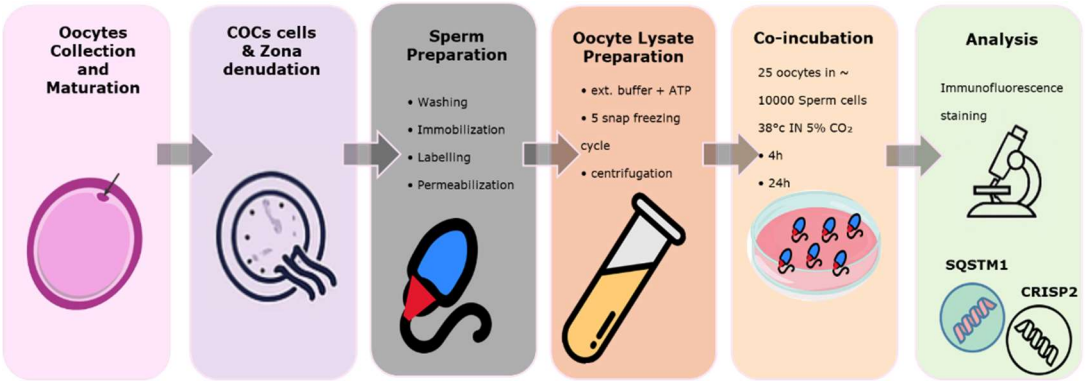

Figure 9 *Workflow of activities carried out during the Period Abroad (November 2024- April 2025) following the same procedure of Sutovsky group, with just slight modifications*

The timeline of the project was extended, because the difficulties encountered in replicating the work were not few, starting from the preparation of gametes for co-incubation. Specifically, regarding boar semen and mitochondrial staining. It was crucial to perform the procedure in such a way as to ensure that the signal remained detectable by immunofluorescence, even after permeabilizing the structure to mimic the early structural changes in spermatozoa.

CRISP2 was suggested as a reference protein marker (Zhang et al., 2022). This is a key component of the perinuclear theca (PT) of the spermatozoon, which resides in the post-acrosomal region (M. Zhang et al., 2021). Its rapid dispersion and subsequent degradation (disappearing before paternal pronucleus formation and mitochondrial degradation) is an early and indicative event of PT solubilization (Zhang et al., 2022), Fig 10.

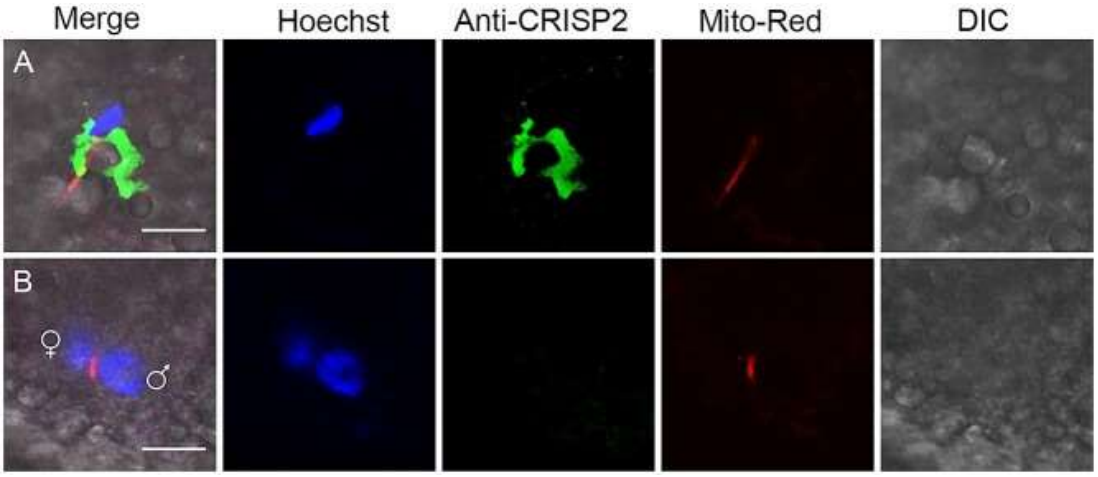

Figure 10 *The imagine represents the behaviour of sperm CRISP 2 in an in-vitro fertilization study, comparing the rapid dispersal of CRISP 2 observed immediately after the incorporation in zygote (row A) and at the formation of the two pronuclei, which typically occurs a few hours after fertilization (row B). In green anti-CRISP 2 detected by Alexa Fluor 488-conjugated; in blue nucleus staining (Hoechst 33342); in red Mito-tracker staining to highlight Mitochondria. Scale bar = 10 µm, DIC: Differential Interference Contrast, reported from (Zhang et al., 2022)*

The dissolution of the PT is an indispensable prerequisite for sperm nuclear decondensation (Zhang et al., 2022). Since the cell-free system aims to recapitulate early proteomic interactions (Zuidema et al., 2023), the observation of the rapid degradation or removal of key sperm proteins (such as CRISP2) by oocyte extracts, in a manner similar to what is observed *in-vitro* fertilization within 5 hours (Zhang et al., 2022), would confirm the effectiveness of the cell-free system in mimicking fertilization events.

At the end of my period abroad, it was possible to perform only a single trial using CRISP2 as the marker and SQSTM1 as the protein of interest, which were visualized by immunofluorescence after 4 hours and 24 hours of incubation with oocyte extract and with only extraction buffer. Results appear to highlight the success of replicating the work, marking a starting point for performing further replicates and continuing with the study of other proteins that could be involved. However, the partial nature of the data obtained does not allow the inclusion in this thesis. A collaboration between the three participating universities is already planned to continue the study of this topic beyond my PhD. The project aims to integrate Sutovsky's work with real-time metabolic analyses using the Seahorse XFp Analyzer, to characterize mitochondrial metabolic profiles in sperm and oocytes in the context of paternal mitochondria loss, evaluate oocyte metabolic activation after fertilization, and observe the effects of paternal mitochondria incorporation.

Seasonal spermatogenesis and oxidative balance in the roe deer

In the previous sections, the importance of the pig in the field of reproduction has been highlighted, particularly regarding the development of new strategies for the preservation of sensitive semen and for the study of maternal mitochondrial inheritance, where the domestic pig represents an ideal model species (Zuidema & Sutovsky, 2020; Elmi, Ventrella, et al., 2019). On the other hand, in the perspective of identifying the most suitable animal model for each of the research topics addressed in this thesis, it is important to introduce another species that represents an interesting model for studying spermatogenesis under photoperiodic influence: the European roe deer (*Capreolus capreolus*). This is a small ruminant widely diffused across Europe and Asia (Elmi et al., 2020; Ventrella et al., 2018) in both agricultural and forested landscapes (Tari et al., 2025).

Population densities vary a lot alongside with habitat type and management: around 3 individuals/km² in open farmland (France), 20.5/km² (Pays et al., 2012) in Hungarian agricultural areas (Tari et al., 2025), 3–30/km² in Italy (Emilia-Romagna) (The Regional Government of Emilia-Romagna, 2024), and 24–46/km² in Polish forests (Borkowski et al., 2021). These wide variations across different regions highlight both the species' adaptability and the strong influence of environmental and management factors (Pays et al., 2012).

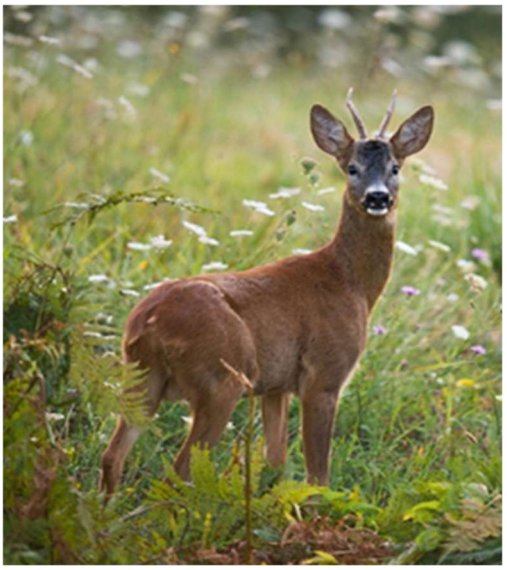

Figure 11 *male sexually mature Roe deer specimens (Bucks) © Filippo Zobbi*

After providing a general overview of population density, it is important to describe the reproductive characteristics, particularly of the male specimens (bucks; Fig. 11), The aim of the study in which I was involved will then be presented. This study is included in its final version in this doctoral thesis and is currently under revision for publication in a peer-reviewed journal.

Peculiarity of the species

The roe deer is a typical seasonal breeder species, with well-defined biological and physiological cycles in males. The primary driver of circannual changes is the photo-period dependent hormonal fluctuations during the year (Elmi et al., 2021, 2020; Ventrella et al., 2018; Goeritz et al., 2003; Blottner et al., 1996). Conventionally the reproduction season of roe deer is analysed in according to per-rut and rut-period (May-August) in which there is an increase in testosterone and oestrogen to stimulate spermatogenesis (Goeritz et al., 2003), but also the functionality of accessory glands, instead, during the rest of the year, there is the regression of spermatogenesis, since to a complete suspension of it, during the winter (October-February) (Lecewicz et al., 2017; Koziorowska-Gilun et al., 2015; Goeritz et al., 2003). Fig. 12 reports a schematic representation of roe deer's reproductive season.

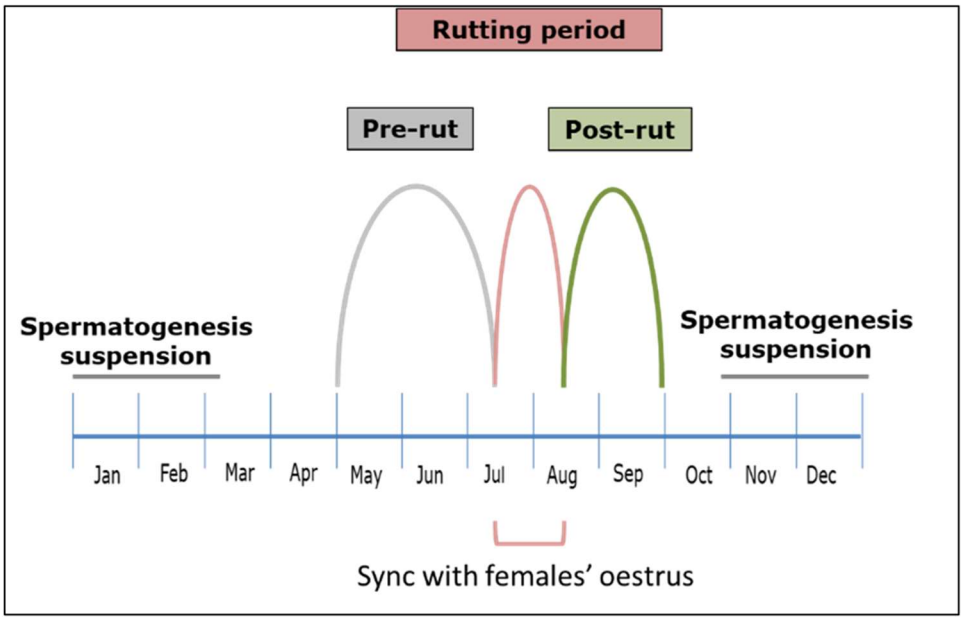

Figure 12 *Graphical representation of Bucks' annual reproductive season, highlighting rutting period subdivision and winter spermatogenesis subspension*

These endocrine changes can also modulate the oxidative status of reproductive tract, since as already seen in boars (Pezo et al., 2021), the high spermatogenesis activity increases ROS production and could not been buffered by antioxidant defence system, leading to oxidative stress to which will be prone the entire reproductive tract (Lecewicz et al., 2017; Koziorowska-Gilun et al., 2015).

This is the reason why in my study we tested two different pathways that are certainly involved in the modelling of reproductive tract: the Angiogenesis, important for the

promotion of testicular tissues' growth and development and Oxidative stress through a gene expression and protein quantification study conducted on bucks' testis, comparing testis obtained from animals hunted during post-rut period Vs animals hunted in pre-rut period. This study was meant to highlight new genes involved in the two different pathways, chosen to understand if there are relevant changes in term of expression or protein content in testicles.

Oxidative Stress: From Literature Insights to Experimental Results

To contextualize the main findings of the work that will be presented in attached file in subsequent section, it is important to briefly summarize what is currently known in the literature regarding oxidative stress in bucks' male reproductive system. In literature it is already well described an enhancement of antioxidant defence system during the mating season, to balance the increased production of ROS (Koziorowska-Gilun et al., 2015) that can damage, as already seen, the spermatozoa through lipid peroxidation, impaired motility and chromatin destabilization (Gadella, 2017; Lecewicz et al., 2017).

Biochemical analyses proved that the activity of key antioxidant enzymes increases during the rutting period. Superoxide Dismutase (SOD), that converts superoxide radicals into hydrogen peroxide, increases its activity in all reproductive tissues. Catalase (CAT), which neutralizes hydrogen peroxide into water and oxygen, is particularly active in the epididymis, while Glutathione Peroxidase (GPx) important for the protection of cells from lipid peroxidation, shows its highest activity in this period in the testis (Koziorowska-Gilun et al., 2015).

For what concerns gene expression study PHGPx (GPx4), a testis-specific isoform of GPx crucial for protecting developing germ cells, and GPx5, an epididymal isoform involved in sperm maturation, are strongly upregulated during this period. Other studies reported seasonal variations in mRNA too for SOD isoforms (Koziorowska-Gilun et al., 2015).

To complete these findings, proteomic analyses have identified additional antioxidant proteins in the epididymis. Peroxiredoxin-2 (PRDX2), an enzyme that efficiently reduces hydrogen peroxide, and Biliverdin Reductase A (BRVA), a protein involved

in neutralizing oxidative products with a purpose of maintain redox balance, also increase in expression during the rut (Lecewicz et al., 2017).

All these findings demonstrate that the antioxidant system in the roe deer male reproductive tract is finely tuned and seasonally regulated, with coordinated changes at the levels of enzymatic activity, gene expression, and protein abundance to protect sperm and maintain tissue function during the peak reproductive period (Lecewicz et al., 2017; Koziorowska-Gilun et al., 2015).

In this framework my work is also included, analysing differences between pre-rut period and post-rut period, which is consider recovery period following the extensive reproductive effort. After initial quantitative Real Time (qPCR) analyses conducted on pooled testicles samples (N=9 pre-rut, N=9 post rut), a subsequent validation phase was conducted using individual quantitative Real Time (qPCR) for each animal. This validation demonstrated statistical relevance in the results obtained for 4 genes (DHCR24, PRDX4, SOD3, SCARA3). Three of them show a statistically significant increase in gene expression: SOD3 (showing an approximately eightfold increase), PRDX4, and SCARA3 exhibit mRNA overexpression in the post-rut testis. An ELISA kit was used to assess total protein levels in the same tissue revealing that SOD3 protein levels followed the same trend as the mRNA, although the changes were not statistically significant.

The study also describes other findings, particularly regarding the angiogenesis pathway, which is crucial for testicular growth and development. For further details on this pathway, the reader is referred to the Experimental Section, where the full methodology and results are presented.

The Porcine Model in Cardiovascular Research

A special emphasis in this thesis has been given to the role of Pig in research to both is related to its importance in livestock (Pezo et al., 2019) as well as model in reproductive research (Zuidema & Sutovsky, 2020).

In this final section of the introduction chapter, another research field will be explored, where the pig once again serves as a precious *"ally"*: cardiac research, because in the experimental section is reported another publication in which I was involved that is

always linked with the theme of mitochondria with particular emphasis on oxidative stress (Tolomeo et al., 2024).

Especially in the preclinical research in cardiothoracic surgery and transplantation, pig is affirmed as most suitable model. This is due to its similarities with human anatomy, physiology, immune system and metabolism (Goutchtat et al., 2025; Meyerholz et al., 2024). In cardiothoracic surgery, to pig model is recognized a significant contribution to the development of stents, the improvement of coronary bypass grafts, and the advancement of cardiac valve xenotransplantation (Goutchtat et al., 2025). Moreover, in the last years pig has been included in a new line of research in heart transplantation, especially in field of heart transplantation obtained from donors after cardiac circulatory death (DCD heart) (Tessari et al., 2025). This inclusion is due to necessity to find new strategies to face the principal problem of DCD heart: Ischemia reperfusion injury (IRI) (Akande et al., 2020).

In fact, although donation after brain death (DBD) remains the gold standard for heart transplantation, as well as for organ transplantation in general, (Longnus et al., 2022), due to its numerous advantages, such as short ischemic period and continuous organ reperfusion during procurement, the available donor pool is insufficient to meet demand (DiChiacchio et al., 2023; Longnus et al., 2022). According to Global Observatory on Donation and Transplantation (GODT) , there are almost three times as many patients on the waiting list as available donors (Global Observatory and Transplantation, 2022). So, the mounting number of patients on the waitlist for cardiac grafts surgery represents a pressing challenge to develop new methods to expand the pool of potential donors.

Ischemia–Reperfusion Injury: A Major Challenge in Transplantation

As stated, ischemia-reperfusion injury is the typical pathologic event of myocardial stroke and so always reported in DCD transplantation procedure (Mantle et al., 2025; Akande et al., 2020). With IRI reference is made to a worsening of tissue damage upon restoration of blood flow to previously ischemic tissue. So that, there is a disruption of cellular homeostasis, with enzyme release, increased production of ROS and intracellular calcium overload (Bugger & Pfeil, 2020).

This damage is largely mediated by oxidative stress and mitochondrial dysfunction (Mantle et al., 2025). Once again it appears clear the critical dual function of mitochondria, since main targets of oxidative damage and critical source of ROS production.

To better understand the IRI and how it irreversibly damages mitochondria is useful to divide the events in two different phases: the ischemic phase and reperfusion phase.

- **Ischemic phase**: the interruption of blood flow deprives cells of oxygen (Mantle et al., 2025; Bugger & Pfeil, 2020), leading to an accumulation of succinate inside mitochondria (Mantle et al., 2025; Tessari et al., 2025; Longnus et al., 2022; Bugger & Pfeil, 2020), since the oxidative phosphorylation is haltered (Mantle et al., 2025) and so ATP synthesis ceases (Bugger & Pfeil, 2020).

  When the mitochondrial membrane potential collapses, ATP-dependent ion pumps cease to function, intracellular sodium accumulates, leading the Na^+/Ca^{2+} exchanger (NCX) to operate in reverse driving calcium influx into the cytosol (Bugger & Pfeil, 2020).
- **Reperfusion phase**: once the oxygen supply is restored, a rapid oxidation of succinate already stored occurs (Mantle et al., 2025; Bugger & Pfeil, 2020), resulting in an excessive reduction of Coenzyme Q (Bugger & Pfeil, 2020), a molecule that acts as a transfer of electrons between the Complex I/II of the Electron Respiratory Chain (Mantle et al., 2025), so electrons are forced to reverse their physiological pathway, coming back to the Complex I (Bugger & Pfeil, 2020). This reverse electron transport is the key mechanism that triggers a massive burst of reactive oxygen species (ROS), which is far more pronounced than the oxidative damage occurring during ischemia (Bugger & Pfeil, 2020).

One of the most catastrophic consequences of the IRI is the opening of the mitochondrial permeability transition pore (mPTP), that is a high-conductance channel located in the inner mitochondrial membrane, regulated by Cyclophilin D (CypD) and the F_oF_1-ATP synthase complex (Mantle et al., 2025; Bugger & Pfeil, 2020). This channel remains inhibited during the ischemic phase due to the low pH level (acidosis) of the mitochondrial matrix (Jurcau & Ardelean, 2022; Bugger & Pfeil, 2020), but its

rapid pH normalization and the ROS increment after the reperfusion promote the pore opening (Jurcau & Ardelean, 2022; Bugger & Pfeil, 2020). If the opening persists for a prolonged period, the phenomenon becomes irreversible. This causes the loss of mitochondrial membrane potential, matrix swelling, disruption of cristae structure (Jurcau & Ardelean, 2022; Akande et al., 2020; Bugger & Pfeil, 2020), since to the release of cytochrome c and apoptosis-inducing Factor (AIF) resulting in apoptosis of the entire cell.

So, these are the key events that concur in cardiomyocyte death, in which, as seen, the mitochondria stand as the central protagonist (Bugger & Pfeil, 2020).

Mitochondria-Targeted Therapeutic Strategies: From Literature Insights to Experimental Results

The central role of mitochondria in IRI leads the effort of researchers to a therapeutic approach aiming to protect and restore their function (Zhang et al., 2025):

One of the possibilities is the replacement of damaged mitochondria with healthy ones isolated in autologous skeletal muscle (Zhang et al., 2025; Doulamis et al., 2024). Although mitochondrial transplantation still seems an ambitious and forward-looking approach, it has shown remarkable feasibility and therapeutic potential in preclinical paediatric porcine DCD models (Doulamis et al., 2024). Mitochondrial Transplantation (MT) could preserve mitochondrial structure and improves cardiac function (Zhang et al., 2025) .

Another possibility is the Mitochondria-targeted Antioxidants, that are compounds such as MitoQ that is mitochondria-targeted antioxidant analogue of Coenzyme Q1, linked to triphenylphosphonium (TPP^+), a lipophilic cation. This binding allows it to selectively and efficiently accumulate inside mitochondria due to the organelle's negative membrane potential (Bugger & Pfeil, 2020). This targeted delivery greatly increases its local concentration (by up to 1000-fold) than untargeted one in rats (Adlam et al., 2005), increasing its antioxidant efficacy against ROS. The efficacy of this it is also demonstrated in porcine models specifically in a study of kidney preservation, where, the adding of MitoQ in preservation solution, reduced oxidative stress, preserved mitochondrial function reducing kidney damages (Parajuli et al., 2012).

As already explained before, the critical threshold in the IRI is reached when there is the prolonged mPTP, that leads to cellular death (Bugger & Pfeil, 2020), so it appears coherent the presence in literature of studies with the purpose of delay this phenomenon, considering mPTP the key therapeutic target for preserving mitochondrial structure (Bugger & Pfeil, 2020). In these studies (Cung et al., 2015; Xie & Yu, 2007) CsA (Cyclosporin A), a natural immunosuppressive drug already used to treat certain autoimmune diseases and to prevent organ transplant rejection by inhibiting T lymphocytes, was employed to pursue this aim. In the context of IRI, CsA can bind CypD (Cyclophilin D), a protein that regulates the opening of the mPTP. When this binding is stable, CypD cannot interact with the pore and, therefore, cannot contribute to its opening. However, despite achieving this effect, long-term outcomes in patients with myocardial infarction have not shown significant benefits (Cung et al., 2015).

In the context of preserving DCD hearts without compromising their use for transplantation, an innovative strategy has been proposed by the research group at the University of Padua, in which I had the privilege of participating during a training period at their facilities (Tolomeo et al., 2024).

The primary aim of the study (Tolomeo et al., 2024), (in Fig. 13 a graphical abstract of the study is reported) was to improve the preservation of DCD hearts through treatment with extracellular vesicles derived from mesenchymal stromal cells (MSC-EVs), with the goal of increasing the pool of organs available for transplantation, assessing their efficacy and safety in a preclinical pig heart transplantation model.

The extracellular vesicles were isolated from mesenchymal stromal cells derived from human umbilical cord perivascular cells (HUCPVCs), purchased from PromoCell and expanded following the guidelines of the International Society for Cellular Therapy (ISCT).

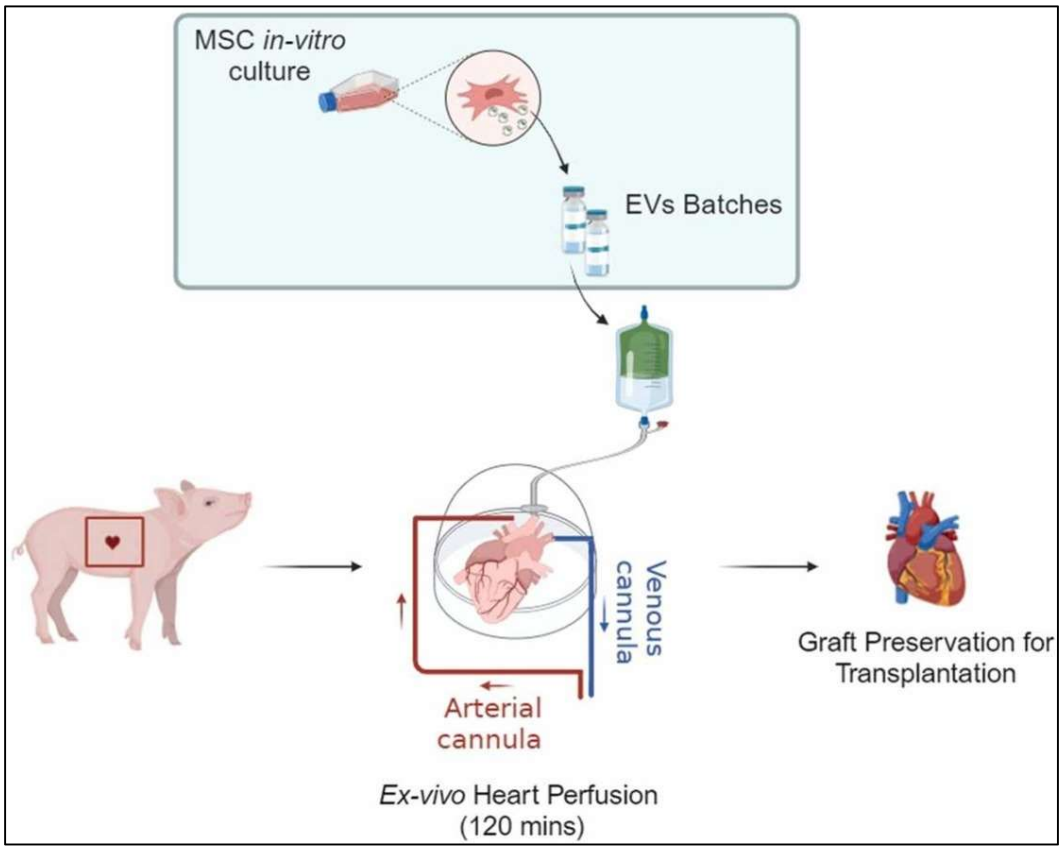

Figure 13 *Graphical abstract of* (Tolomeo et al., 2024)

In this work six female pigs were involved and after mimicking a cardiocirculatory death and after observed a no touch period of 20 minutes according to Italian law, the retrieved hearts were connected to the reperfusion circuit, where hearts were perfused with a mixture of leukocyte-depleted donor blood and a custom preservation solution, gradually warmed to 37°C and maintained at a pressure of 40 mmHg. MSC-EVs, previously characterized, were added to the priming volume at a dose of 1×10^{11} particles, while the control group received an equivalent volume of PBS + NaCl. Perfusion lasted 2 hours and at the end, heart tissue and perfusate samples were collected for further analysis.

The results showed a significant protective effect at the mitochondrial level: transmission electron microscopy (TEM) revealed that MSC-EVs prevented mitochondrial swelling and preserved cristae integrity, reducing the number of abnormal mitochondria compared to controls. Moreover, the treatment reduced oxidative stress, increasing the activity of antioxidant enzymes (SOD, CAT, GPx) in cardiac tissue and significantly decreasing protein carbonyl levels, markers of oxidative damage.

In conclusion, delivery of MSC-EVs via ex situ heart perfusion improved the quality of DCD hearts by maintaining mitochondrial ultrastructure and protecting against oxidative stress, highlighting their potential as an innovative therapeutic strategy for organ preservation in transplantation.

In this section it is reported only the results coherent with the theme of the thesis, but in the entire publication present in experimental section it is possible to see all the different analyses carried out that concur to express the success of this work.

Aim of the study

This thesis should be regarded as an effort to explore different fields of study, all connected, more or less directly, to the investigation of oxidative stress. At the heart of this work lies the preservation of mitochondrial health, a theme that resonates across numerous research areas that may seem distant from each other at first glance yet are all revolving around the same concept: the effect of oxidative stress.

Importantly, oxidative stress is no longer considered merely as a secondary sub-product of ATP production caused by ROS activity, but rather as a phenomenon that must be investigated in a broader perspective, considering the specific cell type in which it occurs, and the different model organisms chosen depending on the specific research question.

During my work, I had the privilege of not being confined to a single animal model or field of study. Instead, working across disciplines within a science-based research context allowed me to transpose knowledge gained in one area to others. This approach revealed unexpected connections: the insights gained from studying sperm preservation and mitophagy in the context of maternal mitochondrial inheritance allowed me to identify broader links to mitochondrial health, even in fields seemingly distant from reproduction, such as organ preservation in cardiovascular research.

In summary, this work highlights how mitochondrial health and ROS signalling serve as a unifying concept across diverse fields of biomedical research, opening new perspectives and connecting seemingly unrelated topics under a common scientific framework. Moreover, during these years, I also had the opportunity to participate in studies not directly related to the specific focus of this thesis, which will be briefly reported in a supplemental section.

Experimental Section

Boar Semen Preservation

Troisio, I., Bertocchi, M., Ventrella, D., Scozzoli, M., Di Vito, M., Truzzi, E., Benvenuti, S., Mattarelli, P., Bacci, M. L., & Elmi, A. (2024). Short- and long-term effects of essential oils on swine spermatozoa during liquid phase refrigeration. *Scientific Reports, 14*(1), 285. https://doi.org/10.1038/s41598-023-51030-2.

This is an experimental study published on Scientific Reports in January 2024 that investigates the use of essential oils as possible alternatives in boar semen preservation. Analysis of 9 essential oils plus patent blend on key morpho-functional parameters including viability, motility and acrosomal reactions. Dose-dependent toxicity was assessed at two different storage times in liquid phase.

scientific reports

Check for updates

OPEN

Short- and long-term effects of essential oils on swine spermatozoa during liquid phase refrigeration

Ilaria Troisio[1,7], Martina Bertocchi[1,7], Domenico Ventrella[1✉], Maurizio Scozzoli[2], Maura Di Vito[3], Eleonora Truzzi[4], Stefania Benvenuti[5], Paola Mattarelli[6], Maria Laura Bacci[1] & Alberto Elmi[1]

The application of essential oils as potential alternatives to antibiotics in swine semen storage is promising, due to their antioxidant and antibacterial properties. However, detrimental effects on spermatozoa should be clarified first. The aim of this study was to evaluate 9 essential oils (EOs; *Satureja montana*, *Pelargonium graveolens*, *Cymbopogon nardus*, *Melaleuca leucadendron*, *Eucaliptus globulus*, *Citrus limon*, *Lavandula angustifolia*, *Lavandula hybrida*, *Mentha piperita*) and a blend (*GL mix*) on key morpho-functional parameters of swine spermatozoa. Test compounds were firstly chemo-characterized and experimental doses were prepared by suspending a fixed number of spermatozoa with 3 different concentrations (0.1, 0.5, 1 mg/mL) of EOs. Experimental doses were stored at 16 °C and sampled after 3 and 120 h for analysis. Overall, *S. montana*, *P. graveolens and L. angustifolia* EOs induced the strongest alterations, with *C. nardus* and *E. globulus* EOs being the best tolerated. Swine spermatozoa represent a good preliminary testing platform to screen toxicity and its different patterns. The comprehensive overview on the potential mechanisms of action of some of the most common EOs, despite of the direct aim of the study being swine reproduction, may be exploited in other fields of research within both veterinary and human medicine.

According to data reported by Lancet and released by WHO (World Health Organization), antimicrobial resistance (AMR) in bacteria caused an estimated 1.27 million deaths in 2019[1], evidence that this is one of the most urgent matters in terms of public health. For this reason, the World health Assembly adopted a global action plan on antimicrobial resistance in 2015 and published a list of priority antibiotic-resistant bacteria in 2017 to identify the most relevant resistant bacteria at a global level for which there is an urgent need for new treatments[2]. The European Commission addressed the argument for the first time in 2001, with the first recommendation on the prudent use of antimicrobial agents in human medicine. Then, in 2011, proposed an actual action plane against the rising threats from antimicrobial resistance. In this circumstance, the Commission introduced the concept of One Health because of the indissoluble link between veterinary medicine, public health, and environmental sectors: *"In order to succeed a holistic approach is needed"*[3]. Finally, in the last year, the European Commission adopted a regulation to establish the criteria for the designation of antimicrobials to be reserved for the treatment of certain infections in humans[4].

In animal husbandry, the use of antimicrobials has always been a common and widespread practice, even for preventive purposes, especially in intensive breeding. Lately, the restrictions imposed by the European Commission have led to the search for alternative preventative approaches such as vaccination, good biosafety practices, and high animal welfare conditions[5,6]. In some cases, finding alternatives has been complicated, as in the case

[1]Department of Veterinary Medical Sciences, Alma Mater Studiorum - University of Bologna, Ozzano dell'Emilia, BO, Italy. [2]Italian Society for Research on Essential Oils (Società Italiana per la Ricerca sugli Oli Essenziali—SIROE), Rome, RM, Italy. [3]Department of Basic Biotechnological Sciences, Intensivological and Perioperative Clinics, Catholic University of the Sacred Heart, Rome, RM, Italy. [4]Department of Chemical and Geological Sciences, University of Modena and Reggio Emilia, Modena, MO, Italy. [5]Department of Life Sciences, University of Modena and Reggio Emilia, Modena, MO, Italy. [6]Department of Agricultural and Food Sciences, Alma Mater Studiorum - University of Bologna, Bologna, BO, Italy. [7]These authors contributed equally: Ilaria Troisio and Martina Bertocchi. ✉email: domenico.ventrella2@unibo.it

of swine breeding and reproduction. In the swine industry, the extensive use of artificial insemination (AI) has contributed to the improvement of fertility performances, potentially one of the most important achievements in the livestock sector within the last 30 years[7]. This contributed to increasing in demand for seminal material from high pedigree boars so that today more than 93% of sows in pig producing countries are inseminated artificially[8].

The most common bacterial populations found in boar semen are Gram-negative belonging to the Enterobacteriaceae family [9–11]. In general, the incidence and relevance of certain bacteria species is correlated with seasonal conditions[12] and specific sources of contamination: bacteria can come from both animal (*E. coli, Enterobacter spp., and Staphylococcus spp*.) and non-animal sources (*Pseudomonas, Bacillus,* and other species)[11]. Contamination points include boars, semen collection areas, water sources, thermometers, air handling systems and mainly poor personnel hygiene[9].

Boar semen extenders are usually added with antibiotics to limit bacterial growth, capable of altering spermatozoa quality, since liquid preservation at 16 °C is still considered the best preservation technique[7,13]. This is related to the cold sensitivity of boar spermatozoa rich in unsaturated fat, and low tolerance to the most common cryopreservation additives[14]. Gentamicin, an aminoglycoside antibiotic, represents one of the most used preservative antimicrobials in porcine semen extenders as of today[12,15], but gentamicin-resistant bacteria have been isolated since 2010 in European AI boar centers[16]. Recently, it has been emphasized that certain factors related to the age and the hygiene-sanitary of boars, as well as the methods used during semen collection, can significantly impact the presence of aerobic and coliform bacteria in semen[11].

So that, a lot could be done with improvements in term of good practice of AI centers along the entire process from collection to the filling of AI doses[7], as shown by an 8-years retrospective study conducted on 28 AI Centers in Europe after the identification and introduction of 9 HCCPs (hygienic critical control points) and the evaluation of hygienic conditions. The analyses show that hygiene management has contributed to reduce contamination of extended ejaculates; in particular, the bacterial contamination rate decreased by 13.5% between audit period 1 and 4[15]. It is important to clarify that most of bacteria detected are considered nonpathogenic, nevertheless high levels of bacterial contamination can lead to negative consequences[9]. High bacterial counts (over 1.4×10^4 CFU/mL) lead to decreased sperm motility and changes in pH. In some cases, bacteria can affect the integrity of sperm membrane which results in reduced viability and damaged acrosomes. Additionally, bacterial concentration and storage time can influence the mitochondrial membrane potential of sperm. Lastly, it was demonstrated that some bacteria can cause agglutination of cells, interfering with motility[12]. Several studies in recent years have focused on the need for finding new strategies to avoid using antibiotics in the extenders. Out of physical methods, such as ultracentrifugation, and microfiltration of seminal plasma[17] that have shown excellent results but turned out to be really expensive. There are also studies that show that colloid centrifugation can reduce bacterial contamination of boar semen without the use of antimicrobials[18], and recently there are some evidences that single-layer centrifugation could enhance chromatin structure in boar semen[19]. Another approach is represented by antimicrobial peptides[20]: substances that can alter the bacterial membrane, potentially killing pathogens.

Among these different alternatives, there are also Essential Oils (EOs): products of the secondary metabolism of plants, which are aromatic and volatile substances responsible of the characteristic fragrance of the plant. Essential oils consist of a mixture of different terpenes, sesquiterpenes and aromatic compounds such as phenols and phenylpropanes[21]. By using different extraction methods (distillation, mechanical pressure, extraction using solvent)[22,23] is it possible to obtain EOs in different compositions. A lot of them have proven antifungal, antiviral, and also antibacterial potentials, as reported by Tariq and colleagues[24], with an exhaustive review in which are listed the mechanisms of action of the most famous compound among the most widely studied.

The aim of the present study was to evaluate 9 EOs (*Satureja montana, Pelargonium graveolens, Cymbopogon nardus, Melaleuca leucadendron, Eucaliptus globulus, Citrus limon, Lavandula angustifolia, Lavandula hybrida, Mentha piperita*) and a blend (*GL mix*) for short and long term potential toxic effects on porcine spermatozoa by evaluating main morpho-functional parameters (viability, acrosomal reactions and total motility). The activity of essential oils on porcine spermatozoa has also been assessed with previous studies in which it has been already tested the potential use of some officinalis Essential Oils as antimicrobial agents for liquid storage[13,25,26].

The outcome of the sequent study may deepen the knowledge around these compounds that can become interesting new proposals as new alternatives for the liquid short and long storage of seminal porcine doses contributing towards fight against antimicrobial resistance.

Results

The results of the chemo-characterization of the different EOs used in the present study are reported in the Supplementary Materials (Tables S1–S10).

The effects of both short- (3 h) and long-term (120 h) exposure to the different EOs on porcine spermatozoa morpho-functional parameters are represented, including the results of the Dunnett's tests used to compare EO-treated samples to the control in the following figures**.** An initial graphical overview of the effects of all test compounds is reported in the Supplementary Materials (Figure S1). However, to better describe the results, the different EOs were divided into subgroups according to the different patterns of toxicity exhibited.

Satureja montana, *Pelargonium graveolens* and *Lavandula angustifolia*

These EOs statistically altered all morpho-functional parameters, as shown in Fig. 1.

The 2 way-ANOVA showed how treatment with *S. montana* altered Viability (V; $p = 0.0001$), Acrosome Reaction (AR; $p = 0.0005$), and Sperm Total Motility (TotM; $p < 0.0001$), while storage time only TotM ($p = 0.0107$). Upon comparison with the control, V (Fig. 1A) was statistically impaired by the middle and the highest concentrations at both timepoints: 0.5 mg/mL (3 h: $p = 0.0257$, 120 h: $p = 0.0190$), 1 mg/mL (3 h: $p = 0.0028$; 120 h:

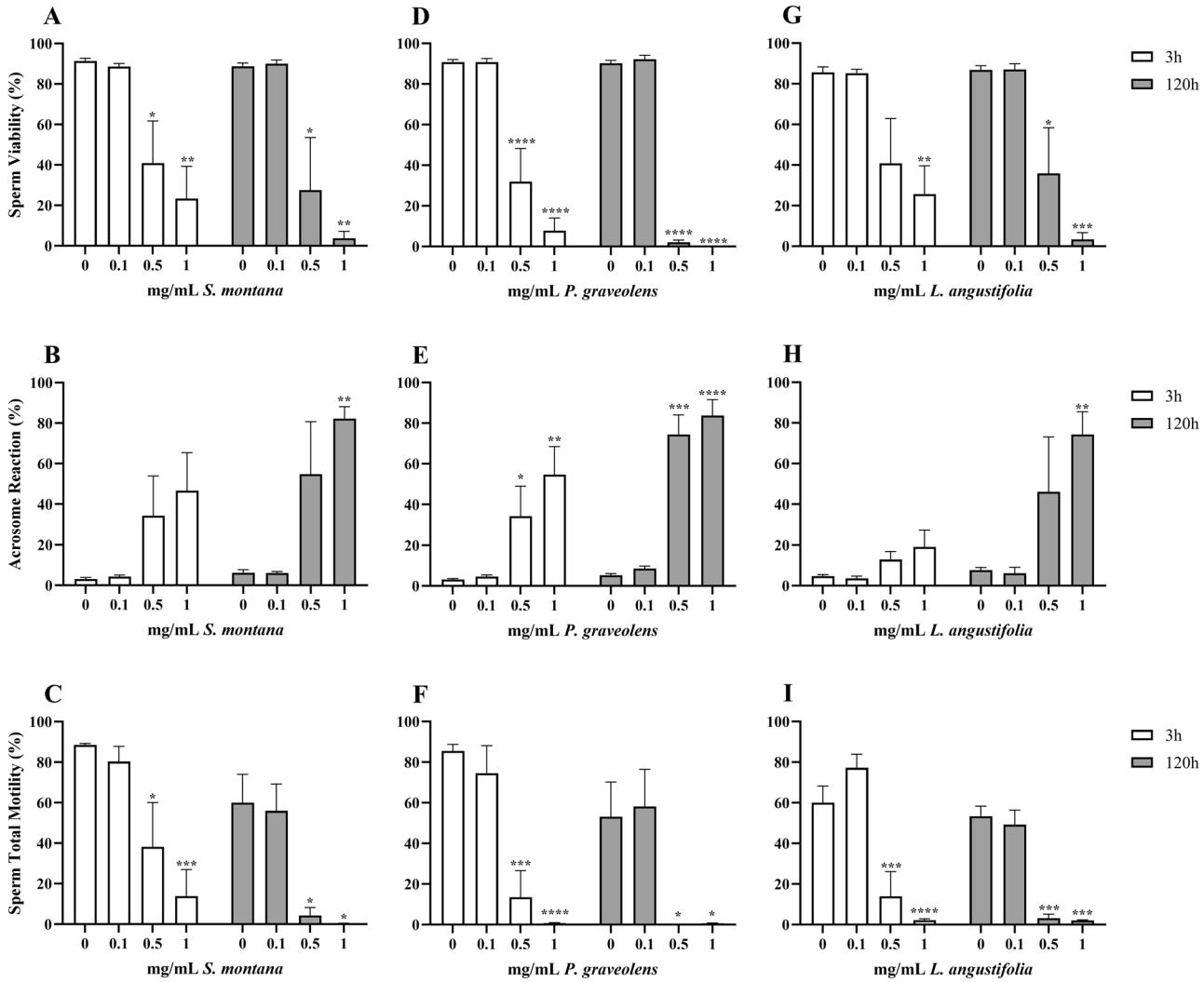

Figure 1. Effects of *S. montana* (**A**–**C**), *P. graveolens* (**D**–**F**) and *L. angustifolia* (**G**–**I**) EOs on sperm viability (**A**, **D**, **G**), acrosome reaction (**B**, **E**, **H**) and sperm total motility (**C**, **F**, **I**). Data are expressed as mean ± standard error of the mean. 0 = control samples (only emulsifiers). * = $p < 0.05$; ** = $p < 0.01$; *** = $p < 0.001$; **** = $p < 0.0001$.

$p = 0.0013$). The same applies to TotM (Fig. 1C): 0.5 mg/mL (3 h: $p = 0.0166$; 120 h: $p = 0.0221$), 1 mg/mL (3 h: $p = 0.0006$; 120 h: $p = 0.141$). On the other hand, AR (Fig. 1B) was only worsened by 1 mg/mL of EO at 120 h ($p = 0.0046$).

Treatment with *P. graveolens* EO statistically altered all three parameters (V, AR and TotM: $p < 0.0001$), while storage time only influenced AR ($p = 0.0093$). The post hoc analysis showed that V (Fig. 1D) was significantly impaired upon exposure to 0.5 and 1 mg/mL of EO at both timepoints ($p < 0.0001$), just like AR (0.5 mg/mL: 3 h $p = 0.0467$, 120 h $p = 0.0002$; 1 mg/mL: 3 h $p = 0.0011$, 120 h $p < 0.0001$; Fig. 1E) and TotM (0.5 mg/mL: 3 h $p = 0.0002$, 120 h $p = 0.0116$; 1 mg/mL: 3 h $p = 0.0002$, 120 h $p = 0.0116$; Fig. 1F).

At last, while treatment with *L. angustifolia* EO influenced all parameters (V and TotM: $p < 0.0001$; AR: $p = 0.0037$), storage time only affected TotM and AR (respectively: $p = 0.0078$ and $p = 0.0247$). The results of Dunnett's tests, in this case, showed that V (Fig. 1G) was statistically reduced at 3 h only by 1 mg/mL ($p = 0.0092$), while by both 0.5 ($p = 0.0265$) and 1 mg/mL ($p = 0.0006$) at 120 h. TotM (Fig. 1I) was compromised at both timepoints upon exposure to 0.5 (3 h: $p = 0.0004$; 120 h: $p = 0.0002$) and 1 mg/mL (3 and 120 h: $p = 0.0001$). On the other hand, AR (Fig. 1H) was only impaired by the highest concentration, after 120 h of exposure impaired ($p = 0.0015$).

Lavandula hybrida and *Citrus limon*

The EOs obtained from *L. hybrida* and *C. limon* showed a very similar pattern of actions on spermatozoa, represented in Fig. 2.

The 2 way-ANOVA showed that treatment with both EOs reduced V ($p < 0.0001$) (Fig. 2A,D) and increased AR ($p = 0.0001$) (Fig. 2B,E). Acrosomal reactions, in both cases, were statistically increased also by storage time (*L. hybrida* EO: $p = 0.0008$; *C. limon* EO: $p = 0.0092$) and interaction between variables (*L. hybrida* EO: $p = 0.0121$;

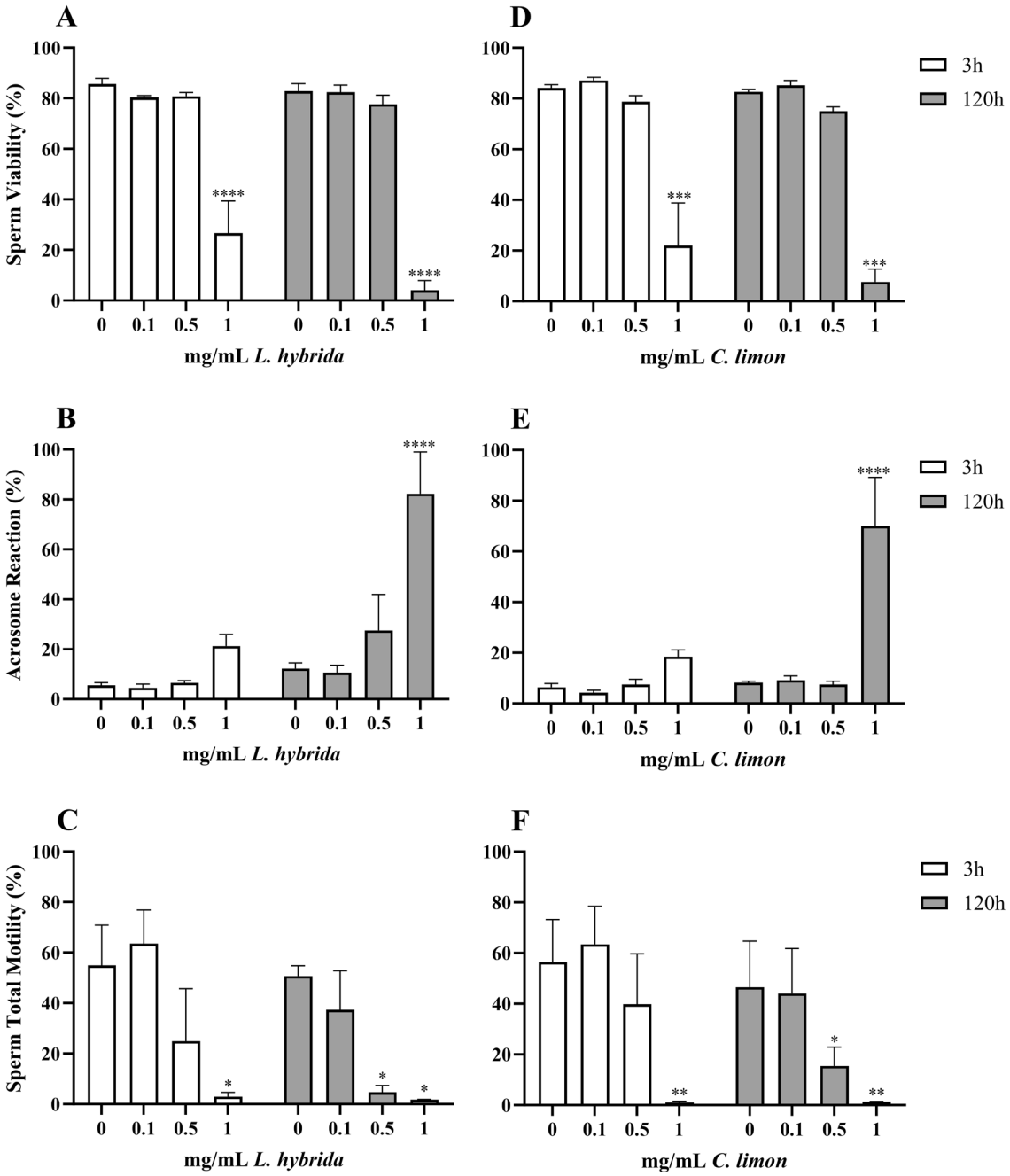

Figure 2. Effects of *L. hybrida* (**A–C**) and *C. limon* (**D–F**) EOs on sperm viability (**A**, **D**), acrosome reaction (**B**, **E**) and sperm total motility (**C**, **F**). Data are expressed as mean ± standard error of the mean. 0 = control samples (only emulsifiers). * = $p < 0.05$; ** = $p < 0.01$; *** = $p < 0.001$; **** = $p < 0.0001$.

C. limon EO: $p = 0.0051$). Also TotM (Fig. 2C,F) was compromised by the treatments (*L. hybrida* EO: $p < 0.0009$; *C. limon* EO: $p = 0.0002$). The post hoc analysis showed that V was statistically altered at both timepoints upon exposure to 1 mg/mL ($p = 0.0001$), while AR was only worsened at 120 h for both EOs ($p < 0.0001$). Upon comparison with the controls, TotM showed a slightly different trend: 0.5 mg/mL (120 h: *L. hybrida* EO $p = 0.0368$, *C. limon* EO $p = 0.0303$), 1 mg/mL (3 h: *L. hybrida* EO $p = 0.0181$, *C. limon* EO $p = 0.0015$; 120 h: *L. hybrida* EO $p = 0.0259$, *C. limon* EO $p = 0.0032$).

Mentha piperita, *Melaleuca leucadendron* and *GL mix*

These EOs and the blend only induced statistically relevant alterations when used at the highest concentration of 1 mg/mL (Fig. 3).

The results of the 2way-ANOVA for the *M. piperita* EO showed that all three parameters were statistically affected by the treatment ($p = 0.0001$), but only AR and TotM by storage time (respectively: $p = 0.0031$ and $p = 0.0017$). The Dunnett's tests highlighted how, for both timepoints, only the samples treated with the highest

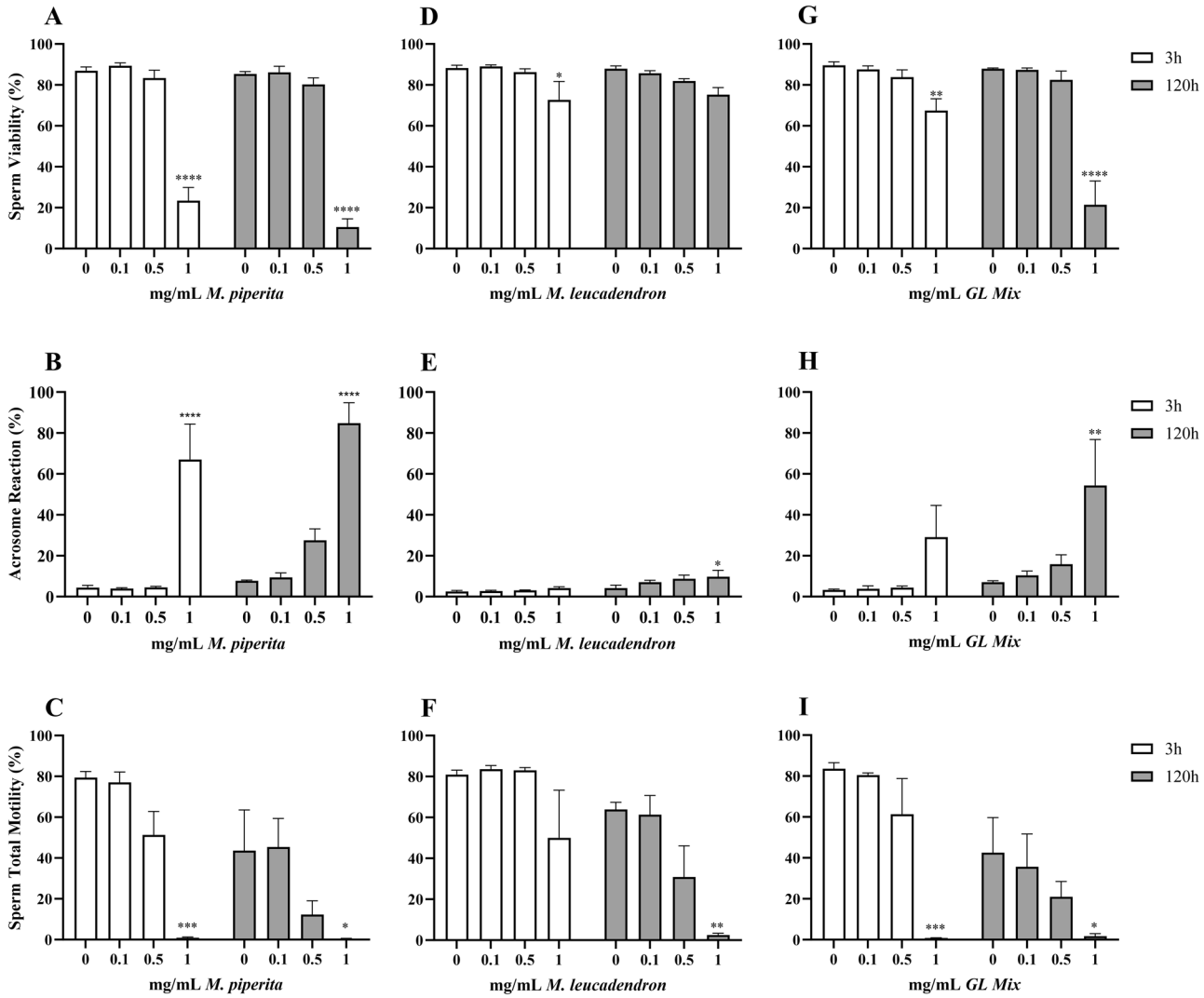

Figure 3. Effects of *M. piperita* (**A**–**C**) and *M. Leucadendron* (**D**–**F**) EOs and *GL Mix* (**G**-**I**) on sperm viability (**A**, **D**, **G**), acrosome reaction (**B**, **E**, **H**) and sperm total motility (**C**, **F**, **I**). Data are expressed as mean ± standard error of the mean. 0 = control samples (only emulsifiers). * = $p < 0.05$; ** = $p < 0.01$; *** = $p < 0.001$; **** = $p < 0.0001$.

concentration of EO statistically differed from the control samples: at 3 h $p < 0.0001$ for all three parameters, at 120 h $p < 0.0001$ for V (Fig. 3A) and AR (Fig. 3B), and $p = 0.0202$ for TotM (Fig. 3C).

Treatment with *M. leucadendron* EO impaired V ($p = 0.0042$; Fig. 3D) and TotM ($p = 0.0013$; Fig. 3F), while storage time altered AR ($p = 0.0009$; Fig. 3E) and TotM ($p = 0.0003$). The post hoc analysis showed that V was significantly worsened by 1 mg/mL at the first timepoint ($p = 0.0206$). For the other two parameters, alterations were only recorded after 120 h, still with the higher concentration (AR: $p = 0.0492$, TotM: $p = 0.0022$).

The 2way-ANOVA showed that treatment with *GL mix* statistically altered: V ($p < 0.0001$; Fig. 3G), AR ($p = 0.0056$; Fig. 3H) and TotM ($p = 0.0001$; Fig. 3I). Viability was also influenced by storage time ($p = 0.0006$) and by the interaction between the variables ($p = 0.0001$); storage time was statistically relevant also on TotM ($p = 0.0008$). Dunnett's tests highlighted that samples added with 1 mg/mL of *GL mix* showed different alterations when compared to the control: at 3 h for V ($p = 0.0034$) and TotM ($p = 0.0002$), at 120 h for all parameters (V: $p < 0.0001$, TotM: $p = 0.0424$, AR: $p = 0.0098$).

Cymbopogon nardus and *Eucaliptus globulus*

These EOs showed minimal to no toxic effects on swine spermatozoa both during short- and long-term storage (Fig. 4).

As for *C. nardus* EO, the 2way analysis of variance showed that there were no interferences on V (Fig. 4A), while storage time statistically impaired AR ($p = 0.0142$; Fig. 4B) and TotM ($p = 0.0049$; Fig. 4C). Upon comparison with the control, the latter was only statistically worsened by 1 mg/mL of EO at 120 h ($p = 0.0277$).

Similarly, looking at the results for the EO of *E. globulus*, V was never impaired (Fig. 4D), while AR (Fig. 4E) and TotM (Fig. 4F) only by storage time (respectively $p = 0.0019$ and $p = 0.0002$).

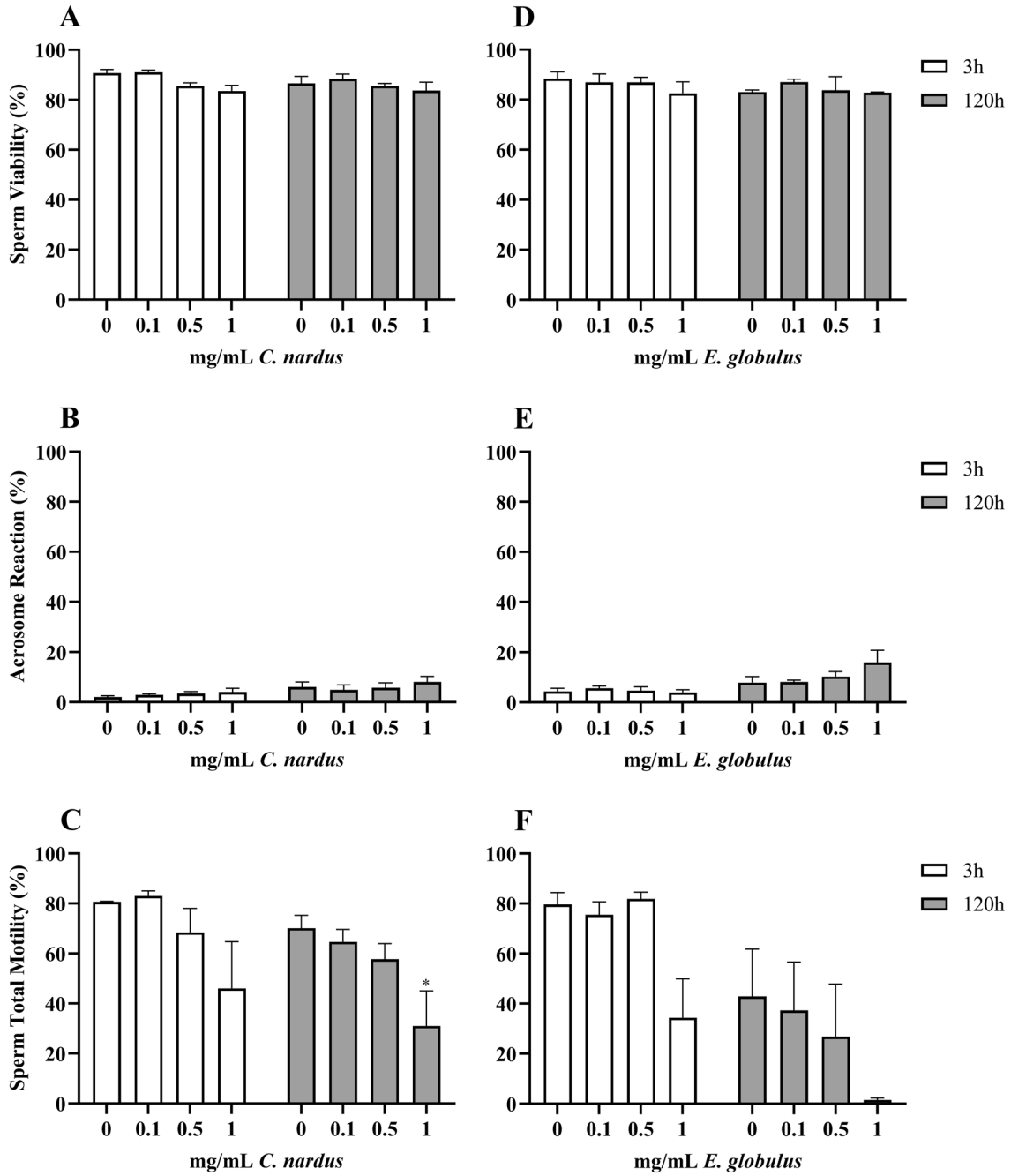

Figure 4. Effects of *C. nardus* (**A**–**C**) and *E. globulus* (**D**–**F**) EOs on sperm viability (**A**), acrosome reaction (**B**) and sperm total motility (**C**). Data are expressed as mean ± standard error of the mean. 0 = control samples (only emulsifiers). * = $p < 0.05$; ** = $p < 0.01$; *** = $p < 0.001$; **** = $p < 0.0001$.

Discussion

The analyses conducted on boar spermatozoa do provide not only necessary preliminary information regarding the potential use of EOs in swine AI seminal doses, but also supply general insights into the different mechanisms of action underlying their biological properties. In particular, the chosen parameters provide data on two key damage mechanisms: membrane disruption (as indicated by viability and percentage of reacted acrosomes) and mitochondrial activity impairment by means of membrane depolarization, potentially leading to the loss of motility[27]. All of the above support the hypothesis that swine spermatozoa, due to their ease of collection and low ethical value, may represent a useful preliminary screening platform for natural substances toxicity. The reason for choosing to evaluate the effects of EOs at two different timepoints (3 and 120 h) is to simulate the usual short- and long-term storage conditions of swine ejaculates at the standard temperature of 16 ± 1 °C. The assessments conducted after 3 h of incubation should provide information regarding the immediate, direct effects of EOs on spermatozoa, while the ones after 120 h should also provide insights regarding the lasting capabilities

of the EOs themselves and their interaction with the given environment. As for the tested concentrations, the 3 chosen one should represent a high one, potentially clearly showing detrimental effects, a low one, still regarded as potentially active against contaminants according to literature but as low as possible, and a middle one.

Overall, it is possible to identify a trend of concentration related effects, that is in according to what was already reported for previous studies EOs such as *R. officinalis* and *T. capitata*[26], and *M. Alternifolia*[13]. However, no evidence of damage was highlighted for all the tested compounds when using the lowest concentration of 0.1 mg/mL, both looking at membranes' alterations and motility. This consideration is important because the literature shows different works proving that some of the EOs analysed in this study already have antibacterial and antifungal effects at very low concentrations, below those considered able to alter morpho-functional sperm parameters.

It can be stated that the first group of EOs (*S. montana*, *P. graveolens* and *L. angustifolia)* exhibits similarities in very strong impairment of sperm quality starting from the concentrations of 0.5 mg/mL. Additionally, it seems that the storage period does not significantly influence viability, whereas in other cases, it appears to have significant effects. The EO obtained from *S. montana* has proven antibacterial activity at a concentration lower than that considered toxic for boar spermatozoa. In particular, as reported by literature, *S. montana* EO reports a MIC (minimum inhibitory concentration) value of 0.39 mg/mL towards *Staphylococcus aureus*[28], where MIC is the lowest concentration required by antimicrobials to clearly inhibit the growth of a bacterium after overnight incubation[29], and MICs far < 0.5 mg/mL also against *Pseudomonas aeruginosa, Streptococcus pyogenes, Streptococcus mutans, Streptococcus sanguis, Streptococcus salivarius, Enterococcus faecalis, Lactobacillus acidophilus*[30]. All of bacteria mentioned above have been isolated from neat boar ejaculates[9]. Therefore, out of the tested EOs, *S. montana* would be a very good candidate for continuing investigating its potential use for swine AI doses.

The second group consisted of *L. hybrida* and *C. limon* EOs. *Lavandula hybrida* is also known as *Lavandula x intermedia*, and is a sterile hybrid of true lavender (*L. angustifolia*) and spike lavender (*L. latifolia*)[31]. Comparative studies between *L. x intermedia* and *L. angustifolia* are available: the former possesses similar or stronger antibacterial and antifungal effects than true lavender oil, in particular against Candida spp. The analysis of antimicrobial activity against oral pathogenic bacteria showed that lavandin oil has MIC values ranging from 0.002 to 0.512 mg/mL[32]. Moreover, *L. hybrida* yields more EOs per kg than *L. Angustifolia*, making it also a cheaper alternative to the true lavender oil[31]. *L. hybrida* and *C. limon* EOs were shown together because of the evident common pattern of alteration. Specifically, viability was only influenced by the highest concentration tested (1 mg/mL), without being affected by storage time. On the other hand, the number of reacted acrosomes significantly increased not only due to 1 mg/mL of both EOs, but the storage period played a decisive role in triggering the capacitation process. Different considerations should be made for motility since, in the case of *L. hybrida*, time did not seem to have any effect, while did for *C. Limon* EO. Overall, this was the only parameter statistically influenced already at the middle concentration (0.5 mg/mL) in this second group, although only after 120 h in both cases. When comparing these findings with the available literature, it shows that *L. hybrida* EO has antifungal activity at very low concentrations and that *C. limon* EO can successfully inhibit the development of *L. monocytogenes* in minced beef meat already at 0.06–0.312 mg/g[33].

The EOs reported in the third group (*M. piperita, M. leucadendron* and *GL mix*) only show morpho-functional impairment upon treatment with the highest concentration of 1 mg/mL. In particular, for *M. piperita* EO, the concentrations of 0.1 and 0.5 mg/mL seem to be very well tolerated, with time storage being relevant only for acrosomal reactions and total motility. This EO has been tested against *S. aureus*, *S. pyogenes* and *S. mutans*, with outcoming MICs of approximately 0.6 mg/mL[34]. Such values are promising, since they are close to the well tolerated concentration of 0.5 mg/mL, but further studies increasing the tested concentration > 0.5 < 1 mg/mL would allow for more accurate applications. Again, *Melaleuca Leucadendron* EO and *GL mix* were only capable of altering spermatozoa upon treatment with 1 mg/mL, but with less intense damages when assessed against *M. piperita*. Not a lot of literature is available for *M. leucadendron*, while *GL mix* is a patent-pending mixture of different EOs, therefore to better understand their potential, further studies are needed.

Proceeding towards the last two tested EOs, it is clear that the pattern of toxicity becomes less and less relevant. *C. nardus* EO seems to be very well tolerated at all tested concentrations, despite a mild reduction in total motility, but only after 120 h of incubation. The hypothesis, in this case, is that such effect at 1 mg/mL may be mediated by a mild interaction with mitochondrial function leading to disruption of cellular energy metabolism thus reduced energy production and cellular dysfunction. As for *E. globulus* EO, the post-hoc tests have highlighted no differences between treated samples and control ones. In this case, the increase of acrosomal reactions and the loss of motility detected is only accounted by the storage time. It still has to be acknowledged that the lack of statistical significance for motility at 120 h upon treatment with 1 mg/mL, potentially due to the statistical approach used and the sample size, does not imply a lack of biological relevance since, indeed, motility is almost completely suppressed. Nonetheless, literature shows a good amount of work that proves antibacterial activity of this EO, both alone and in combination with other agents, even against strains of *methicillin-resistant Staphylococcus aureus* (MRSA) bacteria, with MIC values ranging from 0.032 to 10 mg/mL[35].

To discuss the overall results of the present work, it is important to state that the exact composition of the different EOs changes not only from plant to plant, but also within the same plant during the different phases of its growth cycle. This is why, when investigating and reporting data for EOs, assessing and taking into account their exact composition is pivotal. The complete chemo-characterization of the test compounds is reported in the Supplementary Material (Tables S1–S10). As reported by the tables, our EOs are rich in terpenes (also known as terpenoids or isoprenoids), the largest group of natural compounds, with approximately 25,000 structures reported[36]. Terpenes can have a variety of biological activities, such as antibacterial, antifungal, anti-inflammatory, antioxidant properties. These potential properties of terpenes are currently the subject of numerous scientific studies[37–40], but only a limited amount of these consider the possible use in preserving the quality of semen during storage, thanks to their antimicrobial and antioxidant properties. Nonetheless, a recent work

has shone a light on the role of carvacrol as a mitigating agent for the reduction of boar semen quality during storage under cooling conditions: its ability to decrease the production of oxygen reactive species and regulate mitochondrial activity in porcine sperm makes it a promising antioxidant[41]. Carvacrol is a terpene belonging to the class of monoterpenes, formed by coupling two units of isoprene (C10) and is a component found in various plants. As all terpenes, carvacrol also shows concentration-dependent activity, with higher concentrations leading to harmful effects. Amongst the EOs used in this work, *S. montana* showed the highest carvacrol content (52.56%, Table S1), and was indeed one of the test compounds that induced the strongest alterations on morpho-functional parameters, supporting the predominant biological activity of carvacrol itself. Upon literature search, it seems understandable why this particular EO also shows the lowest MICs for different bacterial populations. However, it is important to note that EOs are complex mixtures made up of many molecules, potentially with both synergic and antagonist effects between each other, thus their proprieties strongly depend on their combination with other compounds, as reported by Bakkali and colleagues[42]. This peculiarity was demonstrated by Elmi and colleagues[13], with a comparative study between tea tree oil (*Melaleuca alternifolia* EO) and its principal component, terpinen-4-ol, on the morpho-functional parameters of swine spermatozoa. The results showed how, despite terpinen-4-ol accounted for > 40% of the used *M. alternifolia* EO, the toxicity patterns were very different and to be ascribable to some synergistic interaction between other constituent compounds. In view of above, since the concept of synergy seems to be extremely relevant, it is not possible to translate results obtained by the use of isolated constituents to the whole mixture within the given EO. Unfortunately, despite all the good potential capabilities, such differences and the need for specific studies and tests on each single batch of EO, represent the main pitfall of their applications.

As for the comparison of the MICs of the different tested EOs against the most common bacteria found in porcine ejaculates, the discussion can be challenging as, according to different studies, the populations of contaminating bacteria are extremely different and various. In addition, each and every batch of EOs will provide different results. Dedicated studies would help shining a light on this matter yet, based on the results hereby presented, it looks like the EO derived from *S. montana* is the most characterized in terms of specific antibacterial capabilities and is active against the majority of the most common bacterial population found in boar ejaculates.

In conclusion, the results of the present study provide a comprehensive overview of the potential mechanisms of action of some of the most common EOs, especially concerning their interaction with porcine male gametes. The most promising ones will now have to undergo testing, as already done for other EOs such as *T. capitata* and *R. officinalis*[25], for their antimicrobial capabilities directly in swine artificial insemination doses. Regardless of the direct aim of the study being swine reproduction, results may be exploited in other fields of research within both veterinary and human medicine.

Materials and methods

Natural substances and reagents

Nine pure EOs and one undisclosed blend provided by APA-CT (Forlì, Italy) were used for the present study, in particular: *Satureja montana, Pelargonium graveolens, Cymbopogon nardus, Melaleuca leucadendron, Eucaliptus globulus, Citrus limon, Lavandula angustifolia, Lavandula hybrida* and *Mentha piperita* EOs, and *GL mix*. The *GL mix* is a patent-pending solution of nine EOs: *Eucaliptus globulus, Satureja hortensis, Citrus aurantium var. dulcis, Thymus vulgaris, Melaleuca alternifolia, Citrus limon, Lavandula hybrida, Melaleuca leucadendron and Thymus capitatus*, dispersed in Glyceryl polyethyleneglycol ricinoleate[27]. The natural substances were kept at 4 °C, in darkened glass bottles to avoid alterations. One aliquot of each substance was used for the chemo-characterization, while, for the in vitro experiments, they were added with 0.5% dimethylglyoxime (DMSO) and Tween 80 (0.002%) to grant uniform emulsification[43].

Chemo-characterization of EOs

The chemo-characterization of EOs was performed according to previously published protocols[25], upon Gas Chromatography-Mass Detector (GC–MS) analysis and Gas Chromatography-Flame Ionization Detector (GC-FID). Qualitative analysis was performed using an Agilent Technologies HP-5 MS cross-linked poly-5% diphenyl–95% dimethyl polysiloxane (30 m × 0.25 mm i.d., 0.25 µm film thickness) capillary column on a 7890A gas chromatograph coupled with a 5975C network mass spectrometer. The semi-quantitative characterization of EOs was carried out on a HP-5 cross-linked poly-5% diphenyl–95% dimethyl polysiloxane (30 m × 0.32 mm i.d., 0.25 µm film thickness) capillary column on a 7890A gas chromatograph with a flame ionization detector (Agilent Technologies, Waldbronn, DE). Compounds were identified by comparing the retention times of the chromatographic peaks with those of authentic reference standards run under the same conditions, the fragmentation spectra, and the linear retention indices (LRIs) relative to C_8–C_{40} n-alkanes obtained on the HP-5 column under the above-mentioned conditions with the literature reference[44].

Porcine spermatozoa collection and evaluations

To estimate cytotoxicity on porcine spermatozoa, the EOs, and *GL mix* were evaluated as formerly reported in other works[13,27].

Three adult boars (Large White × Duroc), 1–2 years old, with a weight ranging from 220 to 250 kg were enrolled for this experimental protocol as ejaculate donors, housed in single pens as dictated by the National law (D.lgs n.122/2011). Semen was collected twice a week by an experienced operator using the hand-gloved technique in a pre-heated (37 °C) thermos, as previously described [13].

Semen collection is considered as a zootechnical routine practice, and does not classify as procedure according to the Lgs. Decree 26/2014. Therefore, no ethical approval was needed for the present study.

After the collection, the sperm-rich fraction (SFR) of each ejaculate was immediately diluted 1:1 (v/v) with an in-house prepared swine fertilization medium (SFM) without any antibiotic[13,45]. The experimental doses were prepared by suspending a fixed number of spermatozoa (15×10^7 spz) in 5 mL of SFM (final concentration = 3×10^7 spz/mL) with 3 different concentrations (1, 0.5 and 0.1 mg/mL) of EOs previously added with emulsifiers as described above. For each experiment, control samples were realized by only adding the emulsifiers. After preparation, the experimental doses were stored for 120 h in a refrigerated bath (AD28R-30, VWR International S.r.l., Milano, IT), set at 16 °C (± 1 °C) and sampled at 3 and 120 h[26,27].

Each test compound was tested on three different ejaculates by each boar for key morpho-functional parameters following previously published protocols.

Viability (V) was assessed by eosin-nigrosin staining. Briefly, 10 µL of the staining solution were mixed with 10 µL of each dose, and 8 µL were immediately smeared on a glass slide. The percentage of live cells (undyed spermatozoa/all spermatozoa) was calculated on a minimum of 200 cells[26], upon microscopy evaluation (Eclipse E600, 40×, Nikon, Tokyo, JP).

The percentage of reacted acrosomes (AR) was assessed using modified Coomassie Blue staining: spermatozoa were fixed using 4% formaldehyde, washed, and suspended in ammonium acetate before being smeared onto a microscope slide and incubated with Coomassie Blue G250 staining solution (0.22%). The percentage of reacted acrosomes (undyed acrosomes/all acrosomes) was calculated from a minimum of 200 cells, upon microscopy evaluation[26]. All slides (both V and AR) were coded and analyzed by a blinded operator to avoid biases.

Total motility (TotM) was analysed by computer-assisted sperm analysis (CASA; Hamilton Thorne CEROS II; Animal Motility II, Software Version 1.9, Beverly, MA, USA), using heated dedicated slides (Leja 4 chamber slides, Leja, IMV technologies, L'Aigle, FR).

As inclusion criteria, only SRFs with V > 85% and TotM > 80% were used for the experimental protocol[27].

Statistical analysis

The statistical analyses were performed using the software GraphPad Prism v.8 (GraphPad Software Inc., San Diego, CA, USA). In order to analyze the results of each parameter and each test compound, 2way-ANOVAs were performed setting treatment, time storage and their interaction as factors. Post-hoc analyses were performed by means of Dunnett's tests, to assess differences between the control samples and the ones treated with different concentrations of test compounds. Significance was set at $p < 0.05$.

Data availability

The data of this manuscript are available from the corresponding author upon reasonable request.

Received: 26 October 2023; Accepted: 29 December 2023
Published online: 02 January 2024

References

1. Murray, C. J. *et al.* Global burden of bacterial antimicrobial resistance in 2019: a systematic analysis. *The Lancet* **399**, 629–655 (2022).
2. Tacconelli, E. Global priority list of antibiotic-resistant bacteria to guide research, discovery, and development new antibiotics.
3. Communication-from-the-commission-to-the-european-parliament-and-the-council. doi:https://doi.org/10.1163/2210-7975_HRD-4679-0058.
4. Gazzetta ufficiale L 353/2021. https://eur-lex.europa.eu/legal-content/IT/TXT/HTML/?uri=OJ:L:2021:353:FULL&from=IT.
5. Barton, M. D. Impact of antibiotic use in the swine industry. *Curr. Opin. Microbiol.* **19**, 9–15 (2014).
6. Diana, A. *et al.* Removing prophylactic antibiotics from pig feed: How does it affect their performance and health?. *BMC Vet. Res.* **15**, 67 (2019).
7. Schulze, M., Nitsche-Melkus, E., Hensel, B., Jung, M. & Jakop, U. Antibiotics and their alternatives in Artificial Breeding in livestock. *Anim. Reprod. Sci.* **220**, 106284 (2020).
8. Schulze, M., Nitsche-Melkus, E., Jakop, U., Jung, M. & Waberski, D. New trends in production management in European pig AI centers. *Theriogenology* **137**, 88–92 (2019).
9. Althouse, G. C. & Lu, K. G. Bacteriospermia in extended porcine semen. *Theriogenology* **63**, 573–584 (2005).
10. Ubeda, J. L. *et al.* Adverse effects of members of the Enterobacteriaceae family on boar sperm quality. *Theriogenology* **80**, 565–570 (2013).
11. Gaczarzewicz, D., Udala, J., Piasecka, M., Blaszczyk, B. & Stankiewicz, T. Bacterial contamination of boar semen and its relationship to sperm quality preserved in commercial extender containing gentamicin sulfate. *Pol. J. Vet. Sci.* **19**, 451–459 (2016).
12. Contreras, M. J. *et al.* Bacteria and boar semen storage: Progress and challenges. *Antibiotics* **11**, 1796 (2022).
13. Elmi, A. *et al.* In vitro effects of tea tree oil (*Melaleuca alternifolia* essential oil) and its principal component terpinen-4-ol on swine spermatozoa. *Molecules* **24**, 1071 (2019).
14. Johnson, L. A., Weitze, K. F., Fiser, P. & Maxwell, W. M. C. Storage of boar semen. *Anim. Reprod. Sci.* **62**, 143–172 (2000).
15. Nitsche-Melkus, E., Bortfeldt, R., Jung, M. & Schulze, M. Impact of hygiene on bacterial contamination in extended boar semen: An 8-years retrospective study of 28 European AI centers. *Theriogenology* **146**, 133–139 (2020).
16. Schulze, M., Dathe, M., Waberski, D. & Müller, K. Liquid storage of boar semen: Current and future perspectives on the use of cationic antimicrobial peptides to replace antibiotics in semen extenders. *Theriogenology* **85**, 39–46 (2016).
17. Barone, F., Ventrella, D., Zannoni, A., Forni, M. & Bacci, M. Can microfiltered seminal plasma preserve the morphofunctional characteristics of porcine spermatozoa in the absence of antibiotics?. *A Preliminary Study. Reprod. Domest. Anim.* **51**, 604–610 (2016).
18. Morrell, J. M. *et al.* Removal of bacteria from boar semen using a low-density colloid. *Theriogenology* **126**, 272–278 (2019).
19. Lacalle, E. *et al.* Single layer centrifugation (SLC) for bacterial removal with Porcicoll positively modifies chromatin structure in boar spermatozoa. *Theriogenology* **201**, 95–105 (2023).
20. Shaoyong, W. *et al.* Evaluation of ε-polylysine as antimicrobial alternative for liquid-stored boar semen. *Theriogenology* **130**, 146–156 (2019).
21. Hoffmann, K. H. Essential oils. *Z. Naturforschung C* **75**, 177–177 (2020).
22. Stratakos, A. C. & Koidis, A. Methods for extracting essential oils. In *Essential Oils in Food Preservation* 31–38 (Flavor and Safety Elsevier, 2016).

23. Kant, R. & Kumar, A. Review on essential oil extraction from aromatic and medicinal plants: Techniques, performance and economic analysis. *Sustain. Chem. Pharm.* **30**, 100829 (2022).
24. Tariq, S. *et al.* A comprehensive review of the antibacterial, antifungal and antiviral potential of essential oils and their chemical constituents against drug-resistant microbial pathogens. *Microb. Pathog.* **134**, 103580 (2019).
25. Elmi, A. *et al.* Antimicrobial capabilities of non-spermicidal concentrations of tea tree (*Melaleuca alternifolia*) and rosemary (*Rosmarinus officinalis*) essential oils on the liquid phase of refrigerated swine seminal doses. *Res. Vet. Sci.* **127**, 76–81 (2019).
26. Elmi, A. *et al. Thymbra capitata* L. Cav. and *Rosmarinus officinalis* L. essential oils: In vitro effects and toxicity on swine spermatozoa. *Molecules* **22**, 21 (2017).
27. Mariotti, M. *et al.* Potential applications of essential oils for environmental sanitization and antimicrobial treatment of intensive livestock infections. *Microorganisms* **10**, 822 (2022).
28. Vitanza, L. *et al. Satureja montana* L. essential oil and its antimicrobial activity alone or in combination with gentamicin. *Microb. Pathog.* **126**, 323–331 (2019).
29. Andrews, J. M. Determination of minimum inhibitory concentrations. *J. Antimicrob. Chemother.* **48**, 5–16 (2001).
30. Chouhan, S., Sharma, K. & Guleria, S. Antimicrobial activity of some essential oils—Present status and future perspectives. *Medicines* **4**, 58 (2017).
31. Pokajewicz, K., Czarniecka-Wiera, M., Krajewska, A., Maciejczyk, E. & Wieczorek, P. P. Lavandula × intermedia—A Bastard lavender or a plant of many values? Part I. Biology and chemical composition of lavandin. *Molecules* **28**, 2943 (2023).
32. Pokajewicz, K., Czarniecka-Wiera, M., Krajewska, A., Maciejczyk, E. & Wieczorek, P. P. Lavandula × intermedia—A bastard lavender or a plant of many values? Part II. Biological activities and applications of lavandin. *Molecules* **28**, 2986 (2023).
33. Ben Hsouna, A., Ben Halima, N., Smaoui, S. & Hamdi, N. Citrus lemon essential oil: Chemical composition, antioxidant and antimicrobial activities with its preservative effect against Listeria monocytogenes inoculated in minced beef meat. *Lipids Health Dis.* **16**, 146 (2017).
34. Nikolić, M. *et al.* Chemical composition, antimicrobial, and cytotoxic properties of five Lamiaceae essential oils. *Ind. Crops Prod.* **61**, 225–232 (2014).
35. Elangovan, S. & Mudgil, P. Antibacterial properties of *Eucalyptus globulus* essential oil against MRSA: A systematic review. *Antibiotics* **12**, 474 (2023).
36. Gershenzon, J. & Dudareva, N. The function of terpene natural products in the natural world. *Nat. Chem. Biol.* **3**, 408–414 (2007).
37. Lei, Y., Fu, P., Jun, X. & Cheng, P. Pharmacological properties of geraniol – A review. *Planta Med.* **85**, 48–55 (2019).
38. Ahmad, N. *et al.* Antimicrobial efficacy of *Mentha piperata*-derived biogenic zinc oxide nanoparticles against UTI-resistant pathogens. *Sci. Rep.* **13**, 14972 (2023).
39. Cai, Z.-M. *et al.* 1,8-Cineole: A review of source, biological activities, and application. *J. Asian Nat. Prod. Res.* **23**, 938–954 (2021).
40. Karpiński, T. M. Essential oils of Lamiaceae family plants as antifungals. *Biomolecules* **10**, 103 (2020).
41. Restrepo, G., Zapata, K., Colorado, P. & Rojano, B. Cooling of porcine semen in an extender supplemented with carvacrol. *Reprod. Domest. Anim.* **58**, 860–866 (2023).
42. Bakkali, F., Averbeck, S., Averbeck, D. & Idaomar, M. Biological effects of essential oils – A review. *Food Chem. Toxicol.* **46**, 446–475 (2008).
43. Bag, A. & Chattopadhyay, R. R. Evaluation of synergistic antibacterial and antioxidant efficacy of essential oils of spices and herbs in combination. *PloS One* **10**, e0131321 (2015).
44. Adams, R. P. *Identification of Essential Oil Components by Gas Chromatography/Mass Spectrometry* (Allured Pub Corp, 2007).
45. Fantinati, P. *et al.* Evaluation of swine fertilisation medium (SFM) efficiency in preserving spermatozoa quality during long-term storage in comparison to four commercial swine extenders. *Animal* **3**, 269–274 (2009).

Acknowledgements

APA-CT kindly provided the test compounds but played no role in designing the study nor in results interpretation and discussion.

Author contributions

M.L.B., M.S. and A.E. conceptualized the work. E.T. and S.B. chemo-characterized the test compounds. M.B., A.E. and D.V. performed the in vitro tests. I.T. and D.V. performed the formal data anlyses. M.D.V. and P.M. supported data interpretation. M.L.B., A.E. and M.S. provided senior support to the study and supported funding. I.T. wrote the manuscript. All authors reviewed the manuscript.

Competing interests

The authors declare no competing interests.

Additional information

Supplementary Information The online version contains supplementary material available at https://doi.org/10.1038/s41598-023-51030-2.

Correspondence and requests for materials should be addressed to D.V.

SUPPLEMENTARY MATERIAL

Short- and long-term effects of Essential Oils on swine spermatozoa during liquid phase refrigeration

Ilaria Troisio, Martina Bertocchi, Domenico Ventrella, Maurizio Scozzoli, Maura Di Vito, Eleonora Truzzi, Stefania Benvenuti, Paola Mattarelli, Maria Laura Bacci, Alberto Elmi.

Table S1. Composition of the essential oil of *Satureja montana*.

Compound	Lit. LRI	Exp. LRI	Area %
carvacrol	1301	1305	52.56
p-cymene	1024	1029	13.79
thymol	1295	1298	6.66
γ-terpinene	1060	1061	5.33
neral	1245	1252	3.85
β-caryophyllene	1420	1424	3.11
borneol	1066	1168	2.19
myrcene	989	993	1.24
α-pinene	936	934	1.15
linalool	1099	1102	0.8
α-terpinene	1017	1017	0.75
octen-3-ol	981	980	0.74
α-thujene	928	927	0.71
limonene	1029	1030	0.68
camphene	950	948	0.65
β-bisabolone	1508	1513	0.65
terpinen-4-ol	1177	1179	0.49
camphor	1143	1147	0.41
geranial	1278	1275	0.29
cis-β-ocimene	1038	1039	0.24
caryophyllene oxide	1589	1594	0.24
trans-β-ocimene	1051	1049	0.22
trans-sabinene hydrate	1064	1067	0.2
α-terpineol	1190	1192	0.16
terpinolene	1090	1089	0.15
α-phellandrene	1004	1005	0.14
β-pinene	975	976	0.11
δ-cadinene	1524	1521	0.1
α-muurolene	1499	1502	0.07
γ-muurolene	1477	1484	0.04
γ-cadinene	1523	1522	0.04
sabinene	973	974	0.01
TOTAL			**97.80**

Experimental retention indices and literature retention indices (HP-5 column) according to NIST 14 (National Institute of Standards and Technology, USA; 14th edition) library database [1], Babushok et al. [2].

Table S2. Composition of the essential oil of *Pelargonium graveolens*.

Compound	Lit. LRI	Exp. LRI	Area %
citronellol	1237	1237	33.77
geraniol	1259	1265	33.38
geranial	1278	1283	3.74
geranyl formate	1300	1307	3.17
isomenthone	1164	1166	2.79
linalool	1099	1102	2.69
γ-eudesmol	1630	1633	2.1
menthone	1154	1155	1.67
δ-cadinene	1524	1520	1.21
cis-rose oxide	1112	1112	0.84
β-caryophyllene	1420	1425	0.79
phenylethyl tiglate	1587	1591	0.68
β-bourbonene	1384	1389	0.67
geranyl butanoate	1562	1563	0.57
germacrene D	1481	1486	0.55
viridiflorene	1496	1501	0.41
trans-rose oxide	1128	1128	0.34
α-copaene	1376	1380	0.33
α-pinene	936	932	0.32
aromadendrene	1440	1446	0.31
neral	1245	1249	0.28
α-cubebene	1351	1358	0.26
geranyl acetate	1386	1387	0.21
α-humulene	1455	1460	0.2
α-terpineol	1190	1191	0.19
p-cymene	1024	1028	0.17
cis-linalool oxide	1072	1072	0.14
myrcene	989	991	0.12
γ-muurolene	1477	1482	0.11
cis-β-ocimene	1038	1038	0.05
α-gurjunene	1409	1412	0.04
β-pinene	975	976	0.03
limonene	1029	1029	0.03
TOTAL			**92.16**

Experimental retention indices and literature retention indices (HP-5 column) according to NIST 14 (National Institute of Standards and Technology, USA; 14th edition) library database [1], Babushok et al. [2].

Table S3. Composition of the essential oil of *Lavandula angustifolia*.

Compound	Lit. LRI	Exp. LRI	Area %
linalool	1099	1103	39.69
linalyl acetate	1263	1266	26.39
cis-β-ocimene	1038	1041	8.51
terpinen-4-ol	1177	1181	3.95
lavandulyl acetate	1290	1295	2.43
β-caryophyllene	1420	1426	2.1
α-terpineol	1190	1193	1.5
α-humulene	1455	1461	1.36
trans-β-ocimene	1051	1049	1.22
α-fenchol	1112	1117	1.13
myrcene	989	992	1.06
geranyl acetate	1386	1387	0.99
borneol	1066	1168	0.86
limonene	1029	1029	0.82
lavandulol	1170	1172	0.76
1,8-cineole	1032	1031	0.65
3-octanone	984	987	0.6
neryl acetate	1368	1369	0.52
caryophyllene oxide	1589	1593	0.29
trans-linalool oxide	1091	1088	0.21
α-pinene	936	933	0.2
camphor	1143	1145	0.2
p-cymene	1024	1024	0.17
γ-terpinene	1060	1059	0.17
α-thujene	928	927	0.13
β-pinene	975	976	0.11
cis-linalool oxide	1072	1073	0.09
p-cymen-8-ol	1186	1185	0.09
α-phellandrene	1004	1005	0.07
camphene	950	947	0.05
sabinene	973	973	0.05
γ-cadinene	1523	1521	0.05
TOTAL			**96.76**

Experimental retention indices and literature retention indices (HP-5 column) according to NIST 14 (National Institute of Standards and Technology, USA; 14th edition) library database [1], Babushok et al. [2].

Table S4. Composition of the essential oil of *Lavandula hybrida.*

Compound	Lit. LRI	Exp. LRI	Area %
linalool	1099	1103	35.16
linalyl acetate	1263	1266	27.97
camphor	1143	1147	6.82
1,8-cineole	1032	1032	4.74
terpinen-4-ol	1177	1181	3.48
borneol	1066	1169	3.03
lavandulyl acetate	1290	1295	2.22
β-caryophyllene	1420	1426	1.72
α-humulene	1455	1462	1.24
myrcene	989	992	0.93
lavandulol	1170	1171	0.87
α-terpineol	1190	1193	0.87
cis-β-ocimene	1038	1039	0.83
p-cymene	1024	1029	0.65
germacrene D	1481	1486	0.55
geranyl acetate	1386	1387	0.54
trans-β-ocimene	1051	1049	0.5
α-pinene	936	933	0.4
β-pinene	975	976	0.39
myrtenal	1196	1195	0.39
trans-linalool oxide	1091	1089	0.34
camphene	950	947	0.28
neryl acetate	1368	1369	0.28
α-fenchol	1112	1116	0.26
octen-3-ol	981	980	0.23
γ-cadinene	1523	1522	0.22
cis-linalool oxide	1072	1073	0.2
trans-α-bergamotene	1444	1441	0.19
δ-cadinene	1524	1530	0.16
α-terpinene	1017	1015	0.14
sabinene	973	973	0.12
caryophyllene oxide	1589	1593	0.12
γ-terpinene	1060	1059	0.11
trans-sabinene hydrate	1064	1067	0.11
α-thujene	928	927	0.08
δ-3-carene	1012	1010	0.07
α-phellandrene	1004	1005	0.04
α-gurjunene	1409	1411	0.03
TOTAL			**96.31**

Experimental retention indices and literature retention indices (HP-5 column) according to NIST 14 (National Institute of Standards and Technology, USA; 14th edition) library database [1], Babushok et al. [2].

Table S5. Composition of the essential oil of *Citrus limon.*

Compound	**Lit. LRI**	**Exp. LRI**	**Area %**
limonene	1029	1035	67.8
β-pinene	975	978	14.82
γ-terpinene	1060	1061	8.61
α-pinene	936	933	2.09
myrcene	989	992	1.53
geranial	1278	1275	1.19
pulegone	1244	1246	0.8
α-thujene	928	926	0.36
terpinolene	1090	1088	0.35
neryl acetate	1368	1368	0.27
α-terpinene	1017	1017	0.25
p-cymene	1024	1026	0.18
α-terpineol	1190	1191	0.14
geranyl acetate	1386	1386	0.14
β-caryophyllene	1420	1425	0.14
trans-β-ocimene	1051	1049	0.13
α-phellandrene	1004	1005	0.08
linalool	1099	1101	0.08
terpinen-4-ol	1177	1178	0.08
camphene	950	947	0.07
citronellol	1237	1233	0.04
menthone	1154	1155	0.03
α-humulene	1455	1460	0.03
α-selinene	1495	1503	0.03
α-muurolene	1499	1506	0.03
TOTAL			**99.27**

Experimental retention indices and literature retention indices (HP-5 column) according to NIST 14 (National Institute of Standards and Technology, USA; 14th edition) library database [1], Babushok et al. [2].

Table S6. Composition of the essential oil of *Mentha piperita.*

Compound	**Lit. LRI**	**Exp. LRI**	**Area %**
menthol	1183	1183	36
menthone	1154	1160	28.07
neomenthol	1166	1169	9.56
1,8-cineole	1032	1032	6.47
menthyl acetate	1295	1298	4.8
β-caryophyllene	1420	1426	2.95
limonene	1029	1029	2.57
β-pinene	975	976	1.42
α-pinene	936	933	0.9
pulegone	1244	1244	0.9
piperitone	1254	1259	0.65
α-terpineol	1190	1194	0.44
sabinene	973	973	0.37
α-humulene	1455	1460	0.32
caryophyllene oxide	1589	1593	0.28
p-cymene	1024	1024	0.18
β-bourbonene	1384	1389	0.18
myrcene	989	992	0.16
viridiflorene	1496	1504	0.14
linalool	1099	1102	0.13
camphene	950	948	0.12
isopulegol	1148	1148	0.12
3-octanol	996	997	0.11
δ-elemene	1337	1341	0.1
α-copaene	1376	1380	0.09
germacrene D	1481	1485	0.08
carvone	1245	1249	0.07
γ-terpinene	1060	1058	0.05
trans-sabinene hydrate	1064	1066	0.05
geranyl formate	1300	1306	0.05
α-terpinyl acetate	1350	1354	0.05
trans-linalool oxide	1091	1088	0.04
trans-pinocarveol	1137	1138	0.04
δ-cadinene	1524	1530	0.04
cis-linalool oxide	1072	1073	0.03
TOTAL			**97.53**

Experimental retention indices and literature retention indices (HP-5 column) according to NIST 14 (National Institute of Standards and Technology, USA; 14th edition) library database [1], Babushok et al. [2].

Table S7. Composition of the essential oil of *Melaleuca leucadendron.*

Compound	**Lit. LRI**	**Exp. LRI**	**Area %**
1,8-cineole	1032	1039	77.3
α-terpineol	1190	1195	5.56
α-pinene	936	934	3.61
terpinen-4-ol	1177	1181	2.93
linalool	1099	1103	1.94
p-cymene	1024	1026	1.28
γ-terpinene	1060	1060	0.96
β-caryophyllene	1420	1426	0.47
borneol	1066	1166	0.45
myrcene	989	993	0.39
β-pinene	975	976	0.36
α-terpinene	1017	1018	0.24
α-phellandrene	1004	1006	0.22
terpinolene	1090	1089	0.15
geranyl formate	1300	1305	0.1
sabinene	973	973	0.06
camphene	950	948	0.03
TOTAL			**96.05**

Experimental retention indices and literature retention indices (HP-5 column) according to NIST 14 (National Institute of Standards and Technology, USA; 14th edition) library database [1], Babushok et al. [2].

Table S8. Composition of the essential oil *GL mix.*

Compound	**Lit. LRI**	**Exp. LRI**	**Area %**
limonene	1029	1031	23.8
carvacrol	1301	1309	14.36
1,8-cineole	1032	1034	9.4
p-cymene	1024	1027	8.14
terpinen-4-ol	1177	1181	6.02
geraniol	1259	1264	5.6
γ-terpinene	1060	1060	5.36
linalool	1099	1103	5.2
menthyl acetate	1295	1297	3.43
β-pinene	975	977	2.67
α-pinene	936	934	2.57
α-terpineol	1190	1193	2.43
α-terpinene	1017	1018	1.96
myrcene	989	993	1.12
β-caryophyllene	1420	1426	1.03
terpinolene	1090	1089	0.75
cis-β-ocimene	1038	1039	0.65
borneol	1066	1167	0.6
sabinene	973	974	0.43
trans-β-ocimene	1051	1049	0.4
camphor	1143	1146	0.35
camphene	950	948	0.29
α-phellandrene	1004	1005	0.29
neral	1245	1250	0.27
geranial	1278	1278	0.17
α-thujene	928	927	0.15
α-fenchol	1112	1115	0.15
thymol	1295	1299	0.13
cis-linalool oxide	1072	1070	0.12
geranyl acetate	1386	1387	0.12
α-humulene	1455	1461	0.12
neryl acetate	1368	1369	0.08
trans-linalool oxide	1091	1086	0.03
TOTAL			**98.19**

Experimental retention indices and literature retention indices (HP-5 column) according to NIST 14 (National Institute of Standards and Technology, USA; 14th edition) library database [1], Babushok et al. [2].

Table S9. Composition of the essential oil of *Cymbopogon nardus.*

Compound	Lit. LRI	Exp. LRI	Area %
citronellal	1157	1161	21.19
camphene	950	949	13.72
limonene	1029	1031	13.11
geraniol	1259	1265	12.05
citronellol	1237	1239	8.59
α-pinene	936	934	5.38
citronellyl acetate	1352	1357	1.65
terpinolene	1090	1088	1.59
linalool	1099	1102	1.46
geranyl acetate	1386	1387	1.43
α-terpinene	1017	1017	1.37
δ-cadinene	1524	1531	1.36
β-elemene	1390	1396	1.35
germacrene D	1481	1485	1.21
α-thujene	928	926	1.13
isopulegol	1156	1146	0.96
p-cymene	1024	1025	0.94
sabinene	973	975	0.68
myrcene	989	992	0.49
γ-cadinene	1523	1521	0.39
α-phellandrene	1004	1004	0.37
α-terpineol	1190	1192	0.33
neral	1245	1247	0.3
borneol	1066	1168	0.19
γ-terpinene	1060	1058	0.18
cubenol	1640	1641	0.18
terpinen-4-ol	1177	1185	0.15
3-octanone	984	987	0.14
β-caryophyllene	1420	1424	0.1
α-humulene	1455	1460	0.09
α-muurolene	1499	1500	0.08
α-fenchol	1112	1113	0.06
lavandulol	1170	1171	0.06
geranial	1278	1280	0.05
α-copaene	1376	1380	0.05
β-pinene	975	974	0.04
trans-β-ocimene	1051	1048	0.04
neryl acetate	1368	1367	0.04
α-selinene	1495	1499	0.04
TOTAL			**98.19**

Experimental retention indices and literature retention indices (HP-5 column) according to NIST 14 (National Institute of Standards and Technology, USA; 14th edition) library database [1], Babushok et al. [2].

Table S10. Composition of the essential oil of *Eucaliptus globulus.*

Compound	**Lit. LRI**	**Exp. LRI**	**Area %**
1,8-cineole	1032	1040	91.44
α-pinene	936	934	2.91
γ-terpinene	1060	1060	2.06
α-phellandrene	1004	1006	0.86
myrcene	989	993	0.68
β-pinene	975	976	0.5
α-terpinene	1017	1018	0.18
terpinen-4-ol	1177	1179	0.05
trans-β-ocimene	1051	1050	0.03
camphene	950	947	0.02
TOTAL			**98.73**

Experimental retention indices and literature retention indices (HP-5 column) according to NIST 14 (National Institute of Standards and Technology, USA; 14th edition) library database [1], Babushok et al. [2].

Figure S1. Graphical overview of the effects of all test compounds on morpho-functional parameters on swine spermatozoa upon short- (3h) and long-term (120h) storage.

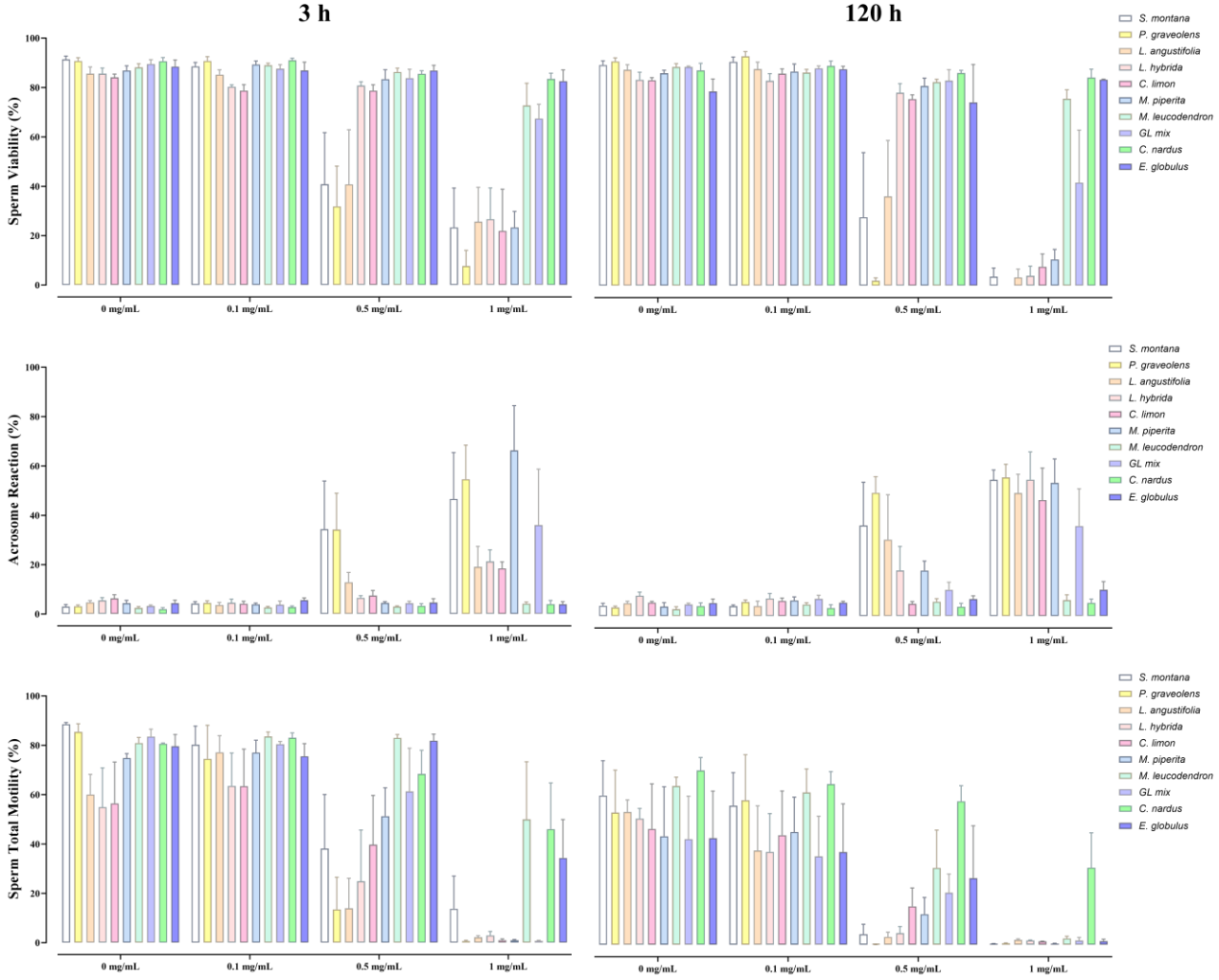

[1] National Institute of Standards and Technology Library Database. Available online: https://webbook.nist.gov/ (accessed on 25 October 2023).

[2] Babushok, V.I.; Zenkevich, I.G. Retention indices for most frequently reported essential oil compounds in GC. Chromatographia 2009, 69, 257–269.

Roe deer as model for photoperiod spermatogenesis regulation

Troisio, I., Ventrella, D., Hausz, B.L., Cesauri, M., Vannetti, N.I., Bacci, M.L., et al. (2026). Molecular Investigations on Angiogenesis and Oxidative Stress in Roe Deer (Capreolus capreolus) Bucks' Testes Throughout the Reproductive Cycle. JOURNAL OF EXPERIMENTAL ZOOLOGY. PART A, ECOLOGICAL AND INTEGRATIVE PHYSIOLOGY, 2026, 1-10. https://doi.org/10.1002/jez.70067

This is an experimental study published on JOURNAL OF EXPERIMENTAL ZOOLOGY. PART A, ECOLOGICAL AND INTEGRATIVE PHYSIOLOGY in January 2026 that deepens two physiological pathways critical for spermatogenesis in this peculiar species which allows processes normally spanning a full reproductive lifespan in other animals to be studied within a single year. This work reveals the role of specific antioxidant proteins in recovery after the reproductive effort and reports for the first time the involvement of *Neuropilin 2 (NRP2),* a protein belonging to angiogenesis pathway that apparently plays a role in the post-rut period.

Journal of Experimental Zoology Part A: Ecological and Integrative Physiology

WILEY

JEZ-A ECOLOGICAL AND INTEGRATIVE PHYSIOLOGY

RESEARCH ARTICLE OPEN ACCESS

Molecular Investigations on Angiogenesis and Oxidative Stress in Roe Deer (*Capreolus capreolus*) Bucks' Testes Throughout the Reproductive Cycle

Ilaria Troisio[1] | Domenico Ventrella[1,2] | Bálint Lóránt Hausz[1] | Mattia Cesauri[3] | Niccolò Ian Vannetti[1] | Maria Laura Bacci[1,2] | Alberto Elmi[3] | Augusta Zannoni[1,2]

[1]Department of Veterinary Medical Sciences, University of Bologna, Bologna, Italy | [2]Health Science and Technologies Interdepartmental Center for Industrial Research (CIRI-SDV), University of Bologna, Bologna, Italy | [3]Department of Veterinary Science, University of Pisa, Pisa, Italy

Correspondence: Domenico Ventrella (domenico.ventrella2@unibo.it)

Received: 22 September 2025 | **Revised:** 8 January 2026 | **Accepted:** 18 January 2026

Funding: RFO, University of Bologna

Keywords: angiogenesis | NRP2 | oxidative stress | Roe deer | SOD3 | spermatogenesis suspension | testicular remodeling

ABSTRACT

Animals with seasonal reproductive cycles, as the Roe deer (Capreolus capreolus), have developed mechanisms to synchronize reproduction with the environmental cycle in order to optimize reproductive success through melatonin. Angiogenesis and oxidative stress are key processes in spermatogenesis, contributing to testicular remodeling and recovery after reproductive effort. This study carried out a gene expression analysis on 18 samples of mature male Roe deer testicles, collected during the local hunting season in pre-rut ($N = 9$) and post-rut ($N = 9$) periods. A quantitative real-time PCR (qPCR) array targeting 84 genes involved in oxidative stress and 84 in angiogenesis were used, followed by validation through individual qPCR of selected genes and related protein quantification by ELISA assays. Post-rut animals showed upregulation of several antioxidant genes: Peroxiredoxin-4 (PRDX4), Scavenger receptors class A member 3 (SCARA3), Superoxide Dismutase 3 (SOD3). Instead, Leptin (LEP) and Thrombospondin II (THBSII), a known angiogenesis inhibitor, are downregulated. A novel insight is represented by the upregulation of Neuropilin (NRP2) in post-rut period that, given to its posttranscriptional silencing too, needs better investigations. The pleiotropic nature of NRP2, including roles in neurodevelopment, immune modulation, and vascular remodeling, makes this gene an interesting candidate for further study, cause its function in reproductive tissues remains poorly understood.

1 | Introduction

The synchronization between reproduction and the environmental cycle has always been a key evolutionary factor for reproductive success in many mammals living in non-equatorial regions (Zerbe et al. 2012). As is well known, in many mammals, reproduction is regulated by the photoperiod (Chemineau et al. 2008), since the light stimulus triggers a hormonal response through melatonin action, responsible for pulsatile secretion of GnRH and gonadotropins (Dardente and Simonneaux 2022). Short-day species (e.g., sheep and goats) reproduce in autumn, while long-day species (e.g., horses) reproduce in spring. In these, we witness a reduction in gonadal activity and a return to anoestrus at the end of the breeding season (Chemineau et al. 2008).

For what specifically concerns the Roe deer (*Capreolus capreolus*), the reproductive season of sexually mature males,

Alberto Elmi and Augusta Zannoni share senior contributions as the last authors.

Summary

- Gene expression in testicular tissue varies between pre-rut and post-rut periods, reflecting physiological adaptations to seasonal reproduction.
- The study combined qPCR arrays and ELISA-based protein validation to provide a robust analysis of oxidative stress and angiogenesis pathways in seasonal spermatogenesis.
- Post-rut upregulation of NRP2, coupled with evidence of translational repression, suggests a complex role worthy of further investigation in reproductive biology.

called bucks, can be easily categorized into three well-distinct periods, during which substantial changes in size and consistency of the reproductive tract occur: pre-rutting (from May to mid-July), rutting period (from mid-July to mid-August), and post-rutting (from mid-August to September) (Klonisch et al. 2006). These seasonal variations can be perceived as adaptations to reduce the energy costs associated with reproduction; indeed, during the winter, bucks show a complete suspension of spermatogenesis. This natural pattern makes the Roe deer an interesting model for studying the seasonal regulation of spermatogenesis under the influence of photoperiod, an area of research already initiated by this research group (Elmi et al. 2021, 2020). Other works already highlighted changes particularly pronounced in size and consistency of reproductive traits during the year, particularly pronounced in testicle size and volume, as could be easily assessed also by an eye evaluation (Goeritz et al. 2003). Moreover, fluctuations in density and volume of the ejaculates with a peak during the rutting period are present (Goeritz et al. 2003). These evidences are also supported by the fluctuation of testosterone, essential for normal spermatogenesis and prevention of apoptotic cell death in androgen-dependent tissues, which presents its highest level in serum and testis between late July and August (the maximum period of meiosis activity in Roe deer) with a sharply decrease and absence during the winter, when there is a complete spermatogenesis suspension (Roelants et al. 2002). Accordingly, it is also proven that LH and FSH gonadotropins, essentials for the activation of Leydig cells' differentiation and Sertoli cells' activation, respectively, show their maximum levels in blood in March with the purpose of maintaining testicular function and preparing the right environment for correct spermatozoa's maturation (Roelants et al. 2002).

It is well acknowledged how the process of angiogenesis, tightly regulated by Vascular Endothelial Growth Factor (VEGF), plays a fundamental role in spermatogenesis by balancing the growth and development of testicular tissue (Caires et al. 2009; Ebisch et al. 2008; Nalbandian et al. 2003). Another role is played by oxidative stress since DNA damage, apoptosis, and epigenetic alterations can be observed in the case of massive activation of reactive oxygen species (ROS) not balanced by antioxidant defense system. The disruption of this fragile balance may undermine the survival of germ cells, activating apoptotic pathways, thereby compromising the entire process of spermatogenesis (Ayad et al. 2022; Takeshima et al. 2020; Aitken and Clarkson 1987). Therefore, the aim of this work was to investigate the differential behavior of these critical pathways in testicular samples collected during the pre-rut and post-rut periods, both at gene expression and protein levels.

2 | Materials and Methods

2.1 | Animals

The samples included in this study were collected from 18 bucks ($N = 18$) during the 2018 hunting season in the Southwestern Bologna Apennines (Italy). Half of them were hunted during the pre-rut period (June 1 to July 15; $n = 9$), while the other half during post-rut period (August 15 to September 30; $n = 9$). To avoid any bias due to possible pathological conditions, animals found dead during the sampling activity were not included in this study. Immediately after their death, carcasses were conferred to local biometric center where scrota, including testicles, were collected from the personnel and, within 2 h, were transferred, at refrigerated temperature (5 ± 1°C), to the laboratories of Department of Veterinary Medical Science of the University of Bologna (Ozzano dell'Emilia, Italy) (Elmi et al. 2021, 2020). Ages were assessed upon teeth eruption and wear patterns evaluations as previously described (Elmi et al. 2020). Since all biological specimens were obtained from hunted animals (in accordance with local legislation), no ethical approval was required.

2.2 | Testicular Tissue Sampling

The detailed methodology for collection and storage of the testicular parenchyma has been previously described (Elmi et al. 2020). Briefly, after the isolation from scrota, testes were weighed and cut in half to collect the middle section of parenchyma, minced, and split into aliquots. For gene expression analyses, aliquots were stored in RNA Stabilization Solution (RNAlater, Thermo Fisher Scientific, Waltham, MA, USA) for 24 h at +4°C and then moved at −80°C after solution removal (for RNA extraction). As for protein assay, aliquots were snap-frozen in liquid nitrogen and immediately stored at −80°C.

2.3 | Homogenization and Extraction of Total RNA and qPCRs Arrays on Pooled Samples

Tissues were firstly homogenized in TRIzolTM Reagent (30 mg/mL) (Molecular Research Center Inc., Cincinnati, OH, USA) and the resulting suspensions were used for total RNA extraction using NucleoSpin RNA (MACHEREY-NAGEL GmbH & Co. KG, Düren, Germany), following the manufacturer's instructions as previously described (Elmi et al. 2020). The RNA quantity was assessed by spectrophotometry measuring the A260/A280 ratio using Nanospectrophotometer (Denovix Inc. Wilmington, DE, USA) followed by a quality evaluation assessment by gel electrophoresis on a 1% agarose gel. After quantification, two different pools (pre-rut and post-rut) were prepared to obtain a final concentration of 250 ng/μL for each of them. The reverse-transcribed total RNA

to cDNA was obtained using RT^2 First Strand Kit (QIAGEN Hilden, Germany).

For each pool, Cow Angiogenesis RT^2 Profiler PCR array (QIAGEN) and Cow Oxidative stress RT^2 Profiler PCR array (QIAGEN) were performed according to the manufacturer's instructions, using 2X RT^2 SYBR Green Mastermix (QIAGEN), and CFX 96 Touch (Bio-Rad Laboratories, Hercules, CA, USA). Each array contained primers for 84 target genes and five housekeeping genes (HKG); seven wells included reverse-transcription controls (RTC), positive PCR controls (PPC), and a genomic DNA contamination control. Gene expression was evaluated using the ΔC_t method (mean reference genes C_t—interest gene C_t), according to the RT2 Profiler PCR Array Handbook.

As a parameter of quantitative gene expression, the threshold cycle (C_t) was used, which is inversely proportional to the amount of template present in the wells. Only genes with C_t values < 35 were reported and evaluated by using the ΔC_t (Δ threshold cycle) method, calculated as ($\Delta C_t = C_t$ mean reference genes–C_t gene of interest). Gene expression was assessed using the fold-change method ($2^{\Delta\Delta C_t}$), where $\Delta\Delta C_t = \Delta C_t$ post-rut–ΔC_t pre-rut, quantifying expression variations between the two groups (post vs. pre).

2.4 | qPCR for the Quantification of Selected Genes on Single Animals

To validate the results obtained from the array performed on the pools, a single qPCR reaction ($N = 18$) was performed for the genes whose expression changes at least three times (up or down, post vs. pre) by using specific primers (QIAGEN). All samples were loaded in duplicate, and qPCRs were performed following the same procedure as before for each HKG and gene of interest. The results are also reported in this case using the fold-change method ($2^{\Delta\Delta C}$t) normalized on the arithmetic mean of the three reference genes (ACTB, B2M, YWHAZ). Primer for reference genes were purchased from QIAGEN (RT2 qPCR Primer Assay for Beta-Actin -ACTB; Beta-2-Microglobulin -B2M; -and tyrosine 3-monooxygenase/tryptophan 5-monooxygenase activation protein zeta -YWHAZ-, Cat. No.; PPB00173A; PPS00031A, PPB01343A, respectively).

The genes of interest of individual analysis were 24-Dehydrocholesterol reductase (DHCR24), Peroxiredoxin-4 (PRDX4), Superoxide Dismutase 3 (SOD3), scavenger receptors class A member 3 (SCARA3) belonging to oxidative stress array, and Coagulation Factor II (F2), Leptin (LEP), Thrombospondin II (THBSII), Neuropilin 2 (NRP2) belonging to angiogenesis array. Primers for genes of interest were purchased from QIAGEN (Hilden, Germany). RT2 qPCR Primer Assay: DHCR24 (Cat. No. PPB09699A); PRDX24 (Cat. No. PPB00807A); SOD3 (Cat. No. PPB09315A); SCARA3 (Cat. No. PPB12336A); F2 (Cat. No. PPB00005A-200); LEP (Cat. No. PPB00093A); THBSII (Cat. No. PPB01550A); NRP2 (Cat. No. PPB12260A-200).

In addition to Roe deer samples, RNA extraction and qPCR were also performed, when needed, on a bovine testis as a positive control. The specificity of the amplified PCR products was confirmed by agarose gel electrophoresis and melting curve analysis.

2.5 | Enzyme-Linked Immunosorbent Assay (ELISA)

According to the qPCR results, we performed the quantification of SOD 3, DHCR24, NRP2, and LEP proteins in testicular tissue using commercially available ELISA Kits (SOD3: MBS062357-96; DHCR24: MBS9349018; NRP2: MBS2802336; LEP: MBS743525 from MyBiosource Inc., San Diego, USA) following the manufacturer's instructions. Tissues were homogenized in phosphate-buffered saline (PBS) according to the dilution ratios suggested by the manufacturer: 1:10 for NRP2, DHCR24, and SOD3, 4:5 for leptin. Absorbance was measured at 450 nm using a Tecan Infinite F50 plate reader equipped with Magellan software (Tecan Group Ltd., Männedorf, Switzerland), and concentrations were calculated based on standard curve readings. All samples were run in duplicates.

2.6 | Statistical Analysis

Descriptive statistics were calculated and reported as means. Data were assessed for normality of distribution using the Shapiro–Wilk test and further analyzed by means of a parametric or nonparametric test accordingly. Welch's *t*-test was used to assess the statistical significance of gene expression differences between the pre-rut and post-rut animal groups. Data from ELISAs were analyzed using an unpaired *t*-test to determine statistically significant differences between the two experimental groups. To evaluate relationships between gene expression and its corresponding protein content, a nonparametric Spearman's rank correlation test was performed. Statistical evaluations and graphic representations were obtained using GraphPad Prism v.8 (GraphPad Software Inc., San Diego, CA, USA). Significance was set for $p < 0.05$.

3 | Results

3.1 | Results of qPCR Arrays on Pooled Samples, Quality Control, and Normalization of Data

Following the qPCR protocol, to confirm that the amplification of the samples occurred specifically, the next step was the evaluation of melting curves, assessing the Tm of the amplified product and the C_t of each gene to evaluate the stability and specificity of the amplification. All the C_t recorded are reported in Supporting Information S1: Table S1 (oxidative stress) and Supporting Information S1: Table S2 (angiogenesis). Among the 84 genes analyzed, 54 genes related to the oxidative stress pathway and 56 genes related to the angiogenesis pathway were detectable, with C_t values below 35 in both groups. Following the kit's instructions, all genes with C_t values greater than 35 were excluded from further analysis, as this threshold is near the limit of detection. A few other genes were found to be non-detectable (N/A) and were not included in the final total number of genes represented in heat maps.

ΔCT values were used to compare reverse RTC and PPC for both pathways of this study. ΔCT values obtained (< 5) suggest no impurities in samples that could have interfered with reverse transcription. CT^{PPC} values fall within the correct range of

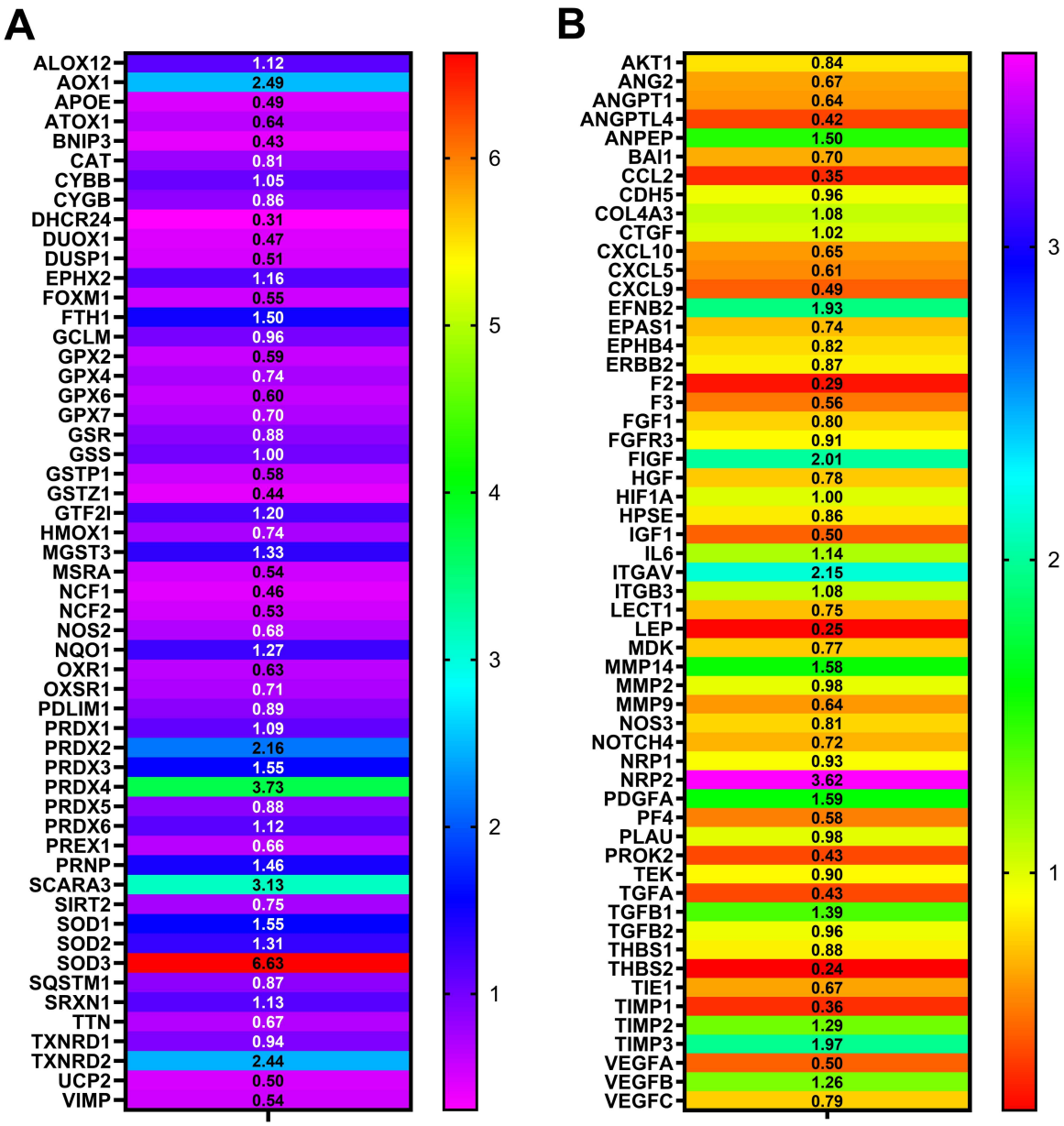

FIGURE 1 | $2^{\Delta\Delta C}$t post-rut versus pre-rut: $2^{\Delta\Delta C}{}_{t}$ oxidative stress assay (A); $2^{\Delta\Delta C}$t angiogenesis assay (B).

20 ± 2, indicating that PCR conditions could be considered appropriate. The normalization of samples' CT values occurred against HKG.

ΔCT values of pre-rut group and post-rut group (gene < 35 C_t) of each pathway are reported in the Heat maps (Supporting Information S1: Figure 1).

To assess variations among groups, data is presented as $2^{\Delta\Delta C}$T, where ΔΔCT = ΔCT post-rut−ΔCT pre-rut. The fold change > 1 or < 1 values indicate, respectively, an increase or decrease in gene expression in post-rut in relation to the pre-rut (control, value = 1) (Figure 1).

For both pathways, we select genes whose expression varied, in term of $2^{\Delta\Delta C}$T value at least ±3 times. Figure 1A shows how the genes of the oxidative stress assay, whose expression varied by at least three times were 4: 24-Dehydrocholesterol Reductase (DHCR24) downregulated by ~0.30 times and Peroxiredoxin 4 (PRDX4), Scavenger receptor class A member 3 (SCARA3), Superoxide dismutase (SOD3) upregulated, respectively, ~ 3.73; ~ 3.14; and ~ 6.63 times.

For the angiogenesis assay too, four genes varied their expression ±3 times. Three are downregulated: Coagulator factor II (F2) ~0.29; Leptin (LEP) ~0.25; Thrombospondin 2 (THBSII) ~0.24; while only one was upregulated: Neuropilin 2 (NRP2) ~3.62.

3.2 | Results of qPCR for the Quantification of Selected Genes on Single Animals

The results of the single qPCRs conducted on each animal for the genes whose expression varied ±3 times are reported in the following figures, plated according to the specific pathway:

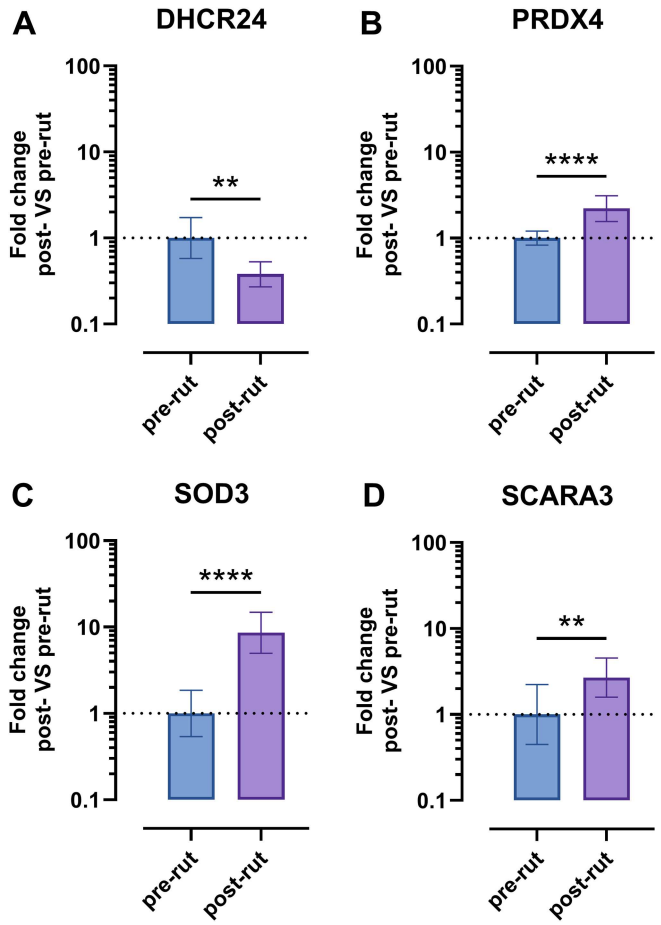

FIGURE 2 | Oxidative stress panel. Data are reported on log10 scales. DHCR24 (A), PRDX4 (B), SOD3 (C), SCARA3 (D); $^{**}p < 0.01$, $^{****}p < 0.0001$.

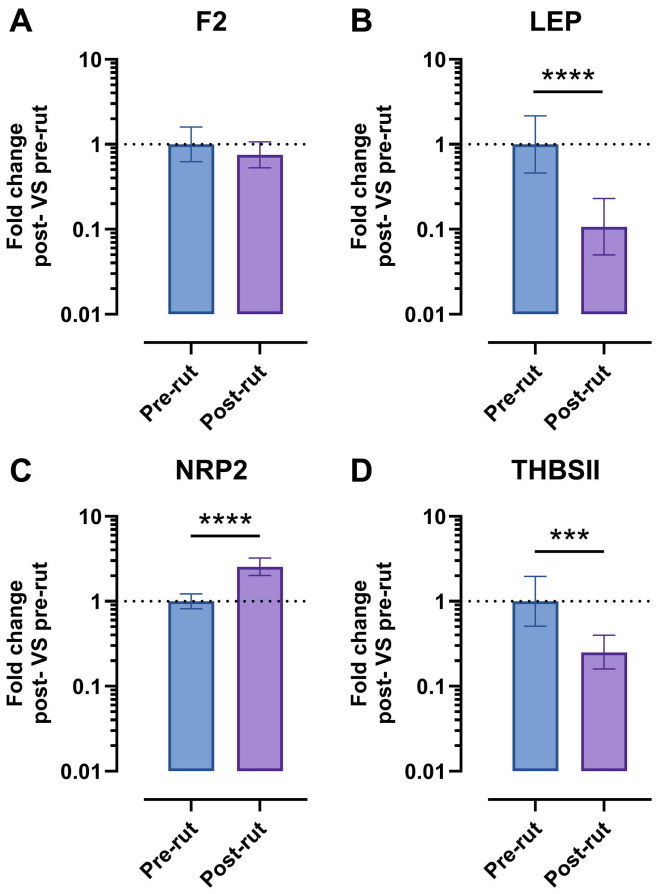

FIGURE 3 | Angiogenesis panel. Data are reported on log10 scales. F2 (A), LEP (B), NRP2 (C), THBSII (D); $^{***}p < 0.001$, $^{****}p < 0.0001$.

Figure 2 (oxidative stress), Figure 3 (angiogenesis). Results are presented as fold of change post-rut single animal versus pre-rut single animal.

The results of the oxidative stress pathway (Figure 2) present statistically significant variations in gene expression among the two groups. Graphs show a decrease in the expression of DHCR24 in the post-rut group ($p = 0.0018$) (Figure 2A). On the other hand, an upregulation of PRDX4 ($p < 0.0001$) (Figure 2B) is clear. At the same time, a sharp increase of about eight times can be noted for SOD3 ($p < 0.0001$) (Figure 2C), while SCARA3 is upregulated about three times ($p = 0.0018$) (Figure 2D).

Figure 3 reports the results of the second pathway analyzed: angiogenesis. A decrease in F2 expression in post-rut group is clear, yet not statistically relevant (Figure 3A). Instead, the decrease in LEP after the rutting period ($p < 0.0001$), as well as THBSII ($p = 0.002$) is statistically verified (Figure 3B,C). The only gene showing an increment in the post-rut is NRP2, with an upregulation of 2.5 times ($p < 0.0001$) (Figure 3D).

3.3 | Results of the ELISAs

The results of protein quantification are shown in Figure 4, presented as box and whiskers plots. Despite following the manufacturer's instructions, all samples assayed for the quantification of DHCR24 were below the sensitivity of the test and were therefore considered unreliable.

Figure 4A shows an increase in SOD3 protein concentration in post-rut animals without relevance from a statistical point of view. Instead, the decrease in NRP2 (Figure 4B) and leptin concentrations (Figure 4C) in the post-rut animals is statistically relevant, with p of 0.0069 and 0.0004, respectively.

3.4 | Correlation Analysis

The results of the nonparametric Spearman's correlation analysis (expressed as ρ) are represented in Figure 5. The table also includes testicular testosterone levels, indicative of the activity of the testes at the moment of sampling, assessed for a previous study of the research team (Elmi et al. 2020).

NRP2 mRNA is positively correlated with SOD3 mRNA (ρ 0.80; $p < 0.0001$) and negatively with leptin mRNA (ρ −0.74; $p < 0.001$). The latter also shows a negative correlation with SOD3 mRNA (ρ −0.94; $p < 0.0001$), which is itself negatively correlated to DHCR24 mRNA (ρ −0.67; $p < 0.01$). Finally, testicular testosterone shows strong positive correlations with DHCR24 mRNA (ρ 0.80; $p < 0.001$) and leptin mRNA expression (ρ 0.76; $p < 0.001$), and negative ones with SOD3 mRNA (ρ −0.70; $p < 0.01$) and NRP2 mRNA (ρ −0.60; $p < 0.01$).

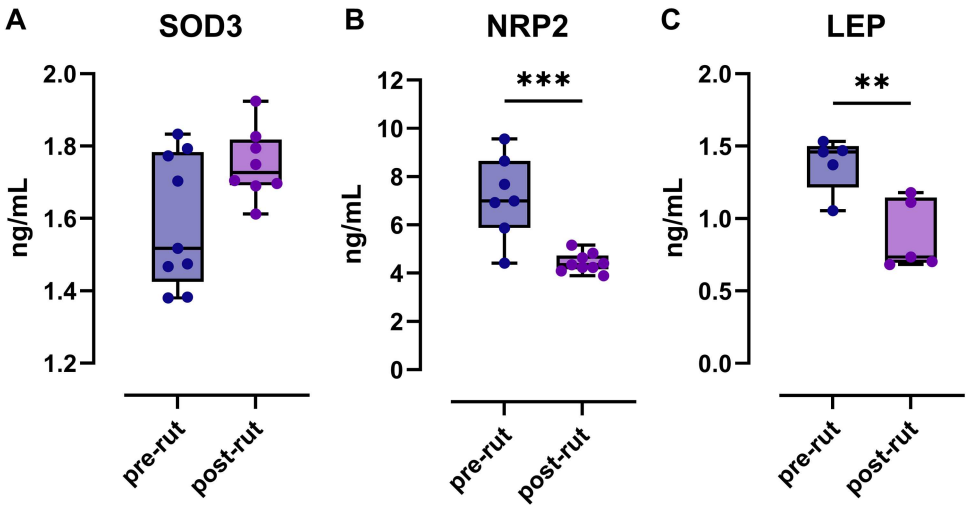

FIGURE 4 | SOD3 (A), NRP2 (B), LEP (C); $^{**}p < 0.01$, $^{***}p < 0.001$.

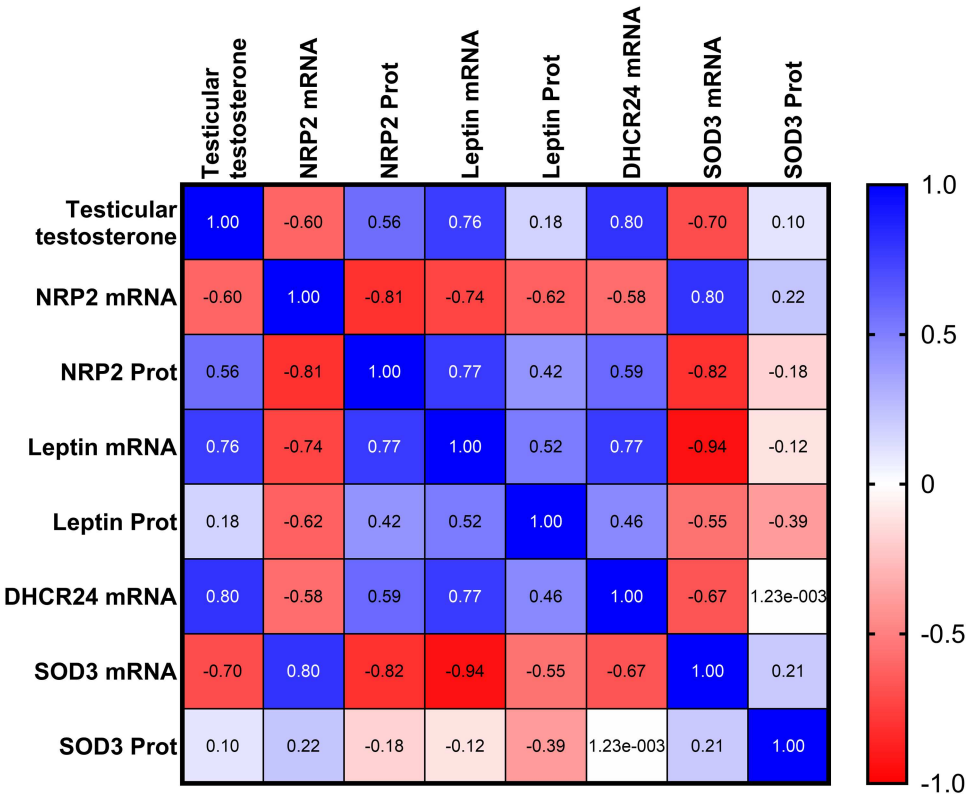

FIGURE 5 | Spearman's rank correlation coefficients (ρ) table for the analyzed parameters, including previously published testicular testosterone (Elmi et al. 2020). Looking at the correlations between gene expression and protein level of the same analyte, NRP2 shows a significant negative correlation (ρ −0.81; $p < 0.001$), while the other analytes show positive relationships, yet not statistically relevant.

4 | Discussion

The distinctive and temporally restricted regulation of spermatogenesis in Roe deer makes it a valuable model deserving deeper exploration, both for understanding species-specific reproductive strategies and for comparative studies. Although literature is witnessing a growing interest in such a field (Kozioł et al. 2020; González-Arto et al. 2016; Wagener et al. 2010; Klonisch et al. 2006; Roelants et al. 2002), many aspects still require clarification. Thus, samples of testicular parenchyma owned to 18 animals hunted in pre- and post-rut period have been included in this study aimed at deepening the knowledge on this finely regulated mechanism using gene and protein expression methodologies.

Gene expression results from angiogenesis and oxidative stress arrays are shown as heat maps (Figure 1). First, mean ΔCT values of the pre- and post-rut pools groups for genes with CT cycle < 35 (Supporting Information S1: Figure 1), then relative gene expression changes are reported using a

$2^{\Delta\Delta C_t}$ method to present results in a clear and standardized way, allowing for comparison (Figure 1). This approach enabled selection of genes which expression varied at least ±3 times, later quantified singularly on a single animal (Figures 2 and 3).

As shown in Figure 2, four genes (DHCR24, PRDX4, SOD3, and SCARA3) belonging to the oxidative stress pathway showed statistically significant variations in fold change expression in the post-rut pool compared to the pre-rut group, considered as the control reference. DCHR24, widely expressed in steroidogenic tissues such as testicular parenchyma (Peri 2016; Zerenturk et al. 2013), encodes a key enzyme involved in final step of cholesterol biosynthesis (London et al. 2015). Its gene expression downregulation in the post-rut period in Roe deer reflects the seasonal decline of androgen levels. Moreover, since seasonal testicular involution is mainly due to reduced spermatogonia proliferation rather than widespread apoptosis (Elmi et al. 2021; Blottner et al. 2007), a reducing DHCR24 expression could reflect a controlled slowing down of metabolism, preserving testicular integrity for the next breeding season. Despite acting through and within diverse mechanisms, the remaining genes belonging to the oxidative stress panel (PRDX4, SOD3, and SCARA3) are involved in antioxidative processes and showed an increase in expression, especially with regard to SOD3 (about eightfold) in pre-rout group. PRDX4 gene encodes for PRDX4 protein, a member of the peroxiredoxin family, that are redox-active enzymes reducing peroxides, particularly hydrogen peroxide (H_2O_2). A testis-specific PRDX4 isoform, PRDX4t, is expressed exclusively in sexually mature testes of many animals and is crucial for sperm nuclear protection during epididymal maturation, aiding in the oxidative folding of protamine (Fujii et al. 2025). SOD3, instead, encodes for glycoprotein SOD3 belonging to a group of metalloenzymes, known as SODs, which play a pivotal role in defending mechanism against ROS. Additionally, SOD3 is predominantly found in the extracellular matrix, potentially supporting areas not accessible to other SODs family members (Kalmari and Colagar 2024). Previous studies analyzing the mRNA expression of this gene in the Cervidae family highlighted significantly higher expression levels during the rutting period, when compared to the pre-rut one in Roe deer epididymis (Koziorowska-Gilun et al. 2015) and to the no-rutting period in European Red deer (Neuman et al. 2025). However, in the latter, despite the mRNA abundance of SOD3 being consistently highest in the testis, no statistically significant seasonal differences were observed (Neuman et al. 2025), which contrasts with the clear seasonal variation indicated by our results. It is important to note that the European Roe deer does not exhibit a complete suspension of spermatogenesis throughout the year, which may limit its suitability as a model for studying seasonal gene expression changes in testis related to reproductive cycles. In the oxidative stress pathway (Figure 2), a marked post-rut versus pre-rut increment of SOD3 is shown (Figure 2C), likely reflecting a critical role in testes recovery, following the massive reproductive effort of the preceding rutting period, also supported by the same trend in PRDX4 (Figure 2B). Looking at the SOD protein levels measured by ELISA, the results mirror the mRNA expression, yet without statistical significance (Figure 4A). SCARA3 is a class A scavenger receptor and is considered a cellular stress response gene (Peng et al. 2020; Yap et al. 2015). To the best of our knowledge, there are no previous evidence for a specific role in the reproductive context in wild mammals; therefore, our findings may represent the first indications of SCARA3 in such a setting. The statistically relevant increment in term of gene expression shown in post-rut group (Figure 2D) is consistent with what was already highlighted for previous genes included in the same panel involved in antioxidant process too.

The angiogenesis plate instead (Figure 3) shows four genes belonging to the same PCR array: F2, LEP, NRP2, and THBSII. In this second panel, not all the genes show significant changes in terms of fold change expression post-rut versus pre-rut when analyzed individually on singular animals. For example, F2, encoding prothrombin which is a key component of the coagulation cascade (Chinnaraj et al. 2018), shows a decrease in gene expression in post-rut pooled samples, yet not statistically significant at the individual level (Figure 3A). On the other hand, a strong statistically significant decrement is highlighted in post-rut group for LEP gene (Figure 3B). Leptin is a hormone produced by adipose tissue functioning as an indicator of body energy reserves (Gaspar-López et al. 2009). In male specimens, especially in seasonal animals, it connects the nutritional status to the reproductive function (Szczesna and Zieba 2015). A previous study on other cervids has already highlighted a decrease in circulating leptin levels after the rutting season, along with a substantial weight loss (Gaspar-López et al. 2009). Our findings provide new evidence that the Roe deer follows a similar pattern. This suggests that leptin plays a consistent role in the metabolic-reproductive axis of seasonal breeders, although the exact mechanism may vary in accordance with the species-specific physiology. Our results on mRNA are further supported by protein concentration data, which show a similar trend in post-rut animals (Figure 4C). Additionally, a statistically significant reduction in THBSII gene expression is observed in post-rut animals (Figure 3D), confirming preliminary data obtained on pooled samples, as shown by heatmap (Figure 1B). THBSII encodes thrombospondin-2 (TSP-2), a well-known inhibitor of angiogenesis (Zhang et al. 2020). While TSP-2 has been extensively studied in the context of cancer research (Pienkowski et al. 2025), its role in spermatogenesis remains poorly understood. The observed decrease may reflect a specific molecular adaptation associated with testicular tissue remodeling following the reproductive season. However, further studies are needed to clarify the significance of these results. Notably, TSP-2 did not show significant gene expression changes in response to photoperiod in *Peromyscus leucopus* (Pyter et al. 2005), suggesting that its regulatory role could be species-specific. The last gene object of discussion is NRP2 that presents an opposite trend compared to the others of the same Panel (Figure 3C). Our results show a discrepancy between NRP2 mRNA and protein concentration in testis parenchyma in post-rut, suggesting a complex regulation. NRP2 is a pleiotropic transmembrane co-receptor, involved in binding different ligands such as 3 semaphorines (SEMA3) and VEGF playing different functions. NRP2, in fact, is considered a potential target in cardiovascular diseases (Harman et al. 2020). Additionally, it guides migration of GnRH neurons, critical for puberty and fertility (Oleari et al. 2019). Moreover, NRP2 knockout mice show reduced GnRH neurons and smaller gonads (Men et al.

2021). The observed mRNA upregulation, alongside with protein downregulation, may result from microRNA-mediated translational repression or increased shedding of soluble NRP2 isoforms. These findings highlight previously unexplored mechanisms regulating NRP2 during seasonal reproduction and needing further investigation.

The Spearman's correlation analysis confirmed a complex interplay between testicular testosterone levels and gene expression of some of the angiogenesis and oxidative stress-related markers analyzed. NRP2 emerges as a central node in the correlation network because of its strong positive correlations between Leptin mRNA and SOD3 mRNA. This indicates a coordinated transcriptional program potentially linking vascular remodeling with antioxidant responses. On the other hand, the negative association between leptin and SOD3 mRNA may indicate that metabolic signaling and antioxidant defense are regulated in opposite directions. A notable finding is the strong negative correlation between NRP2 mRNA and NRP2 protein, highlighting the importance of post-transcriptional and post-translational regulatory mechanisms. Within this gene expression network, testicular testosterone acts as a key functional modulator. Positive correlations with DHCR24 and Leptin mRNA indicate a close association between androgen production and pathways involved in lipid metabolism and cellular homeostasis. In contrast, the negative correlation between testosterone and SOD3 mRNA suggests that increased steroidogenic activity may be accompanied by reduced transcriptional antioxidant defenses, reflecting a functional shift favoring steroidogenesis and vascular support over oxidative stress protection during periods of high reproductive activity.

In such a scenario, it is interesting to note that literature specific to the analyzed genes and proteins is also lacking for other broad-based models of seasonal reproduction, like hamsters (Phodopus sungorus and Cricetulus barabensis). Indeed, these species have been extensively used to investigate testicular involution (Munley et al. 2018; Xue, Xu, Chen, et al. 2022; Xue, Xu, Wu, et al. 2022), with several key regulatory genes been identified, including prolactin receptor (PRLR) (Xue, Xu, Wu, et al. 2022) and RFRP-3, which acts as signal mediator between melatonin and reproductive axis activation (Xue, Xu, Chen, et al. 2022). Unfortunately, assays specifically targeting both the oxidative stress and angiogenetic pathways that would allow us to compare our results are lacking, once again proving the need for further comparative investigations.

5 | Conclusion

This article had the objective to do an extensive and detailed analysis of two important pathways involved in the peculiar seasonal transformation that occurs in Roe deer bucks each year, namely Angiogenesis and Oxidative stress. The decision to first perform a wider analysis and then to select the most promising candidates for more specific individual analyses allowed for a focused yet comprehensive approach that highlights novel genes that have yet to be investigated. Generally speaking, it is proven that the increment of mRNA of some relevant antioxidant genes probably plays a recovery function after the reproductive intense effort. Downregulation of a metabolic reproductive regulatory gene, such as leptin, in the post-rut period, instead, validated by its protein concentration, appears to follow the same trend as other seasonal animals. Finally, the upregulation and translation repression of NRP2 in post-rut period, given to its pleiotropic functions, deserves further in-depth investigation. Considering these preliminary yet substantial scientific findings, continuing to investigate the rapid and substantial changes occurring in this species becomes essential with the aim of advancing fertility research, both in animal models and in a translational framework.

Author Contributions

Ilaria Troisio: methodology, formal analysis, writing – original draft. **Domenico Ventrella:** investigation, funding acquisition, writing – review and editing. **Bálint Lóránt Hausz:** methodology. **Mattia Cesauri:** methodology. **Niccolò Ian Vannetti:** methodology. **Maria Laura Bacci:** conceptualization, project administration, funding acquisition. **Alberto Elmi:** conceptualization, formal analysis, supervision, writing – review and editing. **Augusta Zannoni:** conceptualization, formal analysis, supervision, writing – review and editing.

Acknowledgments

The study was supported by RFO, University of Bologna.

Conflicts of Interest

The authors declare no conflicts of interest.

Data Availability Statement

The data sets generated during and/or analyzed during the current study are available at doi. https://doi.org/10.6092/unibo/amsacta/8515.

References

Aitken, R. J., and J. S. Clarkson. 1987. "Cellular Basis of Defective Sperm Function and Its Association With the Genesis of Reactive Oxygen Species by Human Spermatozoa." *Reproduction* 81, no. 2: 459–469. https://doi.org/10.1530/jrf.0.0810459.

Ayad, B., T. S. Omolaoye, N. Louw, et al. 2022. "Oxidative Stress and Male Infertility: Evidence From a Research Perspective." *Frontiers in Reproductive Health* 4. https://doi.org/10.3389/frph.2022.822257.

Blottner, S., J. Schön, and H. Roelants. 2007. "Apoptosis Is Not the Cause of Seasonal Testicular Involution in Roe Deer." *Cell and Tissue Research* 327, no. 3: 615–624. https://doi.org/10.1007/s00441-006-0328-8.

Caires, K. C., J. de Avila, and D. J. McLean. 2009. "Vascular Endothelial Growth Factor Regulates Germ Cell Survival During Establishment of Spermatogenesis in the Bovine Testis." *Reproduction* 138, no. 4: 667–677. https://doi.org/10.1530/REP-09-0020.

Chemineau, P., D. Guillaume, M. Migaud, J. Thiéry, M. Pellicer-Rubio, and B. Malpaux. 2008. "Seasonality of Reproduction in Mammals: Intimate Regulatory Mechanisms and Practical Implications." Supplement, *Reproduction in Domestic Animals* 43, no. S2: 40–47. https://doi.org/10.1111/j.1439-0531.2008.01141.x.

Chinnaraj, M., W. Planer, and N. Pozzi. 2018. "Structure of Coagulation Factor II: Molecular Mechanism of Thrombin Generation and Development of Next-Generation Anticoagulants." *Frontiers in Medicine* 5. https://doi.org/10.3389/fmed.2018.00281.

Dardente, H., and V. Simonneaux. 2022. "GnRH and the Photoperiodic Control of Seasonal Reproduction: Delegating the Task to Kisspeptin

and RFRP-3." *Journal of Neuroendocrinology* 34, no. 5: e13124. https://doi.org/10.1111/jne.13124.

Ebisch, I. M. W., C. M. G. Thomas, A. M. M. Wetzels, W. N. P. Willemsen, F. C. G. J. Sweep, and R. P. M. Steegers-Theunissen. 2008. "Review of the Role of the Plasminogen Activator System and Vascular Endothelial Growth Factor in Subfertility." *Fertility and Sterility* 90, no. 6: 2340–2350. https://doi.org/10.1016/j.fertnstert.2007.10.026.

Elmi, A., N. Govoni, A. Zannoni, et al. 2021. "Testicular Melatonin and Its Pathway in Roe Deer Bucks (*Capreolus capreolus*) During Capreolus Pre- and Post-Rut Periods: Correlation With Testicular Involution." *Animals: An Open Access Journal From MDPI* 11, no. 7: 1874. https://doi.org/10.3390/ani11071874.

Elmi, A., A. Zannoni, N. Govoni, et al. 2020. "Uncovering the Physiological Mechanisms Underlying the Roe Deer (*Capreolus capreolus*) Testicular Cycle: Analyses of Gelatinases and VEGF Patterns and Correlation With Testes Weight and Testosterone." *Animals: An Open Access Journal From MDPI* 10, no. 3: 444. https://doi.org/10.3390/ani10030444.

Fujii, J., H. Ochi, and S. Yamada. 2025. "A Comprehensive Review of Peroxiredoxin 4, a Redox Protein Evolved in Oxidative Protein Folding Coupled With Hydrogen Peroxide Detoxification." *Free Radical Biology and Medicine* 227: 336–354. https://doi.org/10.1016/j.freeradbiomed.2024.12.015.

Gaspar-López, E., J. Casabiell, J. A. Estevez, et al. 2009. "Seasonal Changes in Plasma Leptin Concentration Related to Antler Cycle in Iberian Red Deer Stags." *Journal of Comparative Physiology B* 179, no. 5: 617–622. https://doi.org/10.1007/s00360-009-0343-7.

Goeritz, F., M. Quest, A. Wagener, et al. 2003. "Seasonal Timing of Sperm Production in Roe Deer: Interrelationship Among Changes in Ejaculate Parameters, Morphology and Function of Testis and Accessory Glands." *Theriogenology* 59, no. 7: 1487–1502. https://doi.org/10.1016/s0093-691x(02)01201-3.

González-Arto, M., A. Vicente-Carrillo, F. Martínez-Pastor, et al. 2016. "Melatonin Receptors MT1 and MT2 Are Expressed in Spermatozoa From Several Seasonal and Nonseasonal Breeder Species." *Theriogenology* 86, no. 8: 1958–1968. https://doi.org/10.1016/j.theriogenology.2016.06.016.

Harman, J. L., J. Sayers, C. Chapman, and C. Pellet-Many. 2020. "Emerging Roles for Neuropilin-2 in Cardiovascular Disease." *International Journal of Molecular Sciences* 21, no. 14: 5154. https://doi.org/10.3390/ijms21145154.

Kalmari, A., and A. H. Colagar. 2024. "Exploration of SOD3 From Gene to Therapeutic Prospects: A Brief Review." *Molecular Biology Reports* 51, no. 1: 980. https://doi.org/10.1007/s11033-024-09919-2.

Klonisch, T., J. Schön, S. Hombach-Klonisch, and S. Blottner. 2006. "The Roe Deer as a Model for Studying Seasonal Regulation of Testis Function." *International Journal of Andrology* 29, no. 1: 122–128. https://doi.org/10.1111/j.1365-2605.2005.00603.x.

Koziorowska-Gilun, M., L. Fraser, P. Gilun, M. Koziorowski, and W. Kordan. 2015. "Activity of Antioxidant Enzymes and Their mRNA Expression in Different Reproductive Tract Tissues of the Male Roe Deer (*Capreolus capreolus*) During the Pre-Rut and Rut Seasons." *Small Ruminant Research* 129: 97–103. https://doi.org/10.1016/j.smallrumres.2015.05.006.

Kozioł, K., D. Broda, M. Romerowicz-Misielak, S. Nowak, and M. Koziorowski. 2020. "Melatonin Concentration in Peripheral Blood and Melatonin Receptors (MT1 and MT2) in the Testis and Epididymis of Male Roe Deer During Active Spermatogenesis." *Theriogenology* 149: 25–37. https://doi.org/10.1016/j.theriogenology.2020.03.025.

London, E., C. A. Wassif, A. Horvath, et al. 2015. "Cholesterol Biosynthesis and Trafficking in Cortisol-Producing Lesions of the Adrenal Cortex." *Journal of Clinical Endocrinology & Metabolism* 100, no. 10: 3660–3667. https://doi.org/10.1210/jc.2015-2212.

Men, M., D.-N. Chen, J.-D. Li, et al. 2021. "Analysis of PLXNA1, NRP1, and NRP2 Variants in a Cohort of Patients With Isolated Hypogonadotropic Hypogonadism." *Molecular Genetics & Genomic Medicine* 9, no. 11: e1816. https://doi.org/10.1002/mgg3.1816.

Munley, K. M., N. M. Rendon, and G. E. Demas. 2018. "Neural Androgen Synthesis and Aggression: Insights From a Seasonally Breeding Rodent." *Frontiers in Endocrinology* 9: 136. https://doi.org/10.3389/fendo.2018.00136.

Nalbandian, A., L. Dettin, M. Dym, and N. Ravindranath. 2003. "Expression of Vascular Endothelial Growth Factor Receptors During Male Germ Cell Differentiation in the Mouse." *Biology of Reproduction* 69, no. 3: 985–994. https://doi.org/10.1095/biolreprod.102.013581.

Neuman, N. M., P. Gilun, M. Koziorowska-Gilun, P. Janiszewski, and A. Dziekońska. 2025. "Antioxidant Enzyme Activity and mRNA Expression in the Reproductive Tissues of Male European Red Deer (*Cervus elaphus elaphus*)." *International Journal of Molecular Sciences* 26, no. 15: 7221. https://doi.org/10.3390/ijms26157221.

Oleari, R., A. Caramello, S. Campinoti, et al. 2019. "PLXNA1 and PLXNA3 Cooperate to Pattern the Nasal Axons That Guide Gonadotropin-Releasing Hormone Neurons." *Development* 146, no. 21: dev176461. https://doi.org/10.1242/dev.176461.

Peng, H., Q. Guo, T. Su, et al. 2020. "Identification of SCARA3 With Potential Roles in Metabolic Disorders." *Aging* 13, no. 2: 2149–2167. https://doi.org/10.18632/aging.202228.

Peri, A. 2016. "Neuroprotective Effects of Estrogens: The Role of Cholesterol." *Journal of Endocrinological Investigation* 39, no. 1: 11–18. https://doi.org/10.1007/s40618-015-0332-5.

Pienkowski, T., K. Wawrzak-Pienkowska, A. Tankiewicz-Kwedlo, M. Ciborowski, K. Kurek, and D. Pawlak. 2025. "Leveraging Glycosylation for Early Detection and Therapeutic Target Discovery in Pancreatic Cancer." *Cell Death & Disease* 16, no. 1: 227. https://doi.org/10.1038/s41419-025-07517-z.

Pyter, L. M., A. K. Hotchkiss, and R. J. Nelson. 2005. "Photoperiod-Induced Differential Expression of Angiogenesis Genes in Testes of Adult *Peromyscus leucopus*." *Reproduction* 129, no. 2: 201–209. https://doi.org/10.1530/rep.1.00448.

Roelants, H., F. Schneider, F. Göritz, J. Streich, and S. Blottner. 2002. "Seasonal Changes of Spermatogonial Proliferation in Roe Deer, Demonstrated by Flow Cytometric Analysis of c-Kit Receptor, in Relation to Follicle-Stimulating Hormone, Luteinizing Hormone, and Testosterone." *Biology of Reproduction* 66, no. 2: 305–312. https://doi.org/10.1095/biolreprod66.2.305.

Szczesna, M., and D. A. Zieba. 2015. "Phenomenon of Leptin Resistance in Seasonal Animals: The Failure of Leptin Action in the Brain." *Domestic Animal Endocrinology* 52: 60–70. https://doi.org/10.1016/j.domaniend.2015.03.002.

Takeshima, T., K. Usui, K. Mori, et al. 2020. "Oxidative Stress and Male Infertility." *Reproductive Medicine and Biology* 20, no. 1: 41–52. https://doi.org/10.1002/rmb2.12353.

Wagener, A., S. Blottner, F. Göritz, W. J. Streich, and J. Fickel. 2010. "Circannual Changes in the Expression of Vascular Endothelial Growth Factor in the Testis of Roe Deer (*Capreolus capreolus*)." *Animal Reproduction Science* 117, no. 3: 275–278. https://doi.org/10.1016/j.anireprosci.2009.05.006.

Xue, H., J. Xu, L. Chen, L. Zhao, M. Wu, and L. Xu. 2022. "RFRP-3 Synchronized With Photoperiods Regulates the Seasonal Reproduction of Striped Hamsters." *Zygote* 30, no. 3: 305–311. https://doi.org/10.1017/S0967199421000496.

Xue, H., J. Xu, M. Wu, L. Chen, and L. Xu. 2022. "Prolactin Receptor Regulates the Seasonal Reproduction of Striped Hamsters." *Zygote* 30, no. 1: 40–47. https://doi.org/10.1017/S0967199421000095.

Yap, N. V. L., F. J. Whelan, D. M. E. Bowdish, and G. B. Golding. 2015. "The Evolution of the Scavenger Receptor Cysteine-Rich Domain of the Class A Scavenger Receptors." *Frontiers in Immunology* 6. https://doi.org/10.3389/fimmu.2015.00342.

Zerbe, P., M. Clauss, D. Codron, et al. 2012. "Reproductive Seasonality in Captive Wild Ruminants: Implications for Biogeographical Adaptation, Photoperiodic Control, and Life History." *Biological Reviews* 87, no. 4: 965–990. https://doi.org/10.1111/j.1469-185X.2012.00238.x.

Zerenturk, E. J., L. J. Sharpe, E. Ikonen, and A. J. Brown. 2013. "Desmosterol and DHCR24: Unexpected New Directions for a Terminal Step in Cholesterol Synthesis." *Progress in Lipid Research* 52, no. 4: 666–680. https://doi.org/10.1016/j.plipres.2013.09.002.

Zhang, K., M. Li, L. Yin, G. Fu, and Z. Liu. 2020. "Role of Thrombospondin-1 and Thrombospondin-2 in Cardiovascular Diseases (Review)." *International Journal of Molecular Medicine* 45, no. 5: 1275–1293. https://doi.org/10.3892/ijmm.2020.4507.

Supporting Information

Additional supporting information can be found online in the Supporting Information section.

Figure S1: Heat maps showing the ΔCt values (ΔCt = mean Ct of reference genes – Ct of the target gene), derived from genes with Ct < 35, for the pre-rut and post-rut groups in the Oxidative Stress (A) and Angiogenesis (B) arrays. Less negative ΔCt values (represented by lighter colours) indicate higher gene expression. **Table S1:** Cycle thresholds (Ct) for the genes belonging to the oxidative stress commercial array. **Table S2:** Cycle thresholds (Ct) for the genes belonging to the angiogenesis commercial array.

SUPPLEMENTARY MATERIALS

Molecular investigations on angiogenesis and oxidative stress in Roe deer (*Capreolus capreolus*) bucks' testes throughout the reproductive cycle

Ilaria Troisio. Domenico Ventrella. Bálint Lóránt Hausz. Mattia Cesauri. Niccolò Ian Vannetti. Maria Laura Bacci. Alberto Elmi. Augusta Zannoni

Table S1 Cycle thresholds (Ct) for the genes belonging to the oxidative stress commercial array.

GENE	PRE-RUT POOL	POST-RUT POOL	GENE	PRE-RUT POOL	POST-RUT POOL	GENE	PRE-RUT POOL	POST-RUT POOL
ALB	39.35	N/A	**GSS**	29.22	28.09	**PRDX2**	28.48	26.24
ALOX12	29.24	27.94	**GSTP1**	28.66	28.31	**PRDX3**	27.92	26.16
AOX1	28.53	26.08	**GSTZ1**	32.92	32.98	**PRDX4**	32.74	29.71
APOE	30.55	30.44	**GTF2I**	27.39	25.99	**PRDX5**	29.62	28.68
ATOX1	25.58	25.1	**HMOX1**	30.97	30.28	**PRDX6**	24.59	23.3
BNIP3	27.08	27.6	**HSPA1A**	35.29	34.48	**PREX1**	32.23	31.7
CAT	28.65	27.83	**LOC788751**	37.09	36.29	**PRNP**	27.69	26.01
CCL5	36.26	35.01	**LPO**	36.46	36.15	**PTGS1**	N/A	39.57
CCS	33.64	33.28	**MB**	34.79	35.12	**PTGS2**	36.25	35.94
CYBB	33.01	31.81	**MBL2**	33.11	32.86	**PXDN**	33.98	33.68
CYGB	30.83	29.91	**MGST3**	27.65	26.11	**RNF7**	35.07	34.4
DHCR24	27.41	27.99	**MPO**	37.17	36.28	**SCARA3**	29.49	26.71
DUOX1	28.66	28.63	**MPV17**	37.61	N/A	**SEPP1**	35.79	34.12
DUOX2	34.95	34.87	**MSRA**	28.37	28.12	**SFTPD**	39.39	37.32
DUSP1	28.63	28.48	**MT3**	38.63	36.31	**SIRT2**	30.3	29.59
EPHX2	28.66	27.32	**NCF1**	27.34	27.34	**SOD1**	25.68	23.92
FOXM1	26.4	26.13	**NCF2**	31.2	30.99	**SOD2**	29.63	28.11
FTH1	25.42	23.7	**NOS2**	31.63	31.05	**SOD3**	32.03	28.17
GCLC	34.52	33.39	**NOX4**	37.86	36.32	**SQSTM1**	29.8	28.87
GCLM	28.5	27.42	**NOX5**	35.46	35.64	**SRXN1**	28.4	27.09
GPX1	N/A	N/A	**NOXA1**	36.63	35.46	**STK25**	34.49	33.73
GPX2	30.87	30.51	**NQO1**	29.39	27.91	**TPO**	N/A	39.25
GPX3	36.48	34.25	**NUDT1**	37.47	36.4	**TTN**	31.05	30.49
GPX4	24.99	24.3	**OXR1**	26.54	26.07	**TXN**	39.89	39.32
GPX5	38.52	38.33	**OXSR1**	27.26	26.62	**TXNRD1**	28.25	27.21
GPX6	32.59	32.19	**PDLIM1**	30.65	29.69	**TXNRD2**	32.36	29.94
GPX7	31.46	30.84	**PNKP**	39.1	37.19	**UCP2**	27.04	26.91
GSR	30.53	29.59	**PRDX1**	25.91	24.66	**VIMP**	32.28	32.03

Table S2 Cycle thresholds (Ct) for the genes belonging to the angiogenesis commercial array.

GENE	PRE-RUT POOL	POST-RUT POOL	GENE	PRE-RUT POOL	POST-RUT POOL	GENE	PRE-RUT POOL	POST-RUT POOL
AKT1	27.24	26.25	**FGF2**	34.03	33.14	**NRP2**	31.37	28.28
ANG	N/A	37.54	**FGFR3**	33.02	31.92	**PDGFA**	30.6	28.7
ANG2	33.25	32.59	**FIGF**	34.83	32.59	**PECAM1**	38.23	36.98
ANGPT1	32.67	32.07	**FLT1**	38.96	37.72	**PF4**	35.2	34.76
ANGPT2	39.48	38	**FN1**	36.67	36.17	**PGF**	34.01	34.51
ANGPTL4	31.09	31.11	**GRO1**	N/A	39.44	**PLAU**	28.47	27.26
ANPEP	31.42	29.6	**HGF**	32.89	32.02	**PLG**	N/A	35.8
BAI1	33.18	32.47	**HIF1A**	28.07	26.83	**PROK2**	24.84	24.82
CCL11	39.64	39.86	**HPSE**	30.7	29.68	**PTGS1**	39.37	39.17
CCL2	31.4	31.68	**ID1**	36.21	35.24	**S1PR1**	40	34.88
CDH5	32.39	31.22	**IFNB1**	N/A	38.75	**SERPINE1**	33.26	33.44
COL18A1	36.1	35.35	**IFNG**	33.93	33.2	**SERPINF1**	33.69	34.54
COL4A3	27.64	26.3	**IGF1**	30.49	30.26	**SPHK1**	36.95	35.16
CTGF	27.56	26.3	**IL1B**	N/A	36.29	**TEK**	31.81	30.72
CXCL10	29.94	29.33	**IL6**	37.01	35.59	**TGFA**	32.65	32.62
CXCL5	32.42	31.9	**ITGAV**	28.29	25.95	**TGFB1**	30.71	29
CXCL8	35.81	36.67	**ITGB3**	32.96	31.61	**TGFB2**	30.22	29.05
CXCL9	31.55	31.35	**JAG1**	35.11	33.49	**TGFBR1**	34.06	33.43
EDN1	37.26	36.43	**KDR**	N/A	N/A	**THBS1**	33.01	31.96
EFNA1	38.28	37.27	**LECT1**	32.93	32.11	**THBS2**	30.91	31.73
EFNB2	29.03	26.85	**LEP**	32.02	32.77	**TIE1**	30.54	29.88
EGF	36.34	35.36	**MDK**	30.43	29.57	**TIMP1**	27.42	27.67
EPAS1	27.56	26.76	**MMP14**	28.77	26.88	**TIMP2**	27.72	26.12
EPHB4	32.24	31.29	**MMP2**	28.7	27.5	**TIMP3**	27.11	24.9
ERBB2	32.75	31.71	**MMP9**	29.46	28.87	**TNF**	37.67	37.49
F2	23.34	23.91	**NOS3**	28.7	27.77	**VEGFA**	30.4	30.18
F3	31.11	30.71	**NOTCH4**	31.46	30.7	**VEGFB**	30.5	28.93
FGF1	27.99	27.08	**NRP1**	28.26	27.13	**VEGFC**	30.92	30.03

Figure S1 Heat maps showing the ΔCt values (ΔCt = mean Ct of reference genes – Ct of the target gene), derived from genes with Ct < 35, for the pre-rut and post-rut groups in the Oxidative Stress (A) and Angiogenesis (B) arrays. Less negative ΔCt values (represented by lighter colours) indicate higher gene expression.

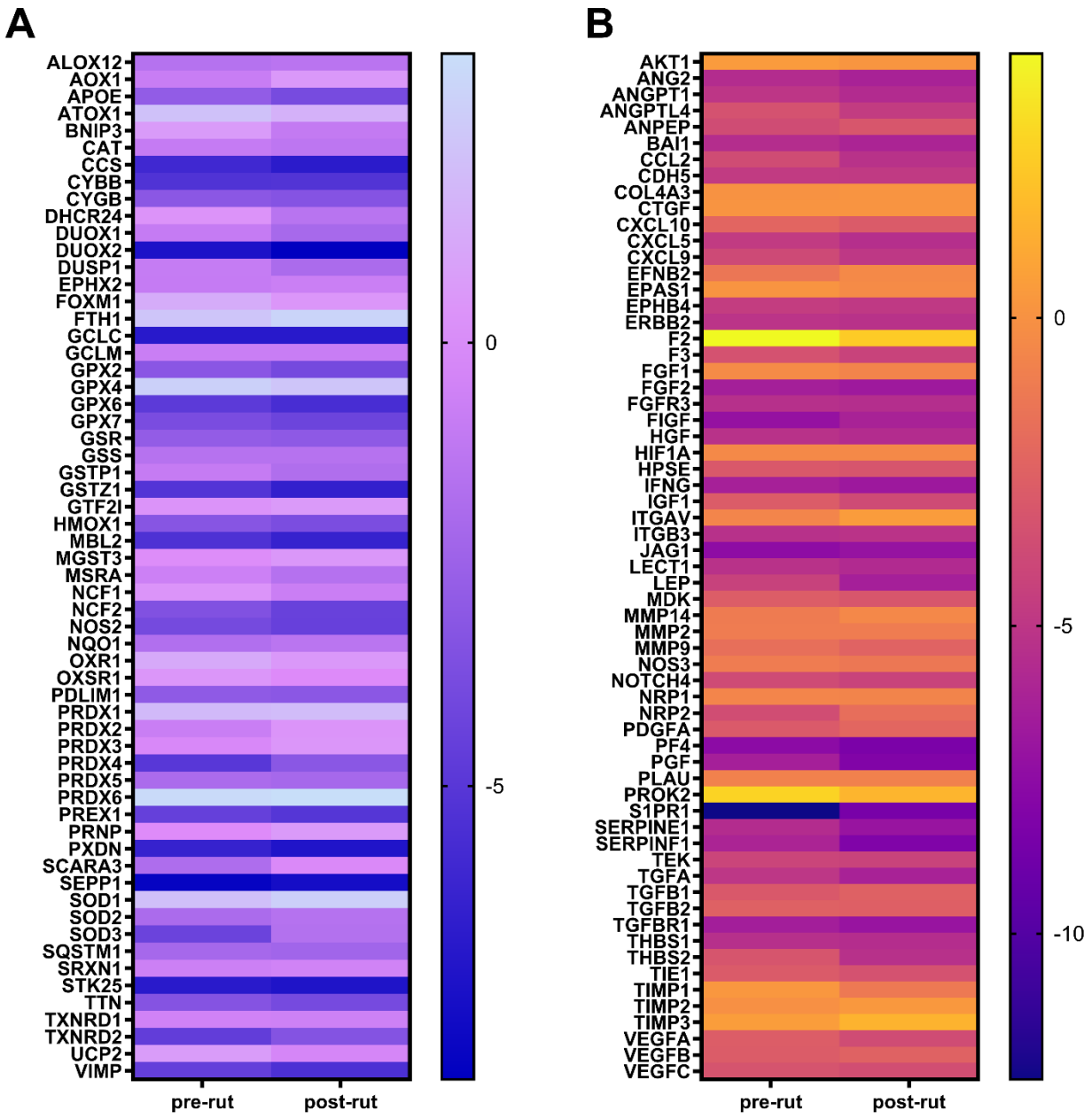

Porcine model in DCD transplantation research

Tolomeo, A. M., Malvicini, R., Ventrella, D., Elmi, A., Lombardi, V., Zanella, F., Andreis, M., De Lazzari, G., Todeschini, G., Caicci, F., Aniballi, C., Troisio, I., Santovito, G., Bacci, M. L., Muraca, M., Fabozzo, A., & Gerosa, G. (2024). Protective effects of mesenchymal stem cells-derived extracellular vesicles against ischemia-reperfusion injury of hearts donated after circulatory death: Preliminary study in a pig model. Biomedicine & Pharmacotherapy, 178, 117256 https://doi.org/10.1016/j.biopha.2024.117256

This work investigates the efficacy of mesenchymal stem cell-derived extracellular vesicles (MSC-EVs) in protecting the heart from ischemia-reperfusion injury in a porcine model. The treatment was found to prevent mitochondrial swelling, cristae loss, and oxidative stress in cardiac tissue. Additionally, MSC-EVs delayed the rise of cardiac-specific enzymes and reduced caspase-3-positive cells, indicating protection against apoptosis and inflammation.

Biomedicine & Pharmacotherapy 178 (2024) 117256

Contents lists available at ScienceDirect

Biomedicine & Pharmacotherapy

journal homepage: www.elsevier.com/locate/biopha

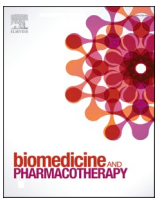

Protective effects of mesenchymal stem cells-derived extracellular vesicles against ischemia-reperfusion injury of hearts donated after circulatory death: Preliminary study in a pig model

Anna Maria Tolomeo [a,b,*,1], Ricardo Malvicini [b,c,d,1], Domenico Ventrella [e], Alberto Elmi [e,f], Valentina Lombardi [a], Fabio Zanella [g], Marco Andreis [a], Giada De Lazzari [b,c], Giulia Todeschini [g], Federico Caicci [h], Camilla Aniballi [e], Ilaria Troisio [e], Gianfranco Santovito [h], Maria Laura Bacci [e], Maurizio Muraca [b], Assunta Fabozzo [g,2], Gino Gerosa [a,b,g,*,2]

[a] Department of Cardiac, Thoracic and Vascular Science and Public Health, University of Padova, Padua, Italy
[b] Institute of Pediatric Research "Città della Speranza", Padua, Italy
[c] Department of Women's and Children's Health, University of Padova, Padua, Italy
[d] Instituto de medicina traslacional, trasplante y bioingeniería (IMeTTyB-CONICET), Buenos Aires, Argentina
[e] Department of Veterinary Medical Sciences, University of Bologna, Bologna, Italy
[f] Department of Veterinary Sciences, University of Pisa, Pisa, Italy
[g] Cardiac Surgery Unit, Hospital University of Padova, Padua, Italy
[h] Department of Biology, University of Padova, Padua, Italy

ARTICLE INFO

Keywords:
Extracellular vesicles
Heart Transplantation
Donation after Circulatory Death
Ischemia-reperfusion injury

ABSTRACT

Introduction: Insufficient supply of cardiac grafts represents a severe obstacle in heart transplantation. Donation after Circulatory Death (DCD), in addition to conventional donation after brain death, is one promising option to overcome the organ shortage. However, DCD organs undergo an inevitable more extended period of warm unprotected ischemia between circulatory arrest and graft procurement. Mesenchymal stromal cell-derived extracellular vesicles (MSC-EVs) have shown remarkable protective effects against ischemia-reperfusion injury. Thus, we aimed to enhance grafts preservation from DCD donors, through treatment with MSC-EVs.

Methods: Female pigs were euthanized by barbiturate overdose and after 20 min of a flat EKG, the chest was opened, the heart harvested and subsequently connected to an extracorporeal perfusion machine. MSC-EVs, isolated by ion exchange chromatography, were added to the perfusion solution (1×10^{11} particles) and the heart was perfused for 2 h. Then, heart tissue biopsies were taken to assess histological changes, mitochondrial morphology, antioxidant enzyme activity and inflammation mediators' expression. Biochemical parameters of myocardial viability were assessed in the perfusate.

Results: The treatment with MSC-EVs significantly prevented mitochondria swelling, mitochondrial cristae loss and oxidative stress in cardiac tissue. The protective effect of MSC-EVs was confirmed by the delayed increase of the cardiac-specific enzymes CK and TnC in the perfusate and the reduction of caspase-3+ cells in tissue sections.

Conclusion: MSC-EVs improve graft quality by preserving the mitochondrial ultrastructure protecting the myocardium against oxidative stress, reducing apoptosis of cardiac cells and preventing the increase of pro-inflammatory cytokines.

Abbreviations: **ALT:**, alanine aminotransferase; **AST:**, aspartate aminotransferase; **CAT:**, catalase; **CK:**, creatinin kinase; **DBD:**, donors after brain death; **DCD:**, Donation after Circulatory Death; **GGT:**, gamma-glutamyl transferase; **GPx:**, glutathione peroxidase; **IRI:**, ischemia-reperfusion injury; **IVS:**, Interventricular septum; **IL-x:**, interleukin-x; **LV:**, left ventricle; **MSC-EVs:**, mesenchymal stromal cell-derived extracellular vesicles; **ROS:**, reactive oxygen species; **RV:**, right ventricle; **SOD:**, superoxide dismutase; **TEM:**, transmission electron microscopy; **TnC:**, troponin C.

* Correspondence to: Department of Cardiac, Thoracic and Vascular Science and Public Health, University of Padova, via Giustiniani 2, 35128, Padua, Italy.
E-mail addresses: annamaria.tolomeo@unipd.it (A.M. Tolomeo), gino.gerosa@unipd.it (G. Gerosa).

[1] These authors contributed equally to this work and share first authorship
[2] These authors share last authorship

https://doi.org/10.1016/j.biopha.2024.117256
Received 10 June 2024; Received in revised form 30 July 2024; Accepted 2 August 2024
Available online 7 August 2024

1. Introduction

Heart transplantation is the treatment of choice in patients where other treatments have failed and there are no other therapeutic alternatives available to improve organ function and the patient's quality of life [1]. It is performed in patients with chronic heart failure, cardiomyopathy, coronary artery disease, and valvular disease, among others [2]. Donor hearts can come from donors after brain death (DBD) or donors after circulatory death (DCD). DCD are those donors from whom life support is withdrawn in a controlled manner and who have suffered extensive and irreversible brain damage, but who do not meet the criteria for brain death. From a clinical point of view, DBD hearts are preferred over DCD hearts since, in the former group, it is possible to maintain adequate perfusion of the organs until procurement is completed, although DCD organs generally come from younger donors with fewer comorbidities [3]. However, due to the increase in life expectancy and technological advances in the treatment of end-stage heart failure and other pathologies, the number of patients on the waiting list demanding a heart transplant currently exceeds the availability of organs [4]. Furthermore, this imbalance tends to worsen over the years given that the characteristics of donors are changing towards older donors. In this sense, as the age of the donor increases, comorbidities such as obesity, diabetes or high blood pressure also increase, which translates into poorer quality of the organs, which aggravates the need for organs and leads to having to accept marginal organs for cardiac transplantation [4].

In this scenario, hearts from DCD have been reconsidered and adopted as an alternative source of organs for transplantation [5,6]. However, the main limitation to the widespread use of DCD organs is that they inevitably suffer a certain degree of ischemic injury during the time of withdrawal of the donor life support [6] and the "no-touch" period (necessary to certify the death of the donor), which varies according to the laws of each country. During this time of unprotected warm ischemia, cellular damage sets in, which is further exacerbated once coronary circulation is restored. This damage, known as ischemia-reperfusion injury (IRI), is characterized by the loss of cellular homeostasis due to intracellular imbalances, such as calcium overload and the production of reactive oxygen species (ROS), which lead to the activation of apoptosis, pyroptosis and cell death due to necrosis [7]. ROS are commonly produced due to cellular metabolism and, at physiological concentrations, are involved in the regulation of growth factor signaling, hypoxic response, inflammation and immune response in mammalian cells [8]. However, in pathological conditions, the increase in these intermediates causes direct damage to cellular DNA, proteins, and lipids, in addition to activating stress response pathways, which initiate a cytokine-mediated cascade that ultimately recruits cells of the immune system, such as neutrophils and macrophages, amplifying tissue damage [9].

Furthermore, mitochondria are critical organelles in a high-energy-consuming organ like the heart and play a central role in its homeostasis. In IRI, mitochondria are one of the main targets of oxidative damage, leading to mitochondrial edema (mitochondrial swelling), loss of mitochondrial cristae, membrane potential and, eventually, cell death [10,11]. Therefore, preserving the integrity and functionality of mitochondria is essential to ensure the organ's viability.

In this sense, mesenchymal stem cells derived-extracellular vesicles (MSC-EVs) have been demonstrated to convey many of the pro-regenerative, anti-apoptotic and anti-inflammatory effects characteristic of their cells of origin. MSCs-EVs limit the excessive inflammatory response inhibiting M1 macrophages polarization and effector T lymphocytes and stimulating the M1 macrophages polarization and the proliferation of regulatory T cells [12–14]. Moreover, in animal models, MSC-EVs enhance the functional recovery of the kidney and heart following IRI, as well as liver regeneration [15,16].

Given all the above, we aimed to achieve an efficient and safe therapeutic based on the rational use of MSC-EVs in a preclinical model of heart transplantation to better preserve the organs and thus contribute to increasing the pool of organs available for transplantation.

2. Materials and methods

2.1. Establishment of the porcine model of cardiac preservation

Animals were anesthetized by intramuscular injection of tiletamine/zolazepam (5 mg/kg). Venous access was performed in the auricular vein, the animals were intubated, and general anesthesia was induced with 8 % sevoflurane. Then, animals were euthanized by administering thiopental (20 mg/kg). According to Italian law, we waited 20 min before proceeding with the procurement of the heart. No medication or intervention was administered during this "no-touch" period, in which

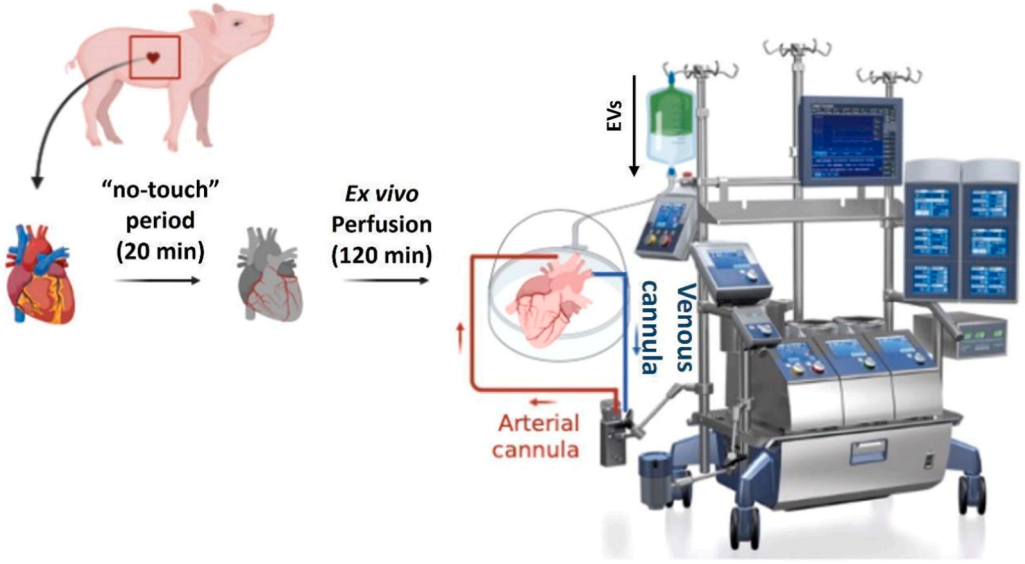

Fig. 1. Schematic representation of the perfusion protocol. After the death of the animal was declared, the heart was left in the animal's body for 20 minutes, according to Italian Law ("no-touch" period). The heart was then removed and connected to a perfusion machine, where it was perfused with a mixture of the animal's own leucodepleted blood and a preservation solution, formulated ad hoc, for 120 min. At the beginning of the perfusion, the extracellular vesicles ($1x10^{11}$ particles) or an equivalent volume of PBS+500 mM NaCl (control group) were added.

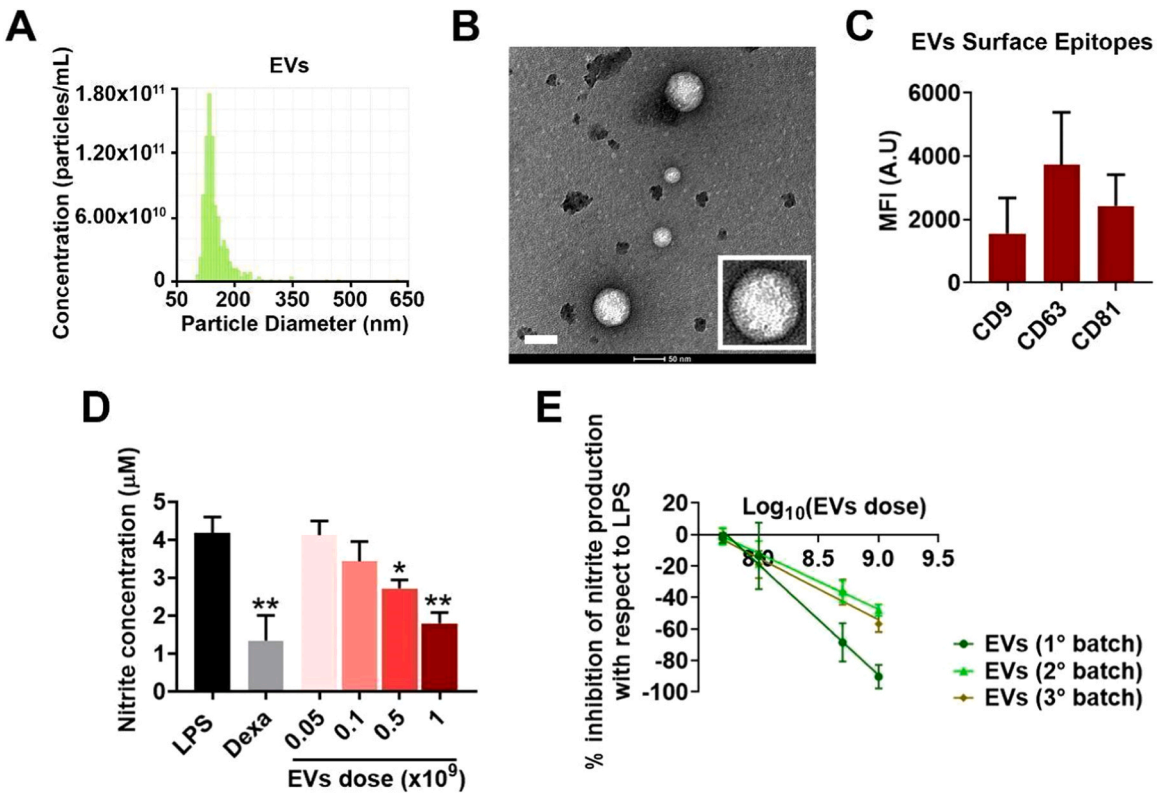

Fig. 2. EV characterization. EV particle size and distribution were assessed by tRPS (A) while TEM assessed its morphology. Scale bar: 50 nm (B). EV surface markers CD9, CD63 and CD81 were assessed by flow cytometry. The biological activity of EVs was evaluated before using them in the *ex-vivo* model. A macrophage assay evaluated EVs' anti-inflammatory activity (D, E). Results were expressed as mean ± SD and significance was determined for independent samples using one-way ANOVA with post-hoc Tukey's test (n = 3). *P<0.05; **P<0.01.

ventilation had been interrupted. After 20 min, the animal's heart was removed and connected to the perfusion machine for 120 min. The perfusion circuit consisted of an air and an oxygen inlet intended to maintain an adequate oxygen pressure, a carbon dioxide inlet to regulate the pH through pCO2, and an inlet to administer drugs and the MSC-EVs (1×10^{11} particles). After 120 min, tissue and perfusate samples were collected for biochemical, histological, inflammation mediators and oxidative stress analysis. The model scheme is outlined in Fig. 1.

Experimental activities with animals were carried out per the current Italian legislation on using animals for experimental purposes (D. Lgs 26/2014). A local ethics committee and the Italian Ministry of Health approved this study. Please see the online supplement for detailed methods.

3. Results

3.1. MSC-EV characterization

TRPS analysis of the MSC-EVs demonstrated a homogeneous population with particle sizes mostly below 100 nm (Fig. 2A). Transmission electron microscopy (TEM) identified the EVs as a group of heterogeneous spheroids with sizes ranging from 30 to 250 nm (Fig. 2B). The RPS and TEM analysis confirmed that almost all the nanoparticles isolated in the present work could be called "small EVs", according to the MISEV2018 criteria [11]. No apoptotic bodies were detected. The EV surface markers were analyzed and the classical tetraspanin (CD63, CD9 and CD81) were identified in our samples (Fig. 2C). To corroborate the biological activity of the EVs preparations before using them in the *ex-vivo* model, and to compare their relative potency, we performed an LPS-stimulated macrophage assay [17]. As can be seen in Fig. 2D and E, EVs preparations used to treat the hearts (one preparation per heart), presented a significant anti-inflammatory activity, although the EV1 preparation exhibited greater relative potency than the other two preparations (Y=-70.3X + 543; IC50=2.75x108 vs Y=-35.5X + 272; IC50=1.17x109 and Y=-40.1X + 253; IC50=1.02x109, respectively).

3.2. Extracellular vesicles ameliorate cardiac damage after ischemia-reperfusion

Biochemical parameters were monitored and analyzed in the perfusion fluid every 30 minutes, during the 120 min of perfusion. A continuous increase in glucose concentration was observed throughout the perfusion, with no observable differences between the two groups (Fig. 3A). Regarding the pH, a slight acidosis was maintained during the first hour of perfusion and was then adjusted to physiological values for both groups (Fig. 3B). An attempt was made to hold a slight hyponatremia to avoid calcium overload, which was more marked in the control group (Fig. 3C). Regarding potassium, normokalaemia levels were maintained throughout the perfusion, to avoid hyperpolarization of cardiac cells (Fig. 3D). Regarding chloride, slight hypochloremia was maintained throughout the perfusion (Fig. 3E). Regarding Magnesium, hypermagnesemia was maintained, since it has been shown that it has anti-arrhythmogenic properties and can prevent calcium overload (Fig. 3F). Regarding ionic calcium, hypocalcemic levels were maintained during perfusion, to avoid calcium overload of cardiomyocytes, which can lead to cell death (Fig. 3G). These results indicate that treatment with extracellular vesicles does not influence the biochemical parameters analyzed, which can be regulated and adjusted thanks to the perfusion system.

Then, the enzymatic activity of cardio-specific enzymes, such as creatinine kinase (CK) and troponin C (TnC), and non-cardio-specific enzymes, such as aspartate aminotransferase (AST), alanine aminotransferase (ALT) and gamma-glutamyl transferase (GGT) was assessed. As can be seen in Fig. 4, treatment with MSC-EVs delays the increase in

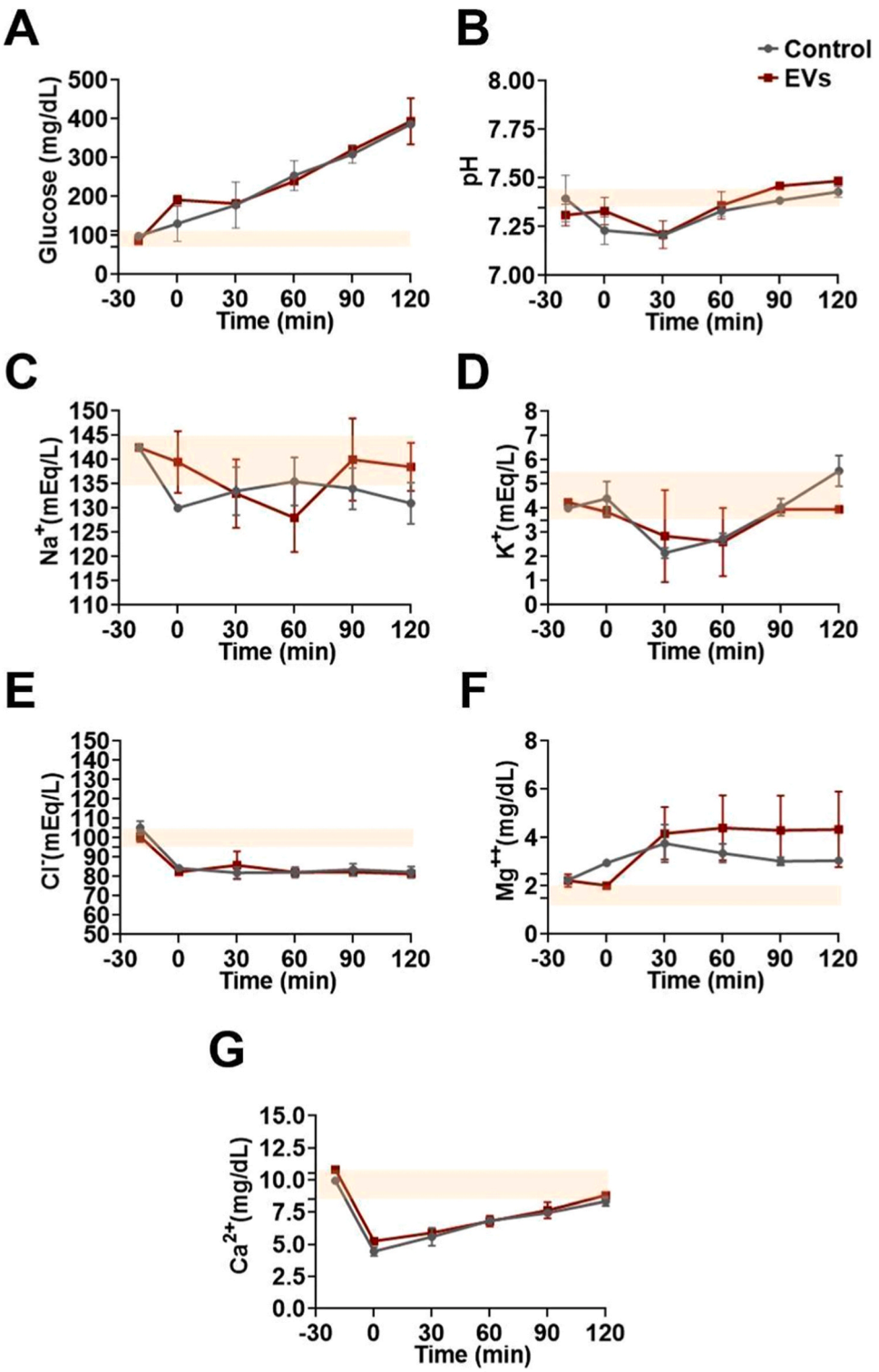

Fig. 3. Biochemical parameters of perfusate. Biochemical analyses of the perfusate were performed every 30 min, throughout the *ex-vivo* perfusion protocol, for the control group and the group treated with EVs. Glucose (A), pH (B), Na+ (C), K+ (D), Cl- (E), Mg++ (F) and Ca++ (G) were analyzed. The usual range of each analyte is indicated in pink. N=3 for each group. Results were expressed as mean ± SD and significance was determined for independent samples using Student's unpaired t-test (n = 3).

the enzyme's activity in the perfusate, compared to the control group, this effect being more noticeable in the first hour of perfusion for CK, TnC and AST (Fig. 4A, B and C, respectively). Likewise, ALT also shows a delay in the increase in perfusion fluid for the EV-treated group, but finally reaches the same levels as the control group (Fig. 4D). Finally, GGT maintains considerably lower and constant levels in the group treated with EVs, compared to the control group (Fig. 4E). These results indicate that treatment with extracellular vesicles would protect cardiac cells from ischemia-reperfusion damage, delaying cellular damage by approximately 30–60 min, compared to the control.

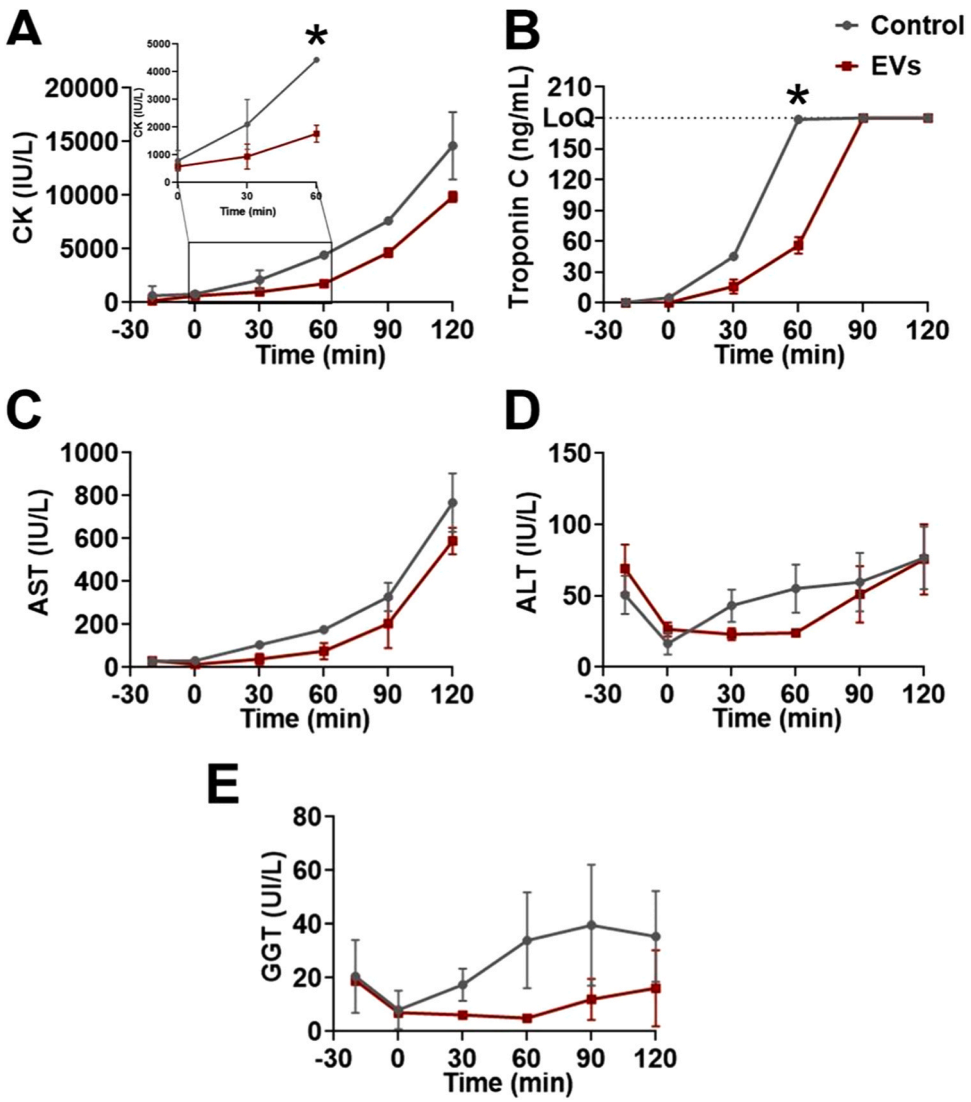

Fig. 4. Analysis of the enzymatic activity in the perfusate. The enzymatic activity of the cardiac-specific enzymes CK and TnC was analyzed in the perfusate (A and B, respectively). Note that for TnC the upper limit of quantification (LoQ) is reached (180 ng/mL). In addition, the activity of AST, ALT and GGT (C, D and E, respectively) was also analyzed. Results were expressed as mean ± SEM and significance was determined for independent samples using Student's unpaired t-test (n = 3) for each group. *P<0.05; **P<0.01.

3.3. MSC-EV administration reduces histological injury in cardiac grafts

Hematoxylin-eosin staining was performed on cardiac tissue sections to evaluate the effect of MSC-EV treatment on the cardiac organ. In this sense, treatment with EVs reduced both edema and hemorrhage areas in the tissue, and the necrotic regions (Fig. 5A). Furthermore, the analysis of caspase-3 by immunohistochemistry revealed that the treatment reduced the number of apoptotic cells, evidenced by a lower number of caspase-3+ cells, than the control group (Fig. 5A). The quantification of the histological score (for hemorrhage, edema, and necrosis) and the number of caspase-3^{+} cells per field at 40X is shown in Fig. 5B.

3.4. MSC-EV reduces mitochondrial damage and oxidative stress

The mitochondrial cristae density in the different cardiac regions was analyzed to evaluate mitochondrial damage. Representative microphotographs of mitochondrial ultrastructure are shown in Fig. 6A. The analysis revealed a loss of the mitochondrial cristae density in the control group. At the same time, the treatment with MSC-EVs effectively maintained the density of the mitochondrial cristae (Fig. 6B). Also, the number of abnormal mitochondria significantly increased in the control group, while treatment with EVs was effective in maintaining the mitochondrial structure (Fig. 6C). These results indicate that treatment with MSC-EVs would help prevent and reduce tissue damage (hemorrhage, edema, and necrosis) and ultrastructural damage to mitochondria.

Moreover, ischemia-reperfusion injury is mainly mediated by an increase in reactive oxygen and nitrogen species and an inadequate or insufficient response of the antioxidant system. This leads to damage to DNA, proteins, lipid peroxidation and mitochondrial dysfunction. In this sense, the enzymatic activities of the antioxidant enzymes superoxide dismutase (SOD), catalase (CAT) and glutathione peroxidase (GPx) were analyzed. A significantly lower activity of the antioxidant enzymes, SOD, and catalase, was found in the groups treated with MSC-EVs compared to the control group. Also, a significantly lower content of carbonylated proteins was observed in the MSC-EV treated group (Fig. 6D).

3.5. Tissue Cytokines, Chemokines and Tissue Repair Mediators Have a Lower Expression after MSC-EVs Treatment

Pro-inflammatory cytokines (such as IL-1ra, IL-2 and IL-6) promote

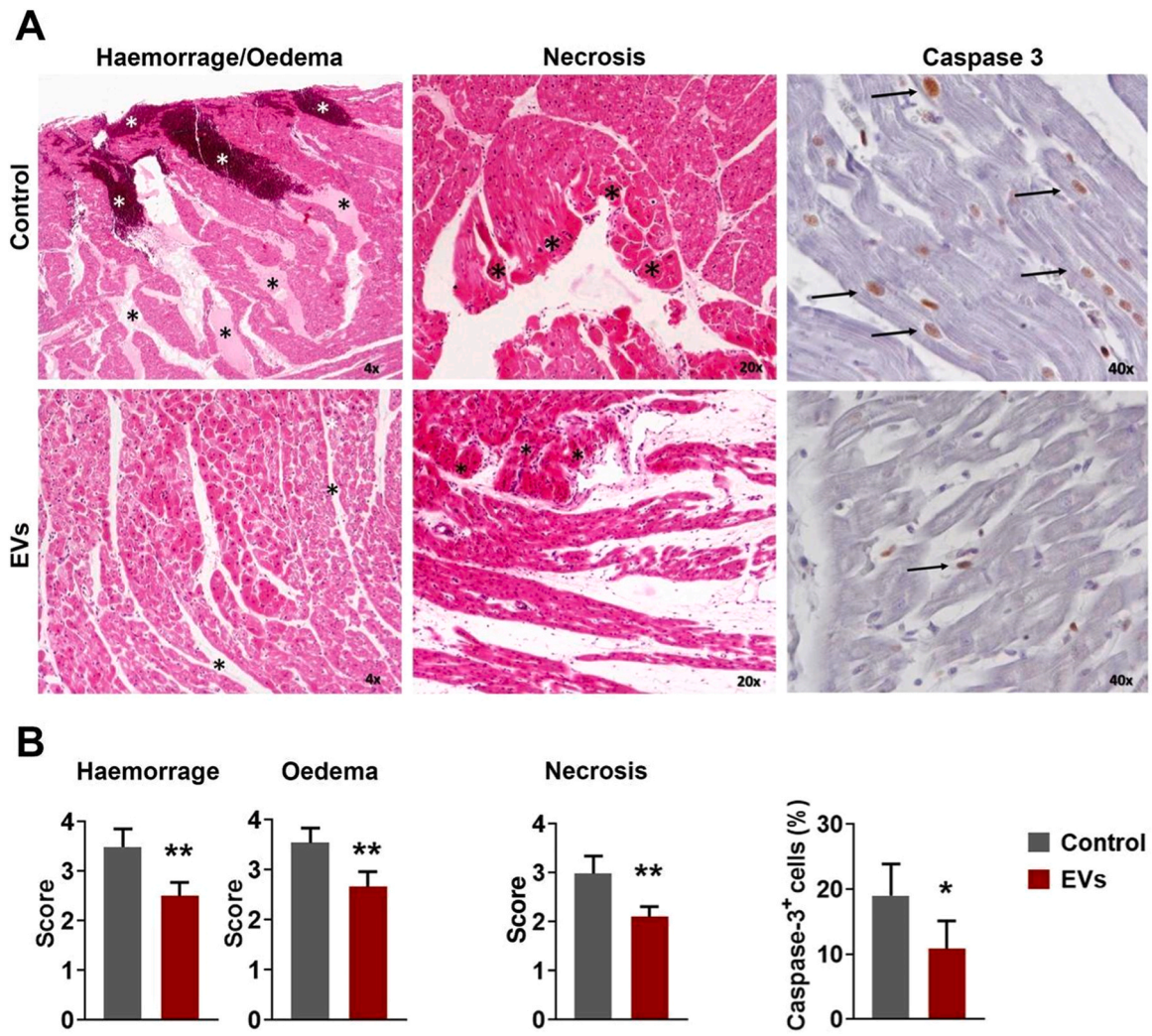

Fig. 5. Histological analysis of the heart**.** Histological section samples of pig hearts were stained with hematoxylin-eosin and analyzed for hemorrhage and edema (*black asterisks and white asterisks, respectively, 4x magnification) and tissue necrosis (black asterisks, 20x magnification). Additionally, immunohistochemical staining for caspase-3 was performed to analyze apoptosis (A). Quantification of the histological score and the total number of caspase-3^{+} cells (10 fields at 40x) (B). Results were expressed as mean ± SD and significance was determined for independent samples using Student's unpaired t-test (n = 3) for each group. *P<0.05; **P<0.01.

the cell proliferation pathway involved in sterile inflammation (during ischemia damage) and immune processes. We found a significant decrease in the concentration of these cytokines in the group treated with EVs with respect to the control group and a non-significative trend for IL-1α, IL-1β and IL-18 (Fig. 7A-B). Both IL-8, a chemokine responsible for the recruitment of neutrophils and macrophages to the injury site and IL-12, a cytokine involved in the macrophage's activation, were influenced by the MSC-EV administration. We found that treatment significantly decreased the levels of these cytokines in the cardiac tissue, with respect to the untreated groups. The anti-inflammatory cytokines, IL-4, and IL-10, typically produced to counteract an ischemic insult, were significantly lower in the treated group with respect to the untreated group (Fig. 7A-B).

4. Discussion

Solid organ transplantation represents the gold standard treatment for patients with terminal organ failure. Heart failure is a perfect example, as heart transplantation remains the treatment of choice for patients with end-stage heart failure and approximately 9 % of patients on the waiting list for heart transplantation ultimately die [18]. Although the World Donation and Transplant Observatory reported 129, 681 solid organs transplanted worldwide in 2020, it is estimated that this covered less than 10 % of the global need [http://www.transplant-observatory.org/]. These data demonstrate a gap between organ transplantation's needs and their availability. Therefore, new strategies for obtaining donor organs must be explored to reduce this gap and increase the number of organs available for transplant. These strategies include DCD donors, representing around 23 % of the organs transplanted in 2020 [http://www.transplant-observatory.org/]. Currently, perfusion machines are being used to improve the function and viability of organs from DCD donors, thus increasing the number of transplants. In this sense, organ perfusion seems a valuable strategy to evaluate pre-transplant graft function and recover organs that would otherwise be discarded [19,20].

An essential advantage of *ex-vivo* organ perfusion is that it offers the potential to explore the effects of various therapeutic strategies on a fully functioning organ. MSC-EVs involve numerous physiological and pathological processes, such as tissue regeneration, immunomodulation, apoptosis, inflammation and viral infections [21–23]. In this scenario, MSC-EVs administration was associated with an elevation in the alveolar fluid clearance rate, in an *ex-vivo* perfusion model of lungs from deceased donors who did not match the criteria for transplantation [24]. Moreover, EVs derived from mesenchymal stem cells have been shown

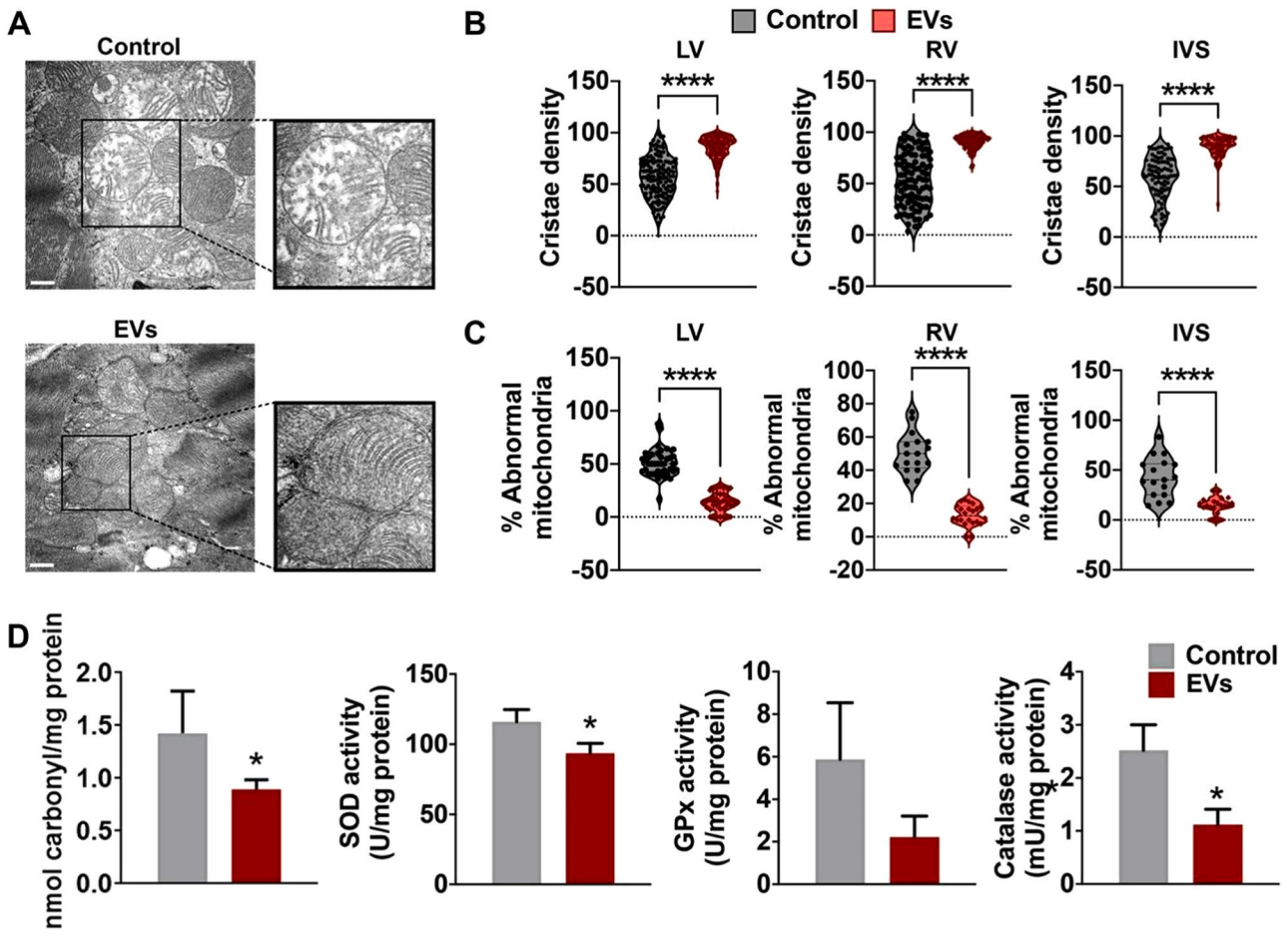

Fig. 6. Analysis of mitochondrial ultrastructure and the oxidative stress. Representative microphotographs of cardiac tissue mitochondria obtained by transmission electron microscopy (A). Analysis of mitochondria was carried out by quantifying the density of mitochondrial cristae (B) and the percentage of abnormal mitochondria (C). 30 photos per group were analyzed. Bar scale = 500 nm. The activity of the antioxidant enzymes SOD, CAT and GPx was evaluated in cardiac tissue homogenates from the regions of the left ventricle, right ventricle, and interventricular septum. In addition, oxidative damage was assessed by quantifying the content of carbonylated proteins (D). Results were expressed as median ± range and significance was determined for independent samples using one-way ANOVA with post-hoc Tukey's test (n = 3). ****P<0.0001 (B and C). Results were expressed as mean ± SD and significance was determined for independent samples using Student's unpaired t-test (n = 3) for each group. *P<0.05 (D).

to have great potential as therapeutic agents for various diseases, including myocardial ischemia, ischemic stroke, and chronic kidney disease [25–27]. In addition, more than 30 clinical trials that use MSC-EVs as therapeutic intervention are registered and are being conducted (https://clinicaltrials.gov/).

Furthermore, EVs have been used to treat myocardial I-R injury in various animal models. In a recent study, adipose tissue derived MSC-EVs (ADMSC-EVs) also showed cardioprotective effects in myocardial I-R injury. Intravenous administration of ADMSC-EVs into rats reduced the levels of creatinine kinase (CK-MB) and troponin C in a myocardial I-R injury model. Similarly, ADMSC-EVs inhibited apoptosis of cardiomyocytes in a hypoxia–reoxygenation model [28]. Moreover, rat bone marrow derived MSC-EVs abrogated ROS production, improved cardiac function, and decreased apoptosis *in-vitro* and in a model of myocardial I-R injury by prompting autophagy via activating adenosine monophosphate–activated protein kinase (AMPK) and AKT pathways [29].

Importantly, although this is a xenogenic model, in which human EVs are used on a pig heart, many studies support the idea that human MSC-EVs can be used across different species, as they have shown immunosuppressive properties, such as the modulation of T-cell responses and the promotion of regulatory T cells in murine models [30, 31]. Moreover, biodistribution studies confirm that human EVs are delivered to different organs, in xenogenic models [32–34].

In this model, we used a dose of 1×10^{11} particles per heart (weight≈120 g). On the other hand, in an experimental model of hypothermic perfusion of discarded human kidneys, an EV dose of approximately $3x10^{10}$ particles per kidney (weight≈130 g) was used [35]. However, there is a lack of studies that perform comprehensive assessments of the *in-vivo* dose-response kinetics and the administration of single *vs* multiple doses, so establishing an EV dose is often an empirical process and may depend on the species. In this regard, the reported effective dose of similar MSC-EVs was 100 μg for rats (~200 g) [36], 200 μg for rabbits (~3 kg) [37], and 1 mg for mini-pigs (~18 kg) [38]. Moreover, even though the manufacturing of GMP-compliant EVs results in a high batch-to-batch consistency, the biological activity may differ among batches for the same dose [39]. In this sense, *in-vitro* functional/potency assays should be performed, to establish the activity of each batch (for example, the IC50) for a given dose of EVs [17].

In our hands, the biochemical analysis of the plasma ions in the perfusate revealed the same behavior and trend in both treated and untreated hearts, as these parameters depend on the composition of the perfusion solution as well as the interventions that can be performed throughout the perfusion system (e.g. administration of drugs, salts, etc.). Regarding the metabolic profile, we found a constant increase in glucose levels in both groups, suggesting that the heart used pyruvate administered in the perfusion solution rather than glucose as metabolic substrate.

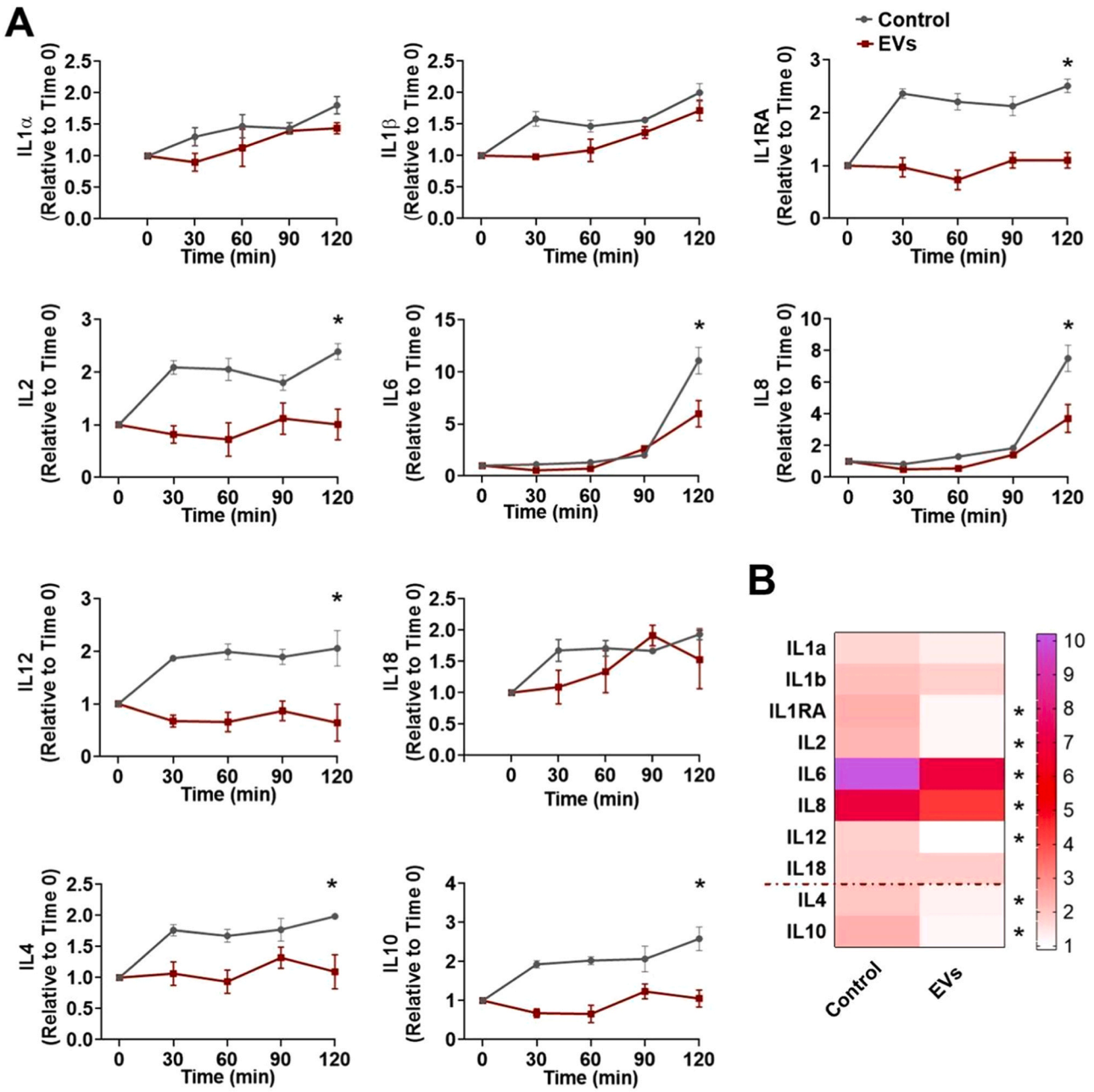

Fig. 7. Analysis of cytokines, chemokines, and inflammatory mediators. Cytokines relative values are expressed relative to time zero and normalized to each group. (B) Heatmap showing the cytokines profile relative expression (to time zero) for both groups. Results were expressed as mean ± SEM and significance was determined for independent samples using Student's unpaired t-test (n = 3). *P < 0.05.

A gradual increase in the activity of the cardiac specific enzymes CK, TnC, AST, ALT, and GGT was also observed, which is indicative of myocardial damage and cell death [40]. However, hearts treated with EVs showed a delay in the increase in troponin, CK, ALT and AST activity of approximately 30 min, compared to the control group, suggesting that EVs exert some type of protection against cellular death in the early phases of perfusion. This finding suggests that MSC-EVs can exert an immediate but transient graft protection (approximately 30 min), pointing to the possible need for repeated MSC-EV administrations to maintain the effect over time. At the end of the perfusion, there were no differences in the levels of ALT and TnC between the groups, but lower levels of activity for CK, AST and GGT were observed in the group treated with EV, compared to the control group.

The histological analysis showed that the treatment with MSC-EVs effectively prevents tissue damage since it reduces oedema, necrosis, and apoptosis, given by a lower number of caspase-3 positive cells. In this respect, Rampino and collaborators reported that discarded human kidneys perfused and treated with EVs showed a lower global score of ischemic kidney damage and renal ultrastructure was preserved, in addition, a lower renal expression of caspase-3 was found [35].

Mitochondria play a critical role in ischemia-reperfusion injury. Given that this organelle plays a fundamental role in calcium overload, ROS production and cell death, preserving the mitochondrial structure and function is crucial to the organ's viability, especially the heart, given its high metabolic demand. In this sense, an essential indicator of mitochondrial integrity is the preservation of the cristae of the inner mitochondrial membrane as it has been shown that the disorganization of mitochondrial cristae leads to mitochondrial stress, poor functioning of the respiratory chain and precedes the release of cytochrome C, with the consequent induction of the intrinsic pathway of apoptosis [41]. In

our model, treatment with MSC-EV proved effective in preserving the integrity of the mitochondrial cristae in the hearts and their ultrastructure, given that a lower number of abnormal mitochondria was observed, than the control group. These data suggest a protective role of EVs on mitochondria, which could explain the lower expression of caspase-3, observed in the treated group.

The prevention of mitochondrial damage by MSC-EVs probably also contributed to the reduction in the rate of ROS production. Indeed, analysis of oxidative stress showed that treatment with MSC-EVs led to a decrease in the expression of the antioxidant enzymes CAT and SOD in cardiac tissue, which is considered a physiological response to a lower exposure to oxidant agents, not only in mammals, but also in other animals [42,43].

Finally, by assessing the inflammatory response as a part of the evaluation of the heart, in our model, we recorded a significantly lower amount of the pro-inflammatory mediators such as IL-1ra, IL-2, IL-6 and IL-8 following the treatment with MSC-EVs. Also, the anti-inflammatory cytokines such as IL-4 and IL-10 showed a lower expression in the group treated with MSC-EVs, further pointing to their protective effect on the cardiac tissue from the ischemic insult.

5. Conclusions

Normothermic re-perfusion supplemented with MSC-EVs may be preferable when dealing with hearts harvested after prolonged warm "unprotected" ischemia. The protective effect of MSC-EVs was confirmed by the delayed increase of the cardiac enzymes CK and TnC in the perfusate, as well as for the prevention of mitochondria swelling, mitochondrial cristae loss and oxidative stress in the donor heart. In conclusion, by creating an adequate perfusion protocol after prolonged warm ischemia in DCD hearts, we showed that MSC-EVs can improve graft quality by protecting the myocardium against ischemic damage.

6. Limitations

In terms of the limitations of this study, it was performed using these three animals/groups, for ethical reasons. Moreover, due to the preliminary nature of the study and the relatively low sample size, the authors opted not to include animals of different sexes to try and obtain reliable data, yet again preliminary, by limiting confounding factors. Nonetheless, it is important to state that enrolled animals were prepubescent, therefore effects imputable to sexual hormones can be ruled out. We realize that this may still represent a limitation to the study, but when working with large animal models, and especially pigs, several husbandry technicalities have to be evaluated. Sourcing of intact males of standard commercial breeds can indeed be challenging since early castration (within the first week after birth) is the standard. In addition, intact males have to be housed singularly and can be extremely aggressive. It is therefore quite common to only include intact males when the given research protocol is either dealing with a sex-influenced pathology or aims at assessing efficacy in a larger population. Based on the results of this preliminary trial, we are planning on moving forward with further studies enrolling a more varied population, therefore also males.

Funding

This work was supported by the "Centro Trapianti Cuore, F99/24CUOR, DGR n. 99 of 12/02/2024" and by the "Fondazione Città della Speranza – Onlus (CDS) within the Pediatric Research Institute Città della Speranza (IRP) —IRP grant 2024–2027".

CRediT authorship contribution statement

Maria Laura Bacci: Writing – review & editing, Validation, Resources, Methodology. **Maurizio Muraca:** Writing – review & editing, Validation, Methodology. **Ilaria Troisio:** Formal analysis, Data curation. **Gianfranco Santovito:** Writing – review & editing, Validation, Methodology, Data curation. **Federico Caicci:** Investigation, Formal analysis, Data curation. **Camilla Aniballi:** Formal analysis. **Giada De Lazzari:** Formal analysis, Data curation. **Giulia Todeschini:** Validation, Investigation, Formal analysis. **Gino Gerosa:** Writing – review & editing, Writing – original draft, Supervision, Funding acquisition, Conceptualization. **Fabio Zanella:** Validation. **Marco Andreis:** Validation, Methodology, Investigation, Formal analysis. **Alberto Elmi:** Resources, Methodology, Investigation. **Assunta Fabozzo:** Writing – review & editing, Writing – original draft, Supervision, Methodology, Conceptualization. **Valentina Lombardi:** Validation. **Ricardo Malvicini:** Writing – review & editing, Writing – original draft, Visualization, Validation, Supervision, Resources, Project administration, Methodology, Investigation, Formal analysis, Data curation, Conceptualization. **Domenico Ventrella:** Validation, Resources, Methodology, Investigation. **Anna Maria Tolomeo:** Writing – review & editing, Writing – original draft, Visualization, Validation, Supervision, Software, Resources, Project administration, Methodology, Investigation, Funding acquisition, Formal analysis, Data curation, Conceptualization.

Declaration of Competing Interest

The authors declare that they have no known competing financial interests or personal relationships that could have appeared to influence the work reported in this paper.

Acknowledgments

The authors would like to thank "Centro Trapianti Cuore anno 2022— DGRV 1637 del 19/12/22" and the "Fondazione Città della Speranza – Onlus (CDS) within the Pediatric Research Institute Città della Speranza (IRP) — IRP grant 2024–2027", for financial support. Furthermore, the author would like to thank Prof. Maria Morini for the histological support to the work. Finally Graphical Abstract and Fig. 1 were created with BioRender.com

Appendix A. Supporting information

Supplementary data associated with this article can be found in the online version at doi:10.1016/j.biopha.2024.117256.

References

[1] T.A. McDonagh, M. Metra, M. Adamo, et al., 2021 ESC Guidelines for the diagnosis and treatment of acute and chronic heart failure, Eur. Heart J. 42 (36) (2021) 3599–3726, https://doi.org/10.1093/EURHEARTJ/EHAB368.
[2] M.R. Costanzo, A. Dipchand, R. Starling, et al., The international society of heart and lung transplantation guidelines for the care of heart transplant recipients, J. Heart Lung Transpl. 29 (8) (2010) 914–956, https://doi.org/10.1016/J.HEALUN.2010.05.034.
[3] K.K. Dhital, H.C. Chew, P.S. Macdonald, Donation after circulatory death heart transplantation, Curr. Opin. Organ Transpl. 22 (3) (2017) 189–197, https://doi.org/10.1097/MOT.0000000000000419.
[4] M.M. Vela, D.G. Sáez, A.R. Simon, Current approaches in retrieval and heart preservation, Ann. Cardiothorac. Surg. 7 (1) (2018) 67–74, https://doi.org/10.21037/ACS.2018.01.06.
[5] G. Gerosa, P. Zanatta, A. Angelini, et al., Overcoming the Boundaries of Heart Warm Ischemia in Donation After Circulatory Death: The Padua Case, in: ASAIO J, 9, Published online February, 2024, https://doi.org/10.1097/MAT.0000000000002141.
[6] A. Iyer, H.C. Chew, L. Gao, et al., Pathophysiological trends during withdrawal of life support: implications for organ donation after circulatory death, Transplantation 100 (12) (2016) 2621–2629, https://doi.org/10.1097/TP.0000000000001396.
[7] T. Zhou, E.R. Prather, D.E. Garrison, L. Zuo, Interplay between ROS and Antioxidants during Ischemia-Reperfusion Injuries in Cardiac and Skeletal Muscle, *Page 417*. 2018;19, Int. J. Mol. Sci. Vol 19 (2) (2018) 417, https://doi.org/10.3390/IJMS19020417.
[8] A. Görlach, E.Y. Dimova, A. Petry, et al., Reactive oxygen species, nutrition, hypoxia and diseases: problems solved? Redox Biol. 6 (2015) 372–385, https://doi.org/10.1016/J.REDOX.2015.08.016.

[9] Ma Y. Role of Neutrophils in Cardiac Injury and Repair Following Myocardial Infarction. Cells 2021, Vol 10, Page 1676. 2021;10 (7):1676. doi:10.3390/CELLS10071676.
[10] X. Chapa-Dubocq, V. Makarov, S. Javadov, Simple kinetic model of mitochondrial swelling in cardiac cells, J. Cell Physiol. 233 (7) (2018) 5310, https://doi.org/10.1002/JCP.26335.
[11] Tolomeo A.M., Fabozzo A., Malvicini R., et al. Temperature-Related Effects of Myocardial Protection Strategies in Swine Hearts after Prolonged Warm Ischemia. Antioxidants. 2022;11(3):476. doi:10.3390/ANTIOX11030476/S1.
[12] R. Malvicini, G. De Lazzari, A.M. Tolomeo, et al., Influence of the isolation method on characteristics and functional activity of mesenchymal stromal cell-derived extracellular vesicles, Cytotherapy 26 (2) (2024) 157–170, https://doi.org/10.1016/J.JCYT.2023.11.001.
[13] A.Del Fattore, R. Luciano, L. Pascucci, et al., Immunoregulatory effects of mesenchymal stem cell-derived extracellular vesicles on T lymphocytes, Cell Transpl. 24 (12) (2015) 2615–2627, https://doi.org/10.3727/096368915X687543.
[14] M. Zhao, M. Kang, J. Wang, et al., Stem Cell-Derived Nanovesicles Embedded in Dual-Layered Hydrogel for Programmed ROS Regulation and Comprehensive Tissue Regeneration in Burn Wound Healing. Adv Mater, Published online, 2024, https://doi.org/10.1002/ADMA.202401369.
[15] M. Quaglia, G. Merlotti, A. Colombatto, et al., Stem cell-derived extracellular vesicles as potential therapeutic approach for acute kidney injury, Front. Immunol. 13 (2022), https://doi.org/10.3389/FIMMU.2022.849891.
[16] A. Psaraki, L. Ntari, C. Karakostas, D. Korrou-Karava, M.G. Roubelakis, Extracellular vesicles derived from mesenchymal stem/stromal cells: The regenerative impact in liver diseases, Hepatology 75 (6) (2022) 1590–1603, https://doi.org/10.1002/HEP.32129.
[17] R. Malvicini, D. Santa-Cruz, G. De Lazzari, et al., Macrophage bioassay standardization to assess the anti-inflammatory activity of mesenchymal stromal cell-derived small extracellular vesicles, Cytotherapy 24 (10) (2022), https://doi.org/10.1016/J.JCYT.2022.05.011.
[18] N. Conrad, A. Judge, J. Tran, et al., Temporal trends and patterns in heart failure incidence: a population-based study of 4 million individuals, Lancet 391 (10120) (2018) 572–580, https://doi.org/10.1016/S0140-6736(17)32520-5.
[19] R. Gelpi, D. Paredes, C. Rodríguez-Villar, et al., The development of a predictive model of graft function in uncontrolled donors after circulatory death: validity of a pulsatile renal preservation machine cut-off value for kidney acceptance, Nephrol. Dial. Transpl. 34 (3) (2019) 531–538, https://doi.org/10.1093/NDT/GFY241.
[20] M. Bissolati, P.G. Gazzetta, R. Caldara, et al., Renal resistance trend during hypothermic machine perfusion is more predictive of postoperative outcome than biopsy score: preliminary experience in 35 consecutive kidney transplantations, Artif. Organs 42 (7) (2018) 714–722, https://doi.org/10.1111/AOR.13117.
[21] D.W. Greening, S.K. Gopal, R. Xu, R.J. Simpson, W. Chen, Exosomes and their roles in immune regulation and cancer, Semin. Cell Dev. Biol. 40 (2015) 72–81, https://doi.org/10.1016/J.SEMCDB.2015.02.009.
[22] O.G. de Jong, B.W.M. van Balkom, R.M. Schiffelers, C.V.C. Bouten, M.C. Verhaar, Extracellular vesicles: potential roles in regenerative medicine, Front. Immunol. 5 (DEC) (2014) 608, https://doi.org/10.3389/FIMMU.2014.00608/BIBTEX.
[23] Z. Hu, W. Wang, Y. Lin, et al., Extracellular vesicle-inspired therapeutic strategies for the COVID-19 (Published online), Adv. Health Mater. (2024) 2402103, https://doi.org/10.1002/ADHM.202402103 (Published online).
[24] S. Gennai, A. Monsel, Q. Hao, J. Park, M.A. Matthay, J.W. Lee, Microvesicles derived from human mesenchymal stem cells restore alveolar fluid clearance in human lungs rejected for transplantation, Am. J. Transpl. 15 (9) (2015) 2404–2412, https://doi.org/10.1111/AJT.13271.
[25] R.C. Lai, F. Arslan, M.M. Lee, et al., Exosome secreted by MSC reduces myocardial ischemia/reperfusion injury, Stem Cell Res. 4 (3) (2010) 214–222, https://doi.org/10.1016/j.scr.2009.12.003.
[26] R.L. Webb, E.E. Kaiser, S.L. Scoville, et al., Human neural stem cell extracellular vesicles improve tissue and functional recovery in the murine thromboembolic stroke model, Transl. Stroke Res. 9 (5) (2018) 530–539, https://doi.org/10.1007/S12975-017-0599-2.
[27] B. Giebel, L. Kordelas, V. Börger, Clinical potential of mesenchymal stem/stromal cell-derived extracellular vesicles, Stem Cell Invest. 4 (10) (2017), https://doi.org/10.21037/sci.2017.09.06.
[28] X. Cui, Z. He, Z. Liang, Z. Chen, H. Wang, J. Zhang, Exosomes from adipose-derived mesenchymal stem cells protect the myocardium against Ischemia/Reperfusion injury through Wnt/β-Catenin signaling pathway, J. Cardiovasc. Pharmacol. 70 (4) (2017) 225, https://doi.org/10.1097/FJC.0000000000000507.
[29] L. Liu, X. Jin, C.F. Hu, R. Li, Z. Zhou, C.X. Shen, Exosomes derived from mesenchymal stem cells rescue myocardial ischaemia/reperfusion injury by inducing cardiomyocyte autophagy Via AMPK and Akt pathways, Cell Physiol. Biochem. 43 (1) (2017) 52–68, https://doi.org/10.1159/000480317.
[30] L. Kordelas, V. Rebmann, A.K. Ludwig, et al., MSC-derived exosomes: a novel tool to treat therapy-refractory graft-versus-host disease, Leukemia 28 (4) (2014) 970–973, https://doi.org/10.1038/leu.2014.41.
[31] Yu B., Zhang X., Li X. Exosomes Derived from Mesenchymal Stem Cells. Int J Mol Sci 2014, Vol 15, Pages 4142-4157. 2014;15(3):4142-4157. doi:10.3390/IJMS15034142.
[32] Li J., Komatsu H., Poku E.K., et al. Biodistribution of Intra-Arterial and Intravenous Delivery of Human Umbilical Cord Mesenchymal Stem Cell-Derived Extracellular Vesicles in a Rat Model to Guide Delivery Strategies for Diabetes Therapies. Pharm 2022, Vol 15, Page 595. 2022;15(5):595. doi:10.3390/PH15050595.
[33] A.M. Tolomeo, G. Zuccolotto, R. Malvicini, et al., Biodistribution of intratracheal, intranasal, and intravenous injections of human mesenchymal stromal cell-derived extracellular vesicles in a mouse model for drug delivery studies, Pharmaceutics 15 (2) (2023), https://doi.org/10.3390/PHARMACEUTICS15020548.
[34] A. Gowen, F. Shahjin, S. Chand, K.E. Odegaard, S.V. Yelamanchili, Mesenchymal stem cell-derived extracellular vesicles: challenges in clinical applications, Front. Cell Dev. Biol. 8 (2020) 518114, https://doi.org/10.3389/FCELL.2020.00149/BIBTEX.
[35] T. Rampino, M. Gregorini, G. Germinario, et al., Extracellular vesicles derived from mesenchymal stromal cells delivered during hypothermic oxygenated machine perfusion repair Ischemic/Reperfusion damage of kidneys from extended criteria donors, Biolog 11 (3) (2022) 350, https://doi.org/10.3390/BIOLOGY11030350/S1.
[36] Yang X., Meng S., Jiang H., Chen T., Wu W. Exosomes derived from interleukin-10-treated dendritic cells can inhibit trinitrobenzene sulfonic acid-induced rat colitis. https://doi.org/103109/003655212010490596. 2010;45(10):1168-1177. doi:10.3109/00365521.2010.490596.
[37] K.L. Wong, S. Zhang, M. Wang, et al., Intra-articular injections of mesenchymal stem cell exosomes and hyaluronic acid improve structural and mechanical properties of repaired cartilage in a rabbit model, e2, Arthrosc. J. Arthrosc. Relat. Surg. 36 (8) (2020) 2215–2228, https://doi.org/10.1016/j.arthro.2020.03.031.
[38] K.T.C. Hede, B.B. Christensen, M.L. Olesen, et al., Mesenchymal stem cell extracellular vesicles as adjuvant to bone marrow stimulation in chondral defect repair in a minipig model, Cartilage 13 (2_suppl) (2021) 254S–266S, doi:10.1177/19476035211029707/ASSET/IMAGES/LARGE/10.1177_19476035211029707-FIG2.JPEG.
[39] H.-C. Lau, D. Woo, H. Jinhee, et al., GMP-compliant manufacturing of biologically active cell-derived vesicles produced by extrusion technology, J. Extra Biol. 1 (12) (2022) e70, https://doi.org/10.1002/JEX2.70.
[40] M. Kemp, J. Donovan, H. Higham, J. Hooper, Biochemical markers of myocardial injury, Br. J. Anaesth. 93 (1) (2004) 63–73, https://doi.org/10.1093/BJA/AEH148.
[41] S. Cogliati, C. Frezza, M.E. Soriano, et al., Mitochondrial cristae shape determines respiratory chain supercomplexes assembly and respiratory efficiency, Cell 155 (1) (2013) 160–171, https://doi.org/10.1016/J.CELL.2013.08.032.
[42] C. Rodriguez, J.C. Mayo, R.M. Sainz, et al., Regulation of antioxidant enzymes: a significant role for melatonin, J. Pineal Res. 36 (1) (2004) 1–9, https://doi.org/10.1046/J.1600-079X.2003.00092.X.
[43] A.M. Tolomeo, A. Carraro, R. Bakiu, et al., Molecular characterization of novel mitochondrial peroxiredoxins from the Antarctic emerald rockcod and their gene expression in response to environmental warming, Comp. Biochem. Physiol. Part C Toxicol. Pharmacol. 225 (2019) 108580, https://doi.org/10.1016/J.CBPC.2019.108580.

Protective effects of mesenchymal stem cells-derived extracellular vesicles against ischemia-reperfusion injury of hearts donated after circulatory death: preliminary study in a pig model.

Supplementary materials and methods

Materials and Methods

2.1. Animals

Six female pigs of commercial hybrid breed (Large White x Landrance x Duroc) weighing between 40 and 55 kilograms were enrolled in the study. The animals were housed at the Department of Veterinary Medical Sciences of the Alma Mater Studiorum University of Bologna, Italy. From a microbiological point of view, the structure is free of Aujeszky's disease and accredited for swine vesicular disease. The animals were housed in multiple boxes with a light: darkness cycle of 12/12 hours, and a temperature of 18±1° C, water ad libitum and appropriate food to the age of the animal.

2.2. Animal preparation

On the day of the experimental test, the animals, fasted for 12 hours, were sedated by intramuscular injection of 5 mg/kg of tiletamine/zolazepam (Zoletil 50/50, Virbac) and left in a quiet place until they reached lateral recumbency. At this time, venous access was achieved by introducing a 20G venous catheter into the lateral auricular vein. The catheter was used to administer drugs and fluids (Lactated Ringer's 5 ml/kg/h). General anesthesia was induced using Sevoflurane (Sevoflo 6-8% in a 1:1 mixture of medical air and oxygen) via a breathing mask and then maintained, after orotracheal intubation, always with Sevoflurane (2-4%). Respiration was mechanically assisted in PCV (pressure-controlled ventilation) mode set at 12 mmHg with 5 mmHg PEEP, respiratory rate was adjusted to maintain normocapnia. Anesthesiological monitoring consisted of evaluation of pulse oximetry (SpO2), capnography and capnometry, respiratory rate, electrocardiogram, and heart rate. A single intravenous bolus of heparin (300 IU/kg; Eparina Vister, TEVA) was administered to anticoagulate the animals.

2.3. Normothermic perfusion protocol

Animals were placed in dorsal *recumbency,* and, upon surgical preparation of the field, the left jugular vein was isolated and cannulated with a 13F double lumen cannula for blood collection and central venous pressure (CVP) monitoring. A catheter was inserted percutaneously in the femoral artery to monitor arterial pressure (AP) Euthanasia was performed by administering thiopental 30 mg/kg (Pentothal Sodium, MSD, Italy); equalization of central venous pressure (CVP) and arterial pressure (AP) was used to establish the time of death of the animal. After the declaration of death, we waited 20 minutes, in accordance with Italian jurisprudence for DCD organ donation. No cardioplegia or other preconditioning was administered to the animal since Italian Law does not allow premedication. During this period ventilation was interrupted. After 20 minutes, a median sternotomy was performed to access the heart. The pericardial sac was then opened, and the heart was exposed and observed for signs of macroscopic damage. The animal's heart was then removed and prepared for perfusion. Arterial cannulation was performed with a standard raccord, the pulmonary artery was cannulated with a 22F straight cannula, and ventilation was performed with a 20F ventilation cannula. The perfusion system was composed of four peristaltic pumps, one for the arterial cannula (inserted in the aortic root), one for the venous cannula (inserted in the pulmonary artery) and two for ventilation. Additionally, we used a heat exchanger to perform hot heart perfusion (the initial perfusate temperature was set at 32°C and then heated to 37°C) and a D100 membrane oxygenator to oxygenate the perfusate. Perfusion was performed at a pressure of 40 mmHg; this value was chosen since it is the average of the values used in other experimental settings [1–3].

At the time of starting the perfusion, a priming solution mixed 1:1 with the animal's blood, which had been leukodepleted, was used. The final composition of the priming solution is described in Table 1. In addition, 250 mg of methylprednisolone, 1 IU of multivitamin and 100 ml of human albumin were added to the priming solution, following the standard protocol for organ harvesting in the clinical practice of ex-vivo cardiac preservation. The control group received 2mL of PBS+ 500mM NaCl, while the group treated with MSC-EV received 1x1011 EV, in a final volume of 1-2mL, depending on the concentration of the preparation. The vesicles were thawed at room temperature before being used and added to the priming solution. A standard maintenance solution for ex vivo cardiac perfusion was used for perfusion maintenance (2 hours). The composition of the maintenance solution is reported in Table 2. The solution maintenance was administered directly into the perfusion circuit at 20 cc/h. If necessary, Thamesol was added to the solution as a pH buffer. During the entire perfusion period, blood samples were taken from the circuit every 30 minutes and biochemical parameters were measured: glucose and lactate, to estimate the metabolic activity of the organ; ions (Na+, K+, Cl-); troponin C (TnC), AST, ALT and creatinine phosphokinase (CK) to evaluate cardiac damage. pH values were measured using iSTAT every 10 minutes of perfusion.

Blood samples taken from the circuit were analyzed at the clinical pathology service (CLINLAB) of the Department of Veterinary Medicine of the Alma Mater Studiorum University of Bologna. Biochemical analysis was performed using a Beckman Coulter AU480 clinical chemistry analyzer, using serum. Hematological analysis was performed using a SIEMES ADVIA 2120 hematology analyzer using K3EDTA whole blood samples. After 2 hours of perfusion, samples were taken for analysis. Samples for histological analysis were fixed in 4% paraformaldehyde in PBS, while the rest of the samples were frozen in liquid nitrogen until use.

Substrate	Concentration
Na+ (mEq/L)	132
K+ (mEq/L)	4,2
Ca++ (mEq/L)	1,2
Cl- (mEq/L)	84
Mg++ (mEq/L)	1
Phosphate (mEq/L)	2,9
Glucose (mg/dl)	148

Table S1. Composition of the priming solution.

Substrate	mg in 500ml H_2O
$CaCl_2 \cdot 2H_2O$	2400
NaCl	1750
Adenosine	750
L-arginine	700
$MgSO_4 \cdot 6H_2O$	400
Glycine	350
L-leucine	343
L-glutamic acid	258
L-aspartic acid	245
Lisine acetate	225
L-histidine	225
L-alanine	174
L-valine	171.5
L-proline	126
L-isoleucine	115.5
L-serine	93
L-tirosine	92
L-treonine	70
L-methionine	59
L-phenialalanine	52
L-triptophan	35
KCl	20

Table S2. Composition of the maintenance solution

2.4. MSC culture

HUCPVC-derived MSCs purchased from PromoCell (Heidelberg, Germany). HUCPVCs were cultured as previously described [4] and expanded until passage four to establish a cell stock for sEV isolation. At this point, cells were characterized according to ISCT guidelines [5]. For sEV isolation, passage four to five HUCPVCs were thawed and cultured in low-glucose Dulbecco's Modified Eagle's Medium (Thermo Fisher Scientific, Waltham, MA, USA) supplemented with 10% fetal bovine serum (FBS) (Thermo Fisher Scientific), 100 U/mL penicillin and 100 mg/mL streptomycin (Thermo Fisher Scientific) at 37°C in a humidified incubator containing 5% carbon dioxide. Next, cells were collected using trypsin 0.1% in Hank's buffer (Thermo Fisher Scientific) and plated in 175 cm2 culture flasks at a density of 4000 cells/cm2 until 70% confluence. Finally, culture medium was changed to alpha minimal essential medium without phenol red (Thermo Fisher Scientific) or FBS. HUCPVCs were cultured in starvation medium for 48 h. Afterward, conditioned medium was collected and centrifuged at 2500 x g for 10 min to eliminate cellular debris and then filtered using a 0.22-mM syringe-driven filter unit (Millex-GP; MilliporeSigma, Burlington, MA, USA). The supernatant was processed immediately and the obtained sEVs were subjected to particle number assessment and protein, lipid and RNA quantification. Next, the sEV preparations were aliquoted and frozen at -80°C until use. Three separate independent isolations from HUCPVCs (passages six to eight), thawed at different times but from the same lot, were performed for each isolation method.

2.5. MSC-EV isolation

MSC-sEVs were isolated by ion exchange chromatography (IEX) or ultrafiltration (UF). Conditioned media was processed as previously described [6]. Briefly, to isolate MSC-sEVs by IEX, either fresh or thawed (at 37°C) conditioned media (150 ml) was applied directly to a column containing an anion exchange resin (4-ml bed volume, Q Sepharose Fast Flow, GE Healthcare, Chicago, IL, USA) that had been equilibrated with 50 mM NaCl in 50 mM phosphate buffer (pH 7.5). Then, the column resin was washed with 100 mM NaCl in 50 mM phosphate buffer (pH 7.5) and then eluted with 8 mL of 500 mM NaCl in 50 mM phosphate buffer (pH 7.5). Eight fractions of 1 ml each were collected. EVs were eluted in fraction 4 and only this fraction was used for the experiments. Samples were stored at -80°C until their use.

2.6. Tunable Resistive Pulse Sensing (tRPS)

Particle concentration and size distribution were analyzed using tunable-resistive-pulse-sensing (TRPS) technology with the qNano instrument (Izon Science, Christchurch, New Zealand). NP100 or NP150 membranes were used for the analysis. The concentration of particles was standardized using a CPC100 calibration solution diluted 1:1,000 (110 nm mean carboxylate polystyrene beads; stock concentration 1.00 × 1012) [4].

2.7. Transmission Electron Microscopy for MSC-EV characterization

MSC-EVs were fixed with 4% PFA for 5 min, and one drop (2.00 × 109 particles) of EVs was placed on a 400-mesh holey-film grid for 10 min. After washing with PBS, the MSC-EVs were stained with 1% uranyl acetate for 2 min. The sample was then washed with PBS and finally observed with a Tecnai G2 (FEI; Thermo Fisher Scientific, Waltham, MA, USA) transmission electron microscope operating at 100 kV. Images were captured with a Veleta (Olympus Soft Imaging System; Münster, Germany) digital camera.

2.8. Immunophenotyping of MSC-EVs

MSC-EVs were characterized by flow cytometry using the MacsPlex Exosome Kit (Miltenyi Biotec, Bergisch Gladbach, Germany), following manufacturer's instructions. Briefly, 1.00 × 109 particles of MSC-EVs were loaded in a 1.5 mL tube and diluted to 120 µL with MACSPlex buffer. Then, a mix of 15 µL of exosome capture beads and 15 µL of antibody were added to each tube and incubated for 1 h at RT in agitation. For blank control, only MACSPlex buffer was used. Then, 500 µL of MACSPlex buffer was added to each tube and the EVs were centrifuged at 3000× g for 5 min. Finally, 500 µL of the supernatant was discarded and the samples were resuspended and transferred to a flow-cytometry tube. Samples were analyzed using a Cytoflex (Beckman Coulter, Brea, CA, USA) flow cytometer.

2.9. Histological analysis

To evaluate microscopic signs of damage, samples were taken from the ventricles and interventricular septum and then analyzed. Immediately after collection, samples were fixed in 10% buffered formalin. After 24 hours of fixation, all samples were embedded in paraffin blocks, then sectioned into 5-micron slices, and then stained with hematoxylin-eosin. Signs of hemorrhage, edema, coagulative necrosis and cellular infiltration were evaluated in the histological samples. Histological scoring was applied according to an evaluation of the percentage of altered cells over the total number of cells observed as follows: 0 (< 1%), 1 (1-25%), 2 (25-50%), 3 (50-75%), 4 (>75%).

To evaluate apoptosis in cardiac tissue, caspase-3 levels were measured by immunohistochemistry. The streptavidin-biotin-peroxidase technique (BIO SPA, Milan, Italy) was followed with Cleaved Caspase-3 antibody (dilution 1:2000, Cell Signaling). After incubating the samples with 0.3% hydrogen peroxide in methanol for 30 minutes, the sections were incubated overnight in a humidified chamber at 4°C with the primary antibody. The sections were then washed in PBS and incubated with the secondary antibody (biotin-linked anti-rabbit IgG) for 30 min at room temperature. They were subsequently incubated with streptavidin-biotin-peroxidase for 25 minutes at room temperature. Then, they were incubated for 10 minutes

in DAB chromogen solution (0.02% diaminobenzidine and 0.001% hydrogen peroxide in PBS), the sections were immediately washed with PBS and then with water. After washing, sections were counterstained (hematoxylin), dehydrated, and fixed with DPX (Fluka). The results were expressed as the total number of positive cells in 10 fields at 40x magnification.

2.10. Transmission Electron Microscopy for Mitochondrial Evaluation

Small cardiac tissue samples (about 1–2 mm3) were fixed in 2% glutaraldehyde plus 2% paraformaldehyde in 0.1 M sodium cacodylate buffer pH 7.4 O.N. at 4 °C, subsequently postfixed in osmium tetroxide 1% in 0.1 M sodium cacodylate buffer for 2 h at 4 °C and embedded in an Epon–Araldite resin mixture. Semithin sections were stained with toluidine blue. Ultrathin sections (60–70 nm) were obtained with a Leica Ultracut EM UC7 ultramicrotome, counterstained with uranyl acetate and lead citrate, and viewed with a Tecnai G2 (FEI) transmission electron microscope operating at 100 kV. Images were captured with a Veleta (Olympus Soft Imaging System, Olympus Italia S.r.l., 20054 Segrate, Italy) digital camera.

2.11. Mitochondrial analysis

Changes in mitochondrial cristae morphology were quantified by counting mitochondria with reduced lamellar density and/or abnormal lamellar structure and expressing these mitochondria relative to the total number of mitochondria counted.

2.12. Preparation of tissue samples

Biopsies derived from pig hearts were homogenized with a Polytron in 4 vol/g tissue of 10 mM Tris-HCl buffer pH 7.6, containing 1 mM DTT (dithiothreitol), 0.5 M sucrose, and 0 KCl. .15 M. The homogenates were centrifuged at 20,000 rpm for 60 min at 4 ◦C (Beckman model J2/21). The supernatants were collected and stored at −80◦C for biochemical analysis. From each animal, a sample was taken from the left ventricle, one from the right ventricle and one from the interventricular septum, which were processed independently. The determination of proteins in the samples was carried out using the BCA method (BCA protein assay kit, Thermofisher).

2.13. Determination of SOD activity

To determine the enzymatic activity of SOD, the supernatant of the cardiac tissue homogenates was used. A commercial kit was used, and the manufacturer's instructions were followed (SOD determination kit, 19160, Sigma). Briefly, the kit uses the highly water-soluble tetrazolium salt, WST-1 [2-(4-iodophenyl)-3-(4-nitrophenyl)-5-(2,4-disulfophenyl)- 2Htetrazolium, monosodium salt] which produces a water-soluble formazan dye upon reduction with a superoxide anion. The reduction rate con ●O2 is linearly related to xanthine oxidase (XO) activity and is inhibited by SOD. Therefore, the IC50 (50% SOD inhibition activity) can be determined by a colorimetric method, measuring the absorbance at 440 nm, which is proportional to the amount of superoxide anion. Thus, SOD activity as inhibition activity can be quantified by measuring the decrease in absorbance at 440 nm. To do this, a solution containing the WST is added to 20µL of sample or standard and mixed. Then, a solution containing xanthine oxidase is added and incubated at 37°C for 20 minutes. Once the incubation is completed, the absorbance is measured at 450nm.

2.14. Determination of CAT activity

To determine the enzymatic activity of CAT, the supernatant of the cardiac tissue homogenates was used. A commercial kit was used, and the manufacturer's instructions were followed (Catalase activity assay kit, ab83464, Abcam). Briefly, the catalase present in the sample reacts with hydrogen peroxide (H2O2) to produce water and oxygen. Unmetabolized H2O2 reacts with a probe to produce a product that can be measured colorimetrically at 570 nm or. Therefore, the catalase activity present in the sample is inversely proportional to the signal obtained. To do this, the samples and standards are added to the wells in a 96-well plate. Stop solution is added to the sample control wells and incubated at 25ºC for 5 min. Then, H2O2

solution is added to the wells and incubated for 30 min at 25ºC, when stop solution is added. Finally, the developer mixture is added, incubated for 10 min at 25ºC and the absorbance is read at 570 nm.

2.15. Determination of GPx activity

To determine the enzymatic activity of GPx, the supernatant of the cardiac tissue homogenates was used. A commercial kit was used, and the manufacturer's instructions were followed (Glutathione peroxidase activity assay kit, ab102530, Abcam). Briefly, glutathione peroxidase (GPx) oxidizes GSH to produce GSSG as part of the reaction in which it reduces cumene hydroperoxide. Glutathione reductase (GR) then reduces GSSG to produce GSH, and in the same reaction consumes NADPH. The decrease in NADPH (measured at 340 nm) is proportional to GPx activity. To do this, 20µL of the sample is loaded into a 96-well plate, then the reaction mixture is added and incubated for 15 min at room temperature to exhaust all the GSSG in the sample. Cumene hydroperoxide is then added and analyzed with a microplate reader after at least 5 minutes.

2.16. Determination of carbonylated proteins

For the determination of carbonylated proteins, the supernatant of the cardiac tissue homogenates was used. A commercial kit was used, and the manufacturer's instructions were followed (Protein Carbonyl Content Assay Kit, ab126287, Abcam). Briefly, the protein carbonylation determination assay is based on the reaction of DNPH with protein carbonyls. The DNP hydrazones formed in this reaction can be quantified at an absorbance of 375 nm. To do this, DNPH is added to the samples and incubated for 10 min. TCA (trichloroacetic acid) is then added to the samples and incubated for 5 min. Then centrifuged for 2 min, the supernatant is discarded, and the pellet is washed with acetone. Finally, a guanidine solution is added to resolubilize the pellet and it is transferred to the 96-well plate to measure the absorbance at 375 nm.

2.17. Tissue Repair Mediators Analysis

Tissue Samples Preparation. The biopsies derived from the pigs' hearts were homogenized with Polytron in 4 vol/g of tissue of 10 mM Tris–HCl Buffer pH 7.6, containing 1 mM DTT (dithiothreitol), 0.5 M sucrose and 0.15 M KCl. The homogenates were centrifuged at 20,000 rpm for 60 min at 4 °C (Beckman model J2/21). The supernatants were collected and stored at −80 °C for biochemical analysis, as described below

Estimation of the Total Amount of Proteins. The total amount of proteins in the cellular extracts was assessed by the Folin phenol reagent method [7], using growing concentrations of bovine serum albumin as standard.

Total protein extracts were analyzed to quantify pro-inflammatory cytokines and chemokines, which were simultaneously measured in each protein extract with Luminex xMAP®® technology (Luminex Corporation, Austin, TX, USA). Each measurement was performed in duplicate. Quantitative analyses were performed with Luminex xPONENT 3.1 Software using a five-parameter logistic curve fitting. Data were expressed as pg per mg tissue.

2.18 Statistical analysis

One-way ANOVA with Kruskal–Wallis test were used for multiple comparisons. Median ± range was used. Student's unpaired t-test was used for independent samples. Data were analyzed using GraphPad software. P-values: * $p < 0.05$; ** $p < 0.01$; *** $p < 0.005$; **** $p < 0.0001$.

References

1. Lucchinetti E, Lou PH, Hatami S, Qi X, Clanachan AS, Freed DH, et al. Enhanced myocardial protection in cardiac donation after circulatory death using Intralipid® postconditioning in a porcine model. Can J Anaesth. 2019;66: 672–685. doi:10.1007/S12630-019-01322-X
2. White CW, Ambrose E, Müller A, Li Y, Le H, Thliveris J, et al. Avoidance of Profound

Hypothermia During Initial Reperfusion Improves the Functional Recovery of Hearts Donated After Circulatory Death. Am J Transplant. 2016;16: 773–782. doi:10.1111/AJT.13574

3. Hatami S, White CW, Ondrus M, Qi X, Buchko M, Himmat S, et al. Normothermic Ex Situ Heart Perfusion in Working Mode: Assessment of Cardiac Function and Metabolism. J Vis Exp. 2019;2019. doi:10.3791/58430

4. Malvicini R, De Lazzari G, Tolomeo AM, Santa-Cruz D, Ullah M, Cirillo C, et al. Influence of the isolation method on characteristics and functional activity of mesenchymal stromal cell-derived extracellular vesicles. Cytotherapy. 2024;26: 157–170. doi:10.1016/J.JCYT.2023.11.001

5. Dominici M, Le Blanc K, Mueller I, Slaper-Cortenbach I, Marini FC, Krause DS, et al. Minimal criteria for defining multipotent mesenchymal stromal cells. The International Society for Cellular Therapy position statement. Cytotherapy. 2006;8: 315–317. doi:10.1080/14653240600855905

6. Malvicini R, Santa-Cruz D, Tolomeo AM, Muraca M, Yannarelli G, Pacienza N. Ion exchange chromatography as a simple and scalable method to isolate biologically active small extracellular vesicles from conditioned media. PLoS One. 2023;18: e0291589. doi:10.1371/JOURNAL.PONE.0291589

7. LOWRY OH, ROSEBROUGH NJ, FARR AL, RANDALL RJ. Protein measurement with the Folin phenol reagent. J Biol Chem. 1951;193: 265–275. doi:10.1016/s0021-9258(19)52451-6

Conclusion

The purpose of this thesis was to create a scientific link between comprehensive research and experimental work, which focuses not on a specific field of research, but on the occurrence of mitochondria dysfunction that is involved in multiple pathophysiological processes. Integrating knowledge from diverse scientific fields and research areas, it is possible to identify unexpected links which may enable research to uncover new insights through the synthesis of these varied findings.

For instance, the study on enrolment of essential oils as potential alternatives for boar semen preservation, revealed that some of the selected oils can be considered safe below certain critical concentrations, paving the way for subsequent steps in the research. It is also highlighted the importance of using boar semen, not only as the endpoint of the study, but also as a model for cytotoxicity research, given the high sensitivity of this particular cell type, as already largely discussed in the Introduction section.

Boar spermatozoa also represent an important tool for studying of cross-species process that involves almost all mammalian species: maternal mitochondrial inheritance. As observed, several encouraging findings have emerged regarding the use of an innovative *porcine cell-free system*, which has already revealed many new candidate proteins that could be investigated in mitophagy studies. In this area of research, there is a pivotal moment that could open many avenues in the scientific field and have significant translational and clinical implications for mitochondrial diseases.

The roe deer experimental study, on the other hand, demonstrates the importance of selecting the appropriate study model to better understand the genes involved in a specific pathway, such as oxidative stress and angiogenesis, exploiting the unique characteristics of this species. roe deer allows the observation of rapid testicular remodelling changes, which occur annually rather than over the reproductive lifespan of a single animal. This enables the analysis from a transcriptomic and proteomic perspective. The findings of this study have important implications for research on a topic of male fertility in pathological conditions.

Finally, it has been shown that the urgency to find alternatives to DBD organ donation has driven research toward solutions that, until a few years ago, might have seemed like science fiction. The use of porcine model, so valuable in cardiac surgery, can once again pave the way for understanding mitochondrial dysfunction, which is among the

primary causes of cardiomyocyte death following ischemia-reperfusion injury. Considering these organelles as therapeutic targets may represent a key step in studying this highly delicate and ethically complex field.

At the outset of my PhD, I had no idea of the profound and intricate implications that scientific inquiry entails. Over these years I have explored these dimensions and broadened my perspective beyond the limits imposed by a single viewpoint, embracing *transdisciplinarity*, which I now regard as an essential key asset for 21st-century science.

References

Abruzzese, G. A., Sanchez-Rodriguez, A., & Roldan, E. R. S. (2024). Sperm Metabolism. *Molecular Reproduction and Development*, *91*(10), e23772. https://doi.org/10.1002/mrd.23772

Adlam, V. J., Harrison, J. C., Porteous, C. M., James, A. M., Smith, R. A. J., Murphy, M. P., & Sammut, I. A. (2005). Targeting an antioxidant to mitochondria decreases cardiac ischemia-reperfusion injury. *FASEB Journal: Official Publication of the Federation of American Societies for Experimental Biology*, *19*(9), 1088–1095. https://doi.org/10.1096/fj.05-3718com

Aitken, R. J., & Drevet, J. R. (2020). The Importance of Oxidative Stress in Determining the Functionality of Mammalian Spermatozoa: A Two-Edged Sword. *Antioxidants (Basel, Switzerland)*, *9*(2), 111. https://doi.org/10.3390/antiox9020111

Akande, O., Chen, Q., Toldo, S., Lesnefsky, E. J., & Quader, M. (2020). Ischemia and reperfusion injury to mitochondria and cardiac function in donation after circulatory death hearts- an experimental study. *PLoS ONE*, *15*(12), e0243504. https://doi.org/10.1371/journal.pone.0243504

Althouse, G. C., & Lu, K. G. (2005). Bacteriospermia in extended porcine semen. *Theriogenology, Proceedings of the V International Conference on Boar Semen Preservation*, *63*(2), 573–584. https://doi.org/10.1016/j.theriogenology.2004.09.031

Anderson, S., Bankier, A. T., Barrell, B. G., de Bruijn, M. H. L., Coulson, A. R., Drouin, J., Eperon, I. C., Nierlich, D. P., Roe, B. A., Sanger, F., Schreier, P. H., Smith, A. J. H., Staden, R., & Young, I. G. (1981). Sequence and organization of the

human mitochondrial genome. *Nature*, *290*(5806), 457–465. https://doi.org/10.1038/290457a0

Annesley, S. J., & Fisher, P. R. (2019). Mitochondria in Health and Disease. *Cells*, *8*(7), 680. https://doi.org/10.3390/cells8070680

Aparicio, I. M., Espino, J., Bejarano, I., Gallardo-Soler, A., Campo, M. L., Salido, G. M., Pariente, J. A., Peña, F. J., & Tapia, J. A. (2016). Autophagy-related proteins are functionally active in human spermatozoa and may be involved in the regulation of cell survival and motility. *Scientific Reports*, *6*(1), 33647. https://doi.org/10.1038/srep33647

Atici, A. E., Crother, T. R., & Noval Rivas, M. (2023). Mitochondrial quality control in health and cardiovascular diseases. *Frontiers in Cell and Developmental Biology*, *11*, 1290046. https://doi.org/10.3389/fcell.2023.1290046

Awda, B. J., Mackenzie-Bell, M., & Buhr, M. M. (2009). Reactive oxygen species and boar sperm function. *Biology of Reproduction*, *81*(3), 553–561. https://doi.org/10.1095/biolreprod.109.076471

Balbach, M., Ghanem, L., Violante, S., Kyaw, A., Romarowski, A., Cross, J. R., Visconti, P. E., Levin, L. R., & Buck, J. (2023). Capacitation induces changes in metabolic pathways supporting motility of epididymal and ejaculated sperm. *Frontiers in Cell and Developmental Biology*, *11*. https://doi.org/10.3389/fcell.2023.1160154

Banaszewska, D., & Andraszek, K. (2021). Assessment of the Morphometry of Heads of Normal Sperm and Sperm with the Dag Defect in the Semen of Duroc Boars. *Journal of Veterinary Research*, *65*(2), 239–244. https://doi.org/10.2478/jvetres-2021-0019

Beckman, K. B., & Ames, B. N. (1998). The free radical theory of aging matures. *Physiological Reviews*, *78*(2), 547–581. https://doi.org/10.1152/physrev.1998.78.2.547

Belmonte, S. A., López, C. I., Roggero, C. M., De Blas, G. A., Tomes, C. N., & Mayorga, L. S. (2005). Cholesterol content regulates acrosomal exocytosis by enhancing Rab3A plasma membrane association. *Developmental Biology*, *285*(2), 393–408. https://doi.org/10.1016/j.ydbio.2005.07.001

Blottner, S., Hingst, O., & Meyer, H. H. D. (1996). Seasonal spermatogenesis and testosterone production in roe deer (Capreolus capreolus). *Reproduction*, *108*(2), 299–305. https://doi.org/10.1530/jrf.0.1080299

Borkowski, J., Banul, R., Jurkiewicz-Azab, J., Hołdyński, C., Święczkowska, J., Nasiadko, M., & Załuski, D. (2021). There is only one winner: The negative impact of red deer density on roe deer numbers and distribution in the Słowiński National Park and its vicinity. *Ecology and Evolution*, *11*(11), 6889–6899. https://doi.org/10.1002/ece3.7538

Brüssow, K.-P., Rátky, J., & Rodriguez-Martinez, H. (2008). Fertilization and early embryonic development in the porcine fallopian tube. *Reproduction in Domestic Animals = Zuchthygiene*, *43 Suppl 2*, 245–251. https://doi.org/10.1111/j.1439-0531.2008.01169.x

Bugger, H., & Pfeil, K. (2020). Mitochondrial ROS in myocardial ischemia reperfusion and remodeling. *Biochimica Et Biophysica Acta. Molecular Basis of Disease*, *1866*(7), 165768. https://doi.org/10.1016/j.bbadis.2020.165768

Contreras, M. J., Núñez-Montero, K., Bruna, P., García, M., Leal, K., Barrientos, L., & Weber, H. (2022). Bacteria and Boar Semen Storage: Progress and

Challenges. *Antibiotics*, *11*(12), 1796. https://doi.org/10.3390/antibiotics11121796

Coy, P., García-Vázquez, F., Visconti, P., & Avilés, M. (2012). Roles of the oviduct in mammalian fertilization. *Reproduction (Cambridge, England)*, *144*(6), 649–660. https://doi.org/10.1530/REP-12-0279

Cung, T.-T., Morel, O., Cayla, G., Rioufol, G., Garcia-Dorado, D., Angoulvant, D., Bonnefoy-Cudraz, E., Guérin, P., Elbaz, M., Delarche, N., Coste, P., Vanzetto, G., Metge, M., Aupetit, J.-F., Jouve, B., Motreff, P., Tron, C., Labeque, J.-N., Steg, P. G., … Ovize, M. (2015). Cyclosporine before PCI in Patients with Acute Myocardial Infarction. *New England Journal of Medicine*, *373*(11), 1021–1031. https://doi.org/10.1056/NEJMoa1505489

Ded, L., Dostalova, P., Zatecka, E., Dorosh, A., Komrskova, K., & Peknicova, J. (2019). *Reproductive Biology and Endocrinology : RB&E*, *17*, 109. https://doi.org/10.1186/s12958-019-0554-z

DiChiacchio, L., Goodwin, M. L., Kagawa, H., Griffiths, E., Nickel, I. C., Stehlik, J., & Selzman, C. H. (2023). Heart Transplant and Donors After Circulatory Death: A Clinical-Preclinical Systematic Review. *The Journal of Surgical Research*, *292*, 222–233. https://doi.org/10.1016/j.jss.2023.07.050

Doulamis, I. P., Tzani, A., Alemany, V. S., Nomoto, R. S., Celik, A., Recco, D. P., Saeed, M. Y., Guariento, A., Plutzky, J., Emani, S. M., del Nido, P. J., & McCully, J. D. (2024). Mitochondrial transplantation normalizes transcriptomic and proteomic shift associated with ischemia reperfusion injury in neonatal hearts donated after circulatory death. *Scientific Reports*, *14*(1), 31236. https://doi.org/10.1038/s41598-024-82578-2

Downing Meisner, A., Klaus, A. V., & O'Leary, M. A. (2005). Sperm head morphology in 36 species of artiodactylans, perissodactylans, and cetaceans (Mammalia). *Journal of Morphology*, *263*(2), 179–202. https://doi.org/10.1002/jmor.10297

Elmi, A., Govoni, N., Zannoni, A., Bertocchi, M., Bernardini, C., Forni, M., Ventrella, D., & Bacci, M. L. (2021). Testicular Melatonin and Its Pathway in Roe Deer Bucks (Capreolus capreolus) during Pre- and Post-Rut Periods: Correlation with Testicular Involution. *Animals : an Open Access Journal from MDPI*, *11*(7), 1874. https://doi.org/10.3390/ani11071874

Elmi, A., Prosperi, A., Zannoni, A., Bertocchi, M., Scorpio, D. G., Forni, M., Foni, E., Bacci, M. L., & Ventrella, D. (2019). Antimicrobial capabilities of non-spermicidal concentrations of tea tree (Melaleuca alternifolia) and rosemary (Rosmarinus officinalis) essential oils on the liquid phase of refrigerated swine seminal doses. *Research in Veterinary Science*, *127*, 76–81. https://doi.org/10.1016/j.rvsc.2019.10.014

Elmi, A., Ventrella, D., Barone, F., Carnevali, G., Filippini, G., Pisi, A., Benvenuti, S., Scozzoli, M., & Bacci, M. (2019). In Vitro Effects of Tea Tree Oil (Melaleuca Alternifolia Essential Oil) and its Principal Component Terpinen-4-ol on Swine Spermatozoa. *Molecules*, *24*(6), 1071. https://doi.org/10.3390/molecules24061071

Elmi, A., Ventrella, D., Barone, F., Filippini, G., Benvenuti, S., Pisi, A., Scozzoli, M., & Bacci, M. (2017). Thymbra capitata (L.) Cav. and Rosmarinus officinalis (L.) Essential Oils: In Vitro Effects and Toxicity on Swine Spermatozoa. *Molecules*, *22*(12), 2162. https://doi.org/10.3390/molecules22122162

Elmi, A., Zannoni, A., Govoni, N., Bertocchi, M., Forni, M., Ventrella, D., & Bacci, M. L. (2020). Uncovering the Physiological Mechanisms Underlying the Roe Deer (Capreolus capreolus) Testicular Cycle: Analyses of Gelatinases and VEGF Patterns and Correlation with Testes Weight and Testosterone. *Animals : an Open Access Journal from MDPI*, *10*(3), 444. https://doi.org/10.3390/ani10030444

Foutouhi, A., & Meyers, S. (2022). Comparative oxidative metabolism in mammalian sperm. *Animal Reproduction Science*, *247*, 107095. https://doi.org/10.1016/j.anireprosci.2022.107095

Gadella, B. M. (2017). Reproductive tract modifications of the boar sperm surface. *Molecular Reproduction and Development*, *84*(9), 822–831. https://doi.org/10.1002/mrd.22821

Gadella, B. M., Tsai, P.-S., Boerke, A., & Brewis, I. A. (2008). Sperm head membrane reorganisation during capacitation. *The International Journal of Developmental Biology*, *52*(5–6), 473–480. https://doi.org/10.1387/ijdb.082583bg

Global Observatory and Transplantation. (2022). *International Report Organ Donation and Transplantation Activities*. https://www.transplant-observatory.org/wp-content/uploads/2023/11/2022-data-global-report_VF_2.pdf

Goeritz, F., Quest, M., Wagener, A., Fassbender, M., Broich, A., Hildebrandt, T. B., Hofmann, R. R., & Blottner, S. (2003). Seasonal timing of sperm production in roe deer: Interrelationship among changes in ejaculate parameters,

morphology and function of testis and accessory glands. *Theriogenology*, *59*(7), 1487–1502. https://doi.org/10.1016/s0093-691x(02)01201-3

Goutchtat, R., Béguier, A., Kasal-Hoc, N., Guerreschi, P., Fayoux, P., Rancan, L., Pattou, F., & Hubert, T. (2025). Pig Models in Translational Surgery. *European Surgical Research. Europaische Chirurgische Forschung. Recherches Chirurgicales Europeennes*, *66*(1), 50–58. https://doi.org/10.1159/000546168

Hirohashi, N., & Yanagimachi, R. (2018). Sperm acrosome reaction: Its site and role in fertilization. *Biology of Reproduction*, *99*(1), 127–133. https://doi.org/10.1093/biolre/ioy045

Jakop, U., Müller, K., Müller, P., Neuhauser, S., Callealta Rodríguez, I., Grunewald, S., Schiller, J., & Engel, K. M. (2022). Seminal lipid profiling and antioxidant capacity: A species comparison. *PLoS ONE*, *17*(3), e0264675. https://doi.org/10.1371/journal.pone.0264675

Jurcau, A., & Ardelean, A. I. (2022). Oxidative Stress in Ischemia/Reperfusion Injuries following Acute Ischemic Stroke. *Biomedicines*, *10*(3), 574. https://doi.org/10.3390/biomedicines10030574

Kahrl, A. F., Snook, R. R., & Fitzpatrick, J. L. (2022). Fertilization mode differentially impacts the evolution of vertebrate sperm components. *Nature Communications*, *13*(1), 6809. https://doi.org/10.1038/s41467-022-34609-7

Kerns, K., Zigo, M., & Sutovsky, P. (2018). Zinc: A Necessary Ion for Mammalian Sperm Fertilization Competency. *International Journal of Molecular Sciences*, *19*(12), 4097. https://doi.org/10.3390/ijms19124097

Koziorowska-Gilun, M., Fraser, L., Gilun, P., Koziorowski, M., & Kordan, W. (2015). Attività degli enzimi antiossidanti e loro espressione di mRNA in diversi tessuti dell'apparato riproduttivo del capriolo maschio (*Capreolus capreolus*) durante la stagione degli amori e la stagione degli amori. *Small Ruminant Research*, *129*, 97–103. https://doi.org/10.1016/j.smallrumres.2015.05.006

Kühlbrandt, W. (2015). Structure and function of mitochondrial membrane protein complexes. *BMC Biology*, *13*, 89. https://doi.org/10.1186/s12915-015-0201-x

Lecewicz, M., Majewska, A., Kordan, W., Wysocki, P., & Koziorowska-Gilun, M. (2017). Changes in the expression of selected antioxidative proteins in roe deer (Capreolus capreolus) epididymis in different periods of the rutting season. *Annals of Animal Science*, *17*(2). https://doi.org/10.1515/aoas-2016-0052

Leung, M. R., Zenezini Chiozzi, R., Roelofs, M. C., Hevler, J. F., Ravi, R. T., Maitan, P., Zhang, M., Henning, H., Bromfield, E. G., Howes, S. C., Gadella, B. M., Heck, A. J. R., & Zeev-Ben-Mordehai, T. (2021). In-cell structures of conserved supramolecular protein arrays at the mitochondria–cytoskeleton interface in mammalian sperm. *Proceedings of the National Academy of Sciences of the United States of America*, *118*(45), e2110996118. https://doi.org/10.1073/pnas.2110996118

Li, S., & Winuthayanon, W. (2017). *Oviduct: Roles in fertilization and early embryo development*. https://doi.org/10.1530/JOE-16-0302

Longnus, S. L., Rutishauser, N., Gillespie, M. N., Reichlin, T., Carrel, T. P., & Sanz, M. N. (2022). Mitochondrial Damage-associated Molecular Patterns as Potential

Biomarkers in DCD Heart Transplantation: Lessons From Myocardial Infarction and Cardiac Arrest. *Transplantation Direct*, *8*(1), e1265. https://doi.org/10.1097/TXD.0000000000001265

Mantle, D., Cufflin, N., Purcell, T. T., & Hargreaves, I. P. (2025). Ischaemia–Reperfusion Injury in Organ Transplantation: Role of Coenzyme Q10. *Journal of Clinical Medicine*, *14*(18), 6486. https://doi.org/10.3390/jcm14186486

Meyerholz, D. K., Burrough, E. R., Kirchhof, N., Anderson, D. J., & Helke, K. L. (2024). Swine models in translational research and medicine. *Veterinary Pathology*, *61*(4), 512–523. https://doi.org/10.1177/03009858231222235

Mills, D. B., Boyle, R. A., Daines, S. J., Sperling, E. A., Pisani, D., Donoghue, P. C. J., & Lenton, T. M. (2022). Eukaryogenesis and oxygen in Earth history. *Nature Ecology & Evolution*, *6*(5), 520–532. https://doi.org/10.1038/s41559-022-01733-y

Mitchell, P. (2011). Chemiosmotic coupling in oxidative and photosynthetic phosphorylation. *Biochimica et Biophysica Acta (BBA) - Bioenergetics, Special Section: Peter Mitchell - 50th anniversary of the chemiosmotic theory*, *1807*(12), 1507–1538. https://doi.org/10.1016/j.bbabio.2011.09.018

Mitchell, P., & Moyle, J. (1967). Respiration-driven proton translocation in rat liver mitochondria. *Biochemical Journal*, *105*(3), 1147–1162. https://doi.org/10.1042/bj1051147

Ngo, C., Suwimonteerabutr, J., Prapasarakul, N., Morrell, J. M., & Tummaruk, P. (2023). Bacteriospermia and its antimicrobial resistance in relation to boar sperm quality during short-term storage with or without antibiotics in a

tropical environment. *Porcine Health Management*, *9*(1), 21. https://doi.org/10.1186/s40813-023-00320-2

Nunnari, J., & Suomalainen, A. (2012). Mitochondria: In sickness and in health. *Cell*, *148*(6), 1145–1159. https://doi.org/10.1016/j.cell.2012.02.035

O'Brien, E., García-Casado, P., Castaño, C., Toledano-Díaz, A., Bóveda, P., & Santiago-Moreno, J. (2021). Sperm Response to in vitro Stress Conditions in Wild and Domestic Species Measured by Functional Variables and ROS Production. *Frontiers in Veterinary Science*, *8*, 650946. https://doi.org/10.3389/fvets.2021.650946

Palma, F. R., Gantner, B. N., Sakiyama, M. J., Kayzuka, C., Shukla, S., Lacchini, R., Cunniff, B., & Bonini, M. G. (2024). ROS production by mitochondria: Function or dysfunction? *Oncogene*, *43*(5), 295–303. https://doi.org/10.1038/s41388-023-02907-z

Parajuli, N., Campbell, L. H., Marine, A., Brockbank, K. G. M., & Macmillan-Crow, L. A. (2012). MitoQ blunts mitochondrial and renal damage during cold preservation of porcine kidneys. *PloS One*, *7*(11), e48590. https://doi.org/10.1371/journal.pone.0048590

Pays, O., Fortin, D., Gassani, J., & Duchesne, J. (2012). Group Dynamics and Landscape Features Constrain the Exploration of Herds in Fusion-Fission Societies: The Case of European Roe Deer. *PLOS ONE*, *7*(3), e34678. https://doi.org/10.1371/journal.pone.0034678

Pezo, F., Romero, F., Zambrano, F., & Sánchez, R. S. (2019). Preservation of boar semen: An update. *Reproduction in Domestic Animals*, *54*(3), 423–434. https://doi.org/10.1111/rda.13389

Pezo, F., Yeste, M., Zambrano, F., Uribe, P., Risopatrón, J., & Sánchez, R. (2021). Antioxidants and their effect on the oxidative/nitrosative stress of frozen-thawed boar sperm. *Cryobiology*, *98*, 5–11. https://doi.org/10.1016/j.cryobiol.2020.11.007

Rj, A. (2017). Reactive oxygen species as mediators of sperm capacitation and pathological damage. *Molecular Reproduction and Development*, *84*(10). https://doi.org/10.1002/mrd.22871

Rodriguez-Martinez, H., Martinez-Serrano, C. A., Alvarez-Rodriguez, M., Martinez, E. A., & Roca, J. (2024). Reproductive physiology of the boar: What defines the potential fertility of an ejaculate? *Animal Reproduction Science, 10th International Conference on Boar Semen Preservation (2024)*, *269*, 107476. https://doi.org/10.1016/j.anireprosci.2024.107476

Ros-Santaella, J. L., Nový, P., Scaringi, M., & Pintus, E. (2024). Antimicrobial peptides and proteins as alternative antibiotics for porcine semen preservation. *BMC Veterinary Research*, *20*(1), 257. https://doi.org/10.1186/s12917-024-04105-9

Sagan, L. (1967). On the origin of mitosing cells. *Journal of Theoretical Biology*, *14*(3), 255–274. https://doi.org/10.1016/0022-5193(67)90079-3

Schulze, M., Ammon, C., Rüdiger, K., Jung, M., & Grobbel, M. (2015). Analysis of hygienic critical control points in boar semen production. *Theriogenology*, *83*(3), 430–437. https://doi.org/10.1016/j.theriogenology.2014.10.004

Siekevitz, P. (1957). Powerhouse of the Cell. *Scientific American*, *197*(1), 131–144. https://doi.org/10.1038/scientificamerican0757-131

Song, W.-H., & Sutovsky, P. (2019). Porcine Cell-Free System to Study Mammalian Sperm Mitophagy. In K. Turksen (A c. Di), *Autophagy in Differentiation and Tissue Maintenance: Methods and Protocols* (pp. 197–207). Springer. https://doi.org/10.1007/7651_2018_158

Song, W.-H., Yi, Y.-J., Sutovsky, M., Meyers, S., & Sutovsky, P. (2016). Autophagy and ubiquitin–proteasome system contribute to sperm mitophagy after mammalian fertilization. *Proceedings of the National Academy of Sciences*, *113*(36), E5261–E5270. https://doi.org/10.1073/pnas.1605844113

Song, W.-H., Zuidema, D., Yi, Y.-J., Zigo, M., Zhang, Z., Sutovsky, M., & Sutovsky, P. (2021). Mammalian Cell-Free System Recapitulates the Early Events of Post-Fertilization Sperm Mitophagy. *Cells*, *10*(9), Articolo 9. https://doi.org/10.3390/cells10092450

Sutovsky, P., & Song, W.-H. (2017). Post-fertilisation sperm mitophagy: The tale of Mitochondrial Eve and Steve. *Reproduction, Fertility, and Development*, *30*(1), 56–63. https://doi.org/10.1071/RD17364

Tari, T., Czimber, K., Faragó, S., Heffenträger, G., Kalmár, S., Kovács, G., Sándor, G., & Náhlik, A. (2025). Roe Deer as a Model Species for Aerial Survey-Based Ungulate Population Estimation in Agricultural Habitats. *Geomatics*, *5*(4), 53. https://doi.org/10.3390/geomatics5040053

Tessari, C., Lucertini, G., Addonizio, M., Geatti, V., Bacich, D., Pradegan, N., Fabozzo, A., Bianco, R., Toscano, G., Tarzia, V., & Gerosa, G. (2025). Ex-Vivo Heart Perfusion Machines in DCD Heart Transplantation Model: The State of Art. *Transplant International*, *38*, 12987. https://doi.org/10.3389/ti.2025.12987

The Regional Government of Emilia-Romagna, U. M. 19. (2024). *Bollettino Ufficiale della Regione Emilia-Romagna — (BURERT)*. Bollettino Ufficiale della Regione Emilia-Romagna — (BURERT). https://bur.regione.emilia-romagna.it

Tolomeo, A. M., Malvicini, R., Ventrella, D., Elmi, A., Lombardi, V., Zanella, F., Andreis, M., Lazzari, G. D., Todeschini, G., Caicci, F., Aniballi, C., Troisio, I., Santovito, G., Bacci, M. L., Muraca, M., Fabozzo, A., & Gerosa, G. (2024). Protective effects of mesenchymal stem cells-derived extracellular vesicles against ischemia-reperfusion injury of hearts donated after circulatory death: Preliminary study in a pig model. *Biomedicine & Pharmacotherapy = Biomedecine & Pharmacotherapie*, *178*, 117256. https://doi.org/10.1016/j.biopha.2024.117256

Troisio, I., Bertocchi, M., Ventrella, D., Scozzoli, M., Di Vito, M., Truzzi, E., Benvenuti, S., Mattarelli, P., Bacci, M. L., & Elmi, A. (2024). Short- and long-term effects of essential oils on swine spermatozoa during liquid phase refrigeration. *Scientific Reports*, *14*(1), 285. https://doi.org/10.1038/s41598-023-51030-2

Vahedi Raad, M., Firouzabadi, A. M., Tofighi Niaki, M., Henkel, R., & Fesahat, F. (2024). The impact of mitochondrial impairments on sperm function and male fertility: A systematic review. *Reproductive Biology and Endocrinology*, *22*(1), 83. https://doi.org/10.1186/s12958-024-01252-4

van der Bliek, A. M., Sedensky, M. M., & Morgan, P. G. (2017). Cell Biology of the Mitochondrion. *Genetics*, *207*(3), 843–871. https://doi.org/10.1534/genetics.117.300262

Ventrella, D., Elmi, A., Barone, F., Carnevali, G., Govoni, N., & Bacci, M. L. (2018). Hair Testosterone and Cortisol Concentrations in Pre- and Post-Rut Roe Deer Bucks: Correlations with Blood Levels and Testicular Morphometric Parameters. *Animals: An Open Access Journal from MDPI*, *8*(7), 113. https://doi.org/10.3390/ani8070113

Wang, Y., Fu, X., & Li, H. (2025). Mechanisms of oxidative stress-induced sperm dysfunction. *Frontiers in Endocrinology*, *16*, 1520835. https://doi.org/10.3389/fendo.2025.1520835

Whitfield, M. (2024). The annulus: Composition, role and importance in sperm flagellum biogenesis and male fertility. *Basic and Clinical Andrology*, *34*(1), 25. https://doi.org/10.1186/s12610-024-00241-2

Wyss, R. K., Méndez-Carmona, N., Sanz, M.-N., Arnold, M., Segiser, A., Fiedler, G. M., Carrel, T. P., Djafarzadeh, S., Tevaearai Stahel, H. T., & Longnus, S. L. (2019). Mitochondrial integrity during early reperfusion in an isolated rat heart model of donation after circulatory death-consequences of ischemic duration. *The Journal of Heart and Lung Transplantation: The Official Publication of the International Society for Heart Transplantation*, *38*(6), 647–657. https://doi.org/10.1016/j.healun.2018.12.013

Xie, J.-R., & Yu, L.-N. (2007). Cardioprotective effects of cyclosporine A in an in vivo model of myocardial ischemia and reperfusion. *Acta Anaesthesiologica Scandinavica*, *51*(7), 909–913. https://doi.org/10.1111/j.1399-6576.2007.01342.x

Zhang, B., Wang, Y., Wu, C., Qiu, S., Chen, X., Cai, B., & Xie, H. (2021). Freeze-thawing impairs the motility, plasma membrane integrity and mitochondria

function of boar spermatozoa through generating excessive ROS. *BMC Veterinary Research*, *17*(1), 127. https://doi.org/10.1186/s12917-021-02804-1

Zhang, M., Bromfield, E. G., Helms, J. B., & Gadella, B. M. (2022). The fate of porcine sperm CRISP2 from the perinuclear theca before and after in vitro fertilization†. *Biology of Reproduction*, *107*(5), 1242–1253. https://doi.org/10.1093/biolre/ioac169

Zhang, M., Bromfield, E. G., Veenendaal, T., Klumperman, J., Helms, J. B., & Gadella, B. M. (2021). Characterization of different oligomeric forms of CRISP2 in the perinuclear theca versus the fibrous tail structures of boar spermatozoa†. *Biology of Reproduction*, *105*(5), 1160–1170. https://doi.org/10.1093/biolre/ioab145

Zhang, X., Yang, Y., Wang, H., Yan, C., Feng, Y., Ma, X., Hu, M., Li, S., & Cheng, C. (2025). Exploring mitochondrial health and transplantation strategies in DCD heart transplantation: A systematic review. *Journal of Translational Medicine*, *23*(1), 789. https://doi.org/10.1186/s12967-025-06805-8

Zigo, M., Netherton, J., Zelenková, N., Kerns, K., Kraus, V., Postlerová, P., Baker, M., & Sutovsky, P. (2024). Bottom-up approach to deciphering the targets of the ubiquitin-proteasome system in porcine sperm capacitation. *Scientific Reports*, *14*(1), 20159. https://doi.org/10.1038/s41598-024-71056-4

Zuidema, D., Jones, A., Song, W.-H., Zigo, M., & Sutovsky, P. (2023). Identification of candidate mitochondrial inheritance determinants using the mammalian cell-free system. *eLife*, *12*, RP85596. https://doi.org/10.7554/eLife.85596

Zuidema, D., & Sutovsky, P. (2020). The domestic pig as a model for the study of mitochondrial inheritance. *Cell and Tissue Research*, *380*(2), 263–271. https://doi.org/10.1007/s00441-019-03100-z

Additional paper

Non-Invasive Hormonal Analysis in Apennine wolf

Troisio, I., Musto, C., Acquisti Casi, N., Govoni, N., Merialdi, G., Ventrella, D., Elmi, A., Delogu, M., & Bacci, M. L. (2025). "***Quantification of steroid hormones in free-ranging Apennine wolf (Canis lupus italicus) hair samples collected post-mortem***" *Wildlife Biology*, 2025, e01507. https://doi.org/10.1002/wlb3.01507

This experimental study published in *Wildlife Biology* in 2025, provides the hormonal profiles of the endangered Apennine wolf through a non-invasive matrix (hair samples) collected post-mortem. This research provides valuable insights into the reproductive and stress-related endocrinology of this subspecies, contributing to conservation efforts and ecological understanding.

WILDLIFE BIOLOGY

Research article

Quantification of steroid hormones in free-ranging Apennine wolf *Canis lupus italicus* hair samples collected post-mortem

Ilaria Troisio[1], Carmela Musto[1], Nicola Acquisti Casi[1], Nadia Govoni[1], Giuseppe Merialdi[2], Domenico Ventrella[1,3], Alberto Elmi[1,4], Mauro Delogu[1] and Maria Laura Bacci[1,3]

[1]Department of Veterinary Medical Sciences, Alma Mater Studiorum – University of Bologna, Ozzano dell'Emilia, Bologna, Italy
[2]Istituto Zooprofilattico Sperimentale della Lombardia e dell'Emilia-Romagna, Bologna, Italy
[3]Health Sciences and Technologies – Interdepartmental Center for Industrial Research (CIRI-SDV), Alma Mater Studiorum – University of Bologna, Bologna, Italy
[4]Department of Veterinary Medical Sciences, University of Pisa, Pisa, Italy

Correspondence: Alberto Elmi (alberto.elmi@unipi.it)

Wildlife Biology
2025: e01507
doi: 10.1002/wlb3.01507
Subject Editor: Cecilia Di Bernardi
Editor-in-Chief: Ilse Storch
Accepted 19 June 2025

After decades of dramatic reductions in their populations, Italian wolves have begun recolonizing parts of their historic range. This growth in populations can lead to potential conflicts with human activities, which remain the main cause of wolf mortality. With the aim of examining animal welfare and their health status, a hormonal dosage on hair was conducted on 20 wolf carcasses originating from the Tuscany and Emilia-Romagna regions. The concentrations of cortisol, testosterone, dehydroepiandrosterone (DHEA), progesterone, and oestradiol (E2) were measured using radioimmunoassay (RIA). Our results, listed as mean ± SD, were cortisol 1.81 ± 1.17, testosterone 2.74 ± 1.6, DHEA 62.92 ± 24.99, P4 53.22 ± 32.8 and E2 0.46 ± 0.23 pg/mg. The study employed a novel approach to analyse hormone levels in this species, but its opportunistic nature resulted in uneven data distribution across sex and age groups. Consequently, comparisons of hormone levels by these categories did not yield relevant differences. Further studies with larger sample sizes are necessary to analyse hormone trends throughout the year and explore differences based on factors such as sex, age, and causes of death.

Keywords: Apennine wolf, cortisol, dehydroepiandrosterone, hair, oestradiol, post-mortem analyses, progesterone, steroids, testosterone

Introduction

Grey wolf *Canis lupus* was once the most common large carnivore in the Northern Hemisphere (Szewczyk et al. 2019) as well as the most studied (Ripple et al. 2014), but several years of mistreatment have caused the decline of numerous wolf populations. During the 18th and 19th centuries, wolves were gradually exterminated from western Europe and the Alps (Breitenmoser 1998, Fabbri et al. 2007), leading to a

worldwide reduction in their historical territory by 68%, particularly in western and central Europe (Szewczyk et al. 2019). The southern Alps' Jura Mountains and Canton of Ticino were sites of the last surviving European populations (Breitenmoser 1998).

In fact, by the end of World War II, in Italy, wolves were almost extinct (Boitani 1984, 1992, Galaverni et al. 2016) but, in the last 40 years, Italian wolves have begun to recolonize parts of their historic range (Galaverni et al. 2016). As clarified by the 2021 survey conducted by the Italian Higher Institute for Environmental Protection and Research (ISPRA, Istituto Superiore per la Protezione e la Ricerca Ambientale), the total number of wolves in the Italian areal is estimated as between 2945 and 3608 divided as follows: 822–1099 wolves in the alpine area and 2020–2645 presenting the same genetic pool ('https://www.isprambiente.gov.it/it/attivita/biodiversita/monitoraggio-nazionale-del-lupo/link). Alongside the expansion of their range, despite wolves preferring areas distant from human settlements, they have been increasingly observed in urban areas (Dini et al. 2024), where the interaction with humans is more frequent and results in livestock depredations, killing of hunting dogs and dog hybridization (David Mech and Luigi 2006), leading to an increase in illegal killing and collision with vehicles (Musto et al. 2021), which mainly involves pups and juveniles (Galaverni et al. 2016). Given the extent of its habitat, the species exhibits significant variation in phenotypic traits. Such variety is also reflected in the taxonomy of the species, which is often updated and revised (Mech 1981, David Mech and Luigi 2006). In Italy, the presence of a local subspecies with unique physical and genetic features, known as the Apennine wolf *Canis lupus italicus*, has been verified (Nowak and Federoff 2002, Montana et al. 2017).

The hypothalamic-pituitary-gonadal (HPG) and hypothalamic-pituitary-adrenal (HPA) axes are the key pathways involved in behavioural modulation (Elmi et al. 2020). The study of stressors and animal welfare provides for the standard approach of the evaluation of activity of the HPA axis. On the other hand, sexual steroids are useful to evaluate the health status of reproductive tissues, necessary for the growth and maintenance of secondary sexual characteristics allowing for successful reproduction. Measuring their concentrations would allow us to assess the activity of the hypothalamic-pituitary-gonadal (HPG) axis (Norman and Litwack 1987). The most prominent indicator of stress is cortisol (CORT) (Ralph and Tilbrook 2016), a stress-reactive hormone (Norman and Litwack 1987), also because it affects the cardiovascular system increasing vasoconstriction, cardiac output, thus mediating the fight or flight response under acute stress (Knezevic et al. 2023). Nonetheless, it is also secreted under favourable circumstances (Bacci et al. 2014). Dehydroepiandrosterone (DHEA), instead, is mainly known as an androgen precursor and for its role in reducing aggressive behaviour (Elmi et al. 2020). In addition, a very wide range of effects are reported: in humans, for example, the presence of specific DHEA receptors in different tissues suggests a potential neuroprotective, anxiolytic and antidepressant role (Nenezic et al. 2023).

Finally, there seems to be an association between lower DHEA levels in older specimens with reduced bone mineral density typical of osteopenia and osteoporosis (Zhou and Glowacki 2018). Another crucial hormone for skeleton and muscle growth is testosterone, also pivotal for the development and differentiation of reproductive tissues (Norman and Litwack 1987). Progesterone (P4) and oestradiol (E2), on the other hand, are mainly known as female steroids. Nevertheless, despite common belief, progesterone also serves important functions in male physiology (Oettel and Mukhopadhyay 2004). Progesterone is synthetized in ovaries by the corpus luteum and, in pregnancy, by the placenta too, although in less measure it is also produced by the adrenal cortex and Leydig cells, testes and in adipose tissue in male specimens (Kolatorova et al. 2022). Lastly, oestradiol is the most common circulating oestrogen, which are primarily produced by ovaries and then adrenal glands and adipose tissue (Vrtačnik et al. 2014, Fuentes and Silveyra 2019). Furthermore, it promotes epithelial proliferation in the endometrium and prepares the mammary gland for lactation during late-phase pregnancy. In males, lower levels of oestrogens are indicative of healthy sperm maturation and erectile function, specifically in humans (Fuentes and Silveyra 2019).

To detect the concentration of hormone accumulation, the use of alternative matrices is becoming increasingly common in a great number of species including wildlife, because these can give information about a longer timespan (Stalder and Kirschbaum 2012, Elmi et al. 2020, Olvera-Maneu et al. 2021). Hair presents many potential applications, mainly in monitoring chronic stress of wild animals (Ghassemi Nejad et al. 2022). The best-known hypothesis that tries to explain how incorporation of hormones in the hair occurs is based upon the same thesis that explains drug incorporation: via passive diffusion from blood at the site of the medulla (Boumba et al. 2006, Russell et al. 2012).

The aim of this work was to analyse the steroid profile of cortisol, testosterone, dehydroepiandrosterone, progesterone and oestradiol, using radioimmunology technique after methanol extraction, in 20 carcasses of Apennine wolf, to evaluate the activity of hypothalamic-pituitary-adrenal (HPA) and hypothalamic-pituitary-gonadal (HPG) axes.

Material and methods

Animals and sampling

Twenty (n = 20) Apennine wolves *Canis lupus italicus*, nine females and 11 males, originating from the Tuscany and Emilia-Romagna regions, were analysed after their demise at the Wildlife and Exotic Fauna Service of the University of Bologna and Experimental Zooprophylactic Institute of Lombardy and Emilia-Romagna of Bologna (IZSLER). The exact recovery location of each carcass is shown in Fig. 1.

Most of the carcasses (13/20, 65%) were retrieved during autumn; out of the remaining ones, six were retrieved in winter (30%) and only one in spring (5%). This pattern aligns closely with the dispersal period of young individuals. The condition of the carcasses was generally good, mainly due to

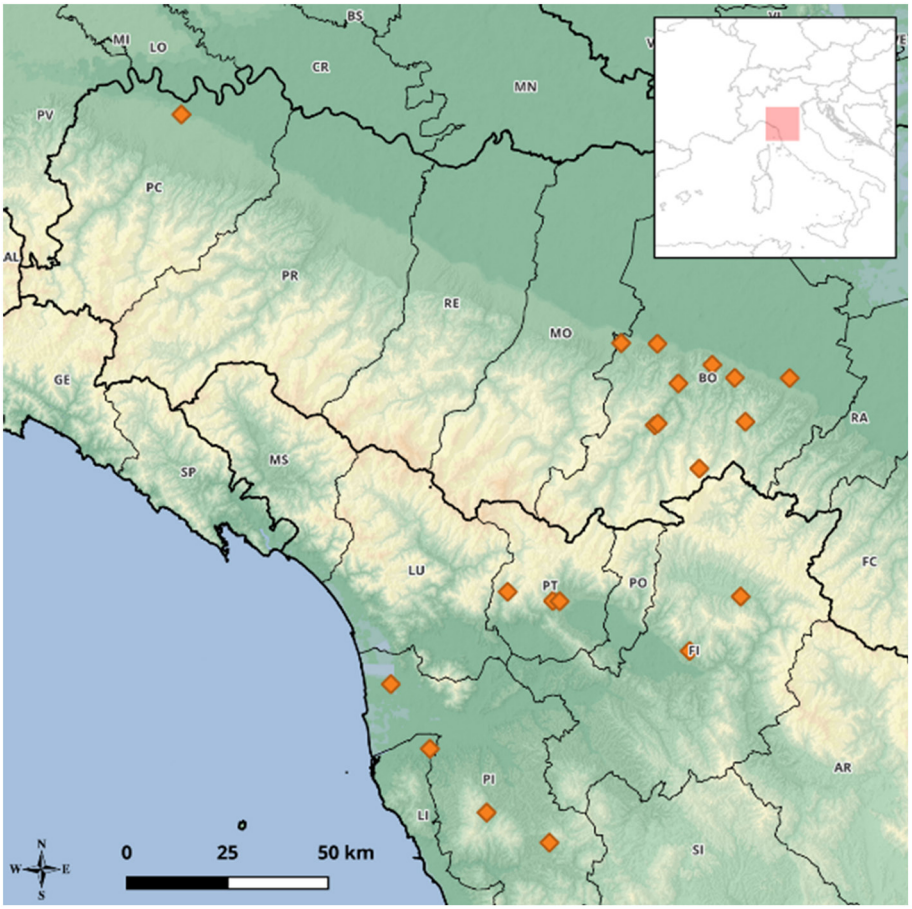

Figure 1. Localization of Apennine wolves' carcasses (map background was sourced from www.mapsforeurope.org).

the cold temperatures slowing down the decomposition processes. On average, carcasses were collected and delivered by the authorities within two to three days of being discovered.

Each wolf underwent a comprehensive necropsy examination for signalling, biometry, phenotypic markers, causes of death body size and weight. Age was estimated based on dental development (Brasington et al. 2023). Each individual was tested for the presence of toxic substances, including pesticides, rodenticides, insecticides, and other common poisons. However, individuals classified as 'poisoned' exhibited both pathological signs consistent with poisoning – acquired coagulopathies, pale mucous membranes, hemothorax, hemoperitoneum, and pulmonary edema – and laboratory confirmation of one or more toxic compounds. Examination of stomach contents was generally of limited diagnostic value, as poisoned individuals often had not eaten for several days prior to death.

Since hair from different body regions grows at varying rates and times, and hormone incorporation may differ across the body (Pereira et al. 2022), each wolf was shaved on a specific section of the rump area measuring 20 × 20 cm. Hair samples were then refrigerated at +4°C in the physiology laboratories (ANFI-ASA) of the Department of Veterinary Medical Sciences at the University of Bologna.

Hair washing and steroid extraction

Hair samples were analysed as previously described (Elmi et al. 2020). Briefly, they were washed with distilled water and isopropanol (Carlo Erba Reagents s.r.l.) to effectively remove organic residues; once dried, hair was pulverized with liquid nitrogen, and then an analytic scale was used to collect the necessary quantity for extraction. Samples were then added to methanol (Carlo Erba Reagents s.r.l.) and incubated overnight for steroids extraction. The ratio between the volume of methanol and the pulverized samples was adjusted on the bases of preliminary tests run in the lab: 1 ml/30 mg for cortisol, testosterone and DHEA, and 1 ml/50 mg for progesterone and oestradiol. Samples were then centrifuged for 30 minutes at 1500 g, and, under a chemical hood, methanol was collected and evaporated to dryness. The quantities of methanol recovered for each hormone analysed were as follows: cortisol: 3 ml; testosterone: 4.5 ml; dehydroepiandrosterone: 4.5 ml; progesterone: 7 ml; oestradiol: 7 ml.

Radioimmunoassay quantification of cortisol, testosterone, and DHEA

The dry extracts were stored at −20°C until suspension in 0.3 ml of RIA buffer (74.26 mmol/l Na_2HPO_4, 12.49 mmol/l EDTA Na, 7.69 mmol/l NaN_3) with 0.1% di BSA (pH 7.5);

100 µl were used cortisol and testosterone, while 10 µl for DHEA (30 mg hair equivalent for cortisol, 50 mg hair equivalent testosterone and 4.5 mg for DHEA). Tritiated antigens were added (30 pg/0.1ml; PerkinElmer Inc.) along with polyclonal anti-DHEA antibodies (0.1 ml, 1:10000), anti-cortisol antibodies (0.1ml, 1:20000), and anti-testosterone antibodies (0.1 ml, 1:50000), all produced in our laboratory in rabbits. After an overnight incubation at +4°C, a solution of charcoal-dextran (charcoal 0.25%, dextran 0.02% in phosphate buffer) was added to separate the steroids not bound to antibodies, followed by centrifugation (15 min, 3000 g). The supernatant was transferred into vials with scintillation fluid, and radioactivity was measured using a beta counter (Packard C1600). The sensitivity of the cortisol, DHEA, and testosterone assays was 6.02 pg/tube, 2.58 pg/tube, and 1.07 pg/tube, respectively, with intra-assay coefficients of variation of 4.9, 5.7, and 5.2%, respectively. Cross-reactions of various steroids with the rabbit anti-cortisol antibody, obtained using a well-established method (Abraham 1974), were cortisol (100%), cortisone (5.3%), 11α-deoxycortisol (5.0%), corticosterone (9.5%), 20α-dihydrocortisone (0.4%), prednisolone (4.60%), progesterone, and testosterone (< 0.001%). Cross-reactions of the anti-DHEA antibody were: dehydroepiandrosterone (100%), dehydroepiandrosterone sulfate (39%), androstenedione (10%), testosterone (0.25%), progesterone, and cortisol (< 0.001%). Cross-reactions for the anti-testosterone antibody were testosterone (100%), dihydrotestosterone (25.4%), androstenedione (0.43%), cortisol, and progesterone (< 0.001%).

To determinate the parallelism between the standard calibration curves and endogenous hormones in the hair, serial dilutions with RIA buffer as above-described (1:1–1:8) were made. Regression analysis was used to determinate the parallelism between the two hormone levels in the same assay. The results of the analyses were expressed in pg/mg of hair.

Radioimmunoassay quantification of oestradiol and progesterone

Samples for oestradiol and progesterone analyses were suspended in 0.4 ml of RIA buffer and subsequently loaded into RIA tubes, 100 µl for E2 (100 mg hair equivalent) and 10 µl for P4 (10 mg hair equivalent). The above-described analysis was then performed using specific polyclonal antibodies produced in-house in rabbits (1:10000 for P4; 1:20000 for E2). The sensitivity of the oestradiol and P4 assays was 1.63 pg/tube and 2.16 pg/tube, respectively. Cross-reactions of the anti-E2 antibody, assessed using the previously mentioned method, were: oestradiol 17b (100%), estrone-estriol (1.2%), oestradiol 17a (0.62%), testosterone, and progesterone (< 0.0001%). Cross-reactions of the anti-P4 antibody were observed: progesterone (100%), 11-a-OH-progesterone (9.7%), 20-a-OH-progesterone (0.3%), 17-a-OH-progesterone (1.5%), testosterone, and oestradiol (< 0.001%). The results of the analyses were expressed in pg/mg of hair.

Statistical analysis

Statistical analyses were conducted using GraphPad Prism ver. 8 software (GraphPad Software Inc.). Descriptive analysis results were presented as mean and standard deviation for continuous variables and as a percentage of the total sampled subjects for qualitative variables. Data distribution was evaluated using the Shapiro–Wilk test. For inferential analysis of each hormone, subjects were categorized by sex and age classes. The Mann–Whitney non-parametric test was used for sex, while the Kruskal–Wallis non-parametric test was used for age, categorized as young, subadult, and adult. To evaluate the relationships between the different analysed hormones, a non-parametric Spearman rank correlation test was performed. The level of statistical significance for all analyses was set at $p < 0.05$.

Results

The data that support the findings of this study are openly available in AMSActa Institutional Research Repository at http://doi.org/10.6092/unibo/amsacta/7786.

Sampled population specifics

Table 1 reports the generic data of the animals received for necropsy investigation, including age category, gender, weight and cause of death.

The sampled population consisted of 11 male (55%) and nine female (45%) specimens. The age was categorized into three age groups: young (< 12 months, 35%), subadult (> 12 < 24 months, 35%) and adult (> 24 months, 30%).

As for the cause of death, 55% of the animals died due to vehicular trauma, 10% due to poisoning, 10% from bite wound trauma, 10% because of gunshot trauma, 10% passed away from combined poisoning and vehicle trauma and, finally, 5% died of cachexia.

Table 1. Specifics of the sampled population.

ID	Age	Gender	Weight (kg)	Cause of death
1	Young	Male	25.0	Poisoning
2	Subadult	Male	20.4	Cachexia
3	Young	Male	16.2	Bite wound trauma
4	Young	Female	16.5	Vehicular trauma
5	Subadult	Male	29.4	Vehicular trauma
6	Adult	Male	37.8	Bite wound trauma
7	Subadult	Female	27.2	Vehicular trauma
8	Adult	Male	34.5	Vehicular trauma
9	Adult	Male	34.7	Poisoning
10	Subadult	Male	30.5	Gunshot trauma
11	Adult	Female	26.4	Vehicular trauma
12	Young	Female	29.0	Vehicular trauma
13	Subadult	Female	29.2	Vehicular trauma
14	Subadult	Male	28.0	Vehicular trauma
15	Young	Female	21.0	Vehicular trauma
16	Young	Female	23.0	Vehicular trauma and poisoning
17	Adult	Male	37.0	Vehicular trauma and poisoning
18	Young	Female	21.0	Vehicular trauma
19	Subadult	Female	28.1	Gunshot trauma
20	Adult	Male	36.0	Vehicular trauma

Young 0–12 months; subadult 12–24 months; adult > 24 months. To every specimen has been associated an animal ID number.

Table 2. Descriptive statistics of the quantified hormones.

ID	Cortisol (pg/mg)	Testosterone (pg/mg)	DHEA (pg/mg)	P4 (pg/mg)	E2 (pg/mg)
1	0.61	4.68	110.51	94.72	0.89
2	2.50	0.95	33.42	21.72	0.19
3	4.90	1.84	57.34	40.35	0.25
4	2.04	2.27	60.54	30.35	0.36
5	0.95	4.59	70.20	64.76	0.35
6	0.98	2.80	75.95	29.73	0.83
7	0.77	1.96	33.13	54.23	0.78
8	1.46	1.21	45.21	26.59	0.34
9	1.20	3.21	72.75	42.69	0.37
10	2.24	3.15	34.55	76.90	0.67
11	1.62	1.52	43.68	42.71	0.51
12	1.40	1.25	45.71	/	/
13	3.08	1.67	49.42	35.65	0.42
14	1.45	4.00	98.43	95.67	0.54
15	1.35	1.74	57.85	37.33	0.21
16	1.86	1.15	33.77	20.25	0.16
17	1.25	2.76	58.85	22.12	0.27
18	1.77	6.23	93.82	126.68	0.84
19	0.35	6.06	111.22	113.58	0.51
20	4.38	1.80	71.96	35.23	0.53

DHEA: dehydroepiandrosterone; P4: progesterone: E2: oestradiol.

Female specimens' weight ranged from 16.50 to 29.20 kg, with a mean of 24.60 ± 4.43 kg; while males ranged between 16.20 and 37.80 kg, with mean of 29.95 ± 7.07 kg.

Hormone concentrations

Table 2 reports the concentrations, expressed in pg/mg of hair, of the five hormones of this study.

Mean concentrations ± SD of hormones were: 1.81 ± 1.17 pg/mg for cortisol, 2.74 ± 1.6 pg/mg for testosterone, 62.92 ± 24.99 pg/mg for DHEA, 53.22 ± 32.8 pg/mg for P4 and, finally, 0.46 ± 0.23 pg/mg for E2.

Hormone concentration categorized by sex

The Mann–Whitney non-parametric test highlighted no significative differences when comparing male (n = 11) versus female (n = 9) specimens for all hormones, as graphically shown in Fig. 2.

Hormone concentration categorized by age

The Kruskal–Wallis non-parametric test was used to evaluate potential differences between age groups; no differences were recorded, as shown in Fig. 3.

Spearman's rank correlation analysis

The correlation coefficients (ρ) between hormones are represented in Fig. 4.

Out of the analysed hormones, cortisol was the only one not showing correlations to other analytes. On the other hand, TEST was positively correlated to DHEA ($\rho = 0.78$, $p < 0.0001$), P4 ($\rho = 0.78$, $p < 0.0001$) and E2 ($\rho = 0.63$, $p = 0.004$). DHEA was also positively correlated to P4 and E2, yet less strongly (respectively, $\rho = 0.51$, $p = 0.027$ and $\rho = 0.46$, $p = 0.046$). Finally, P4 and E2 were also positively correlated ($\rho = 0.66$, $p = 0.002$).

Discussion

The present work was aimed at quantifying cortisol, testosterone, dehydroepiandrosterone, progesterone and oestradiol, by means of RIA methods, in hair samples collected on Apennine wolf carcasses, to evaluate the activity of hypothalamic-pituitary-adrenal (HPA) and hypothalamic-pituitary-gonadal (HPG) axes.

The first article of the Declaration of Principle of Wolf Conservation adopted by the Wolf Specialist Group of the Species Survival Commission of International Union for Conservation of Nature (IUCN) in 1973 states that 'Wolves have a right to exist in a wild state in viable populations'. This fundamental right does not reside in the value to mankind, but rather on the right to co-exist as a part of the natural ecosystem, as any other animal species (Boitani 2000).

To date, the wolf has regained its lost areal and such recolonization has seen the involvement of peri-urban territories, thus increasing interactions with human activities. In fact, in 2016 70% of packs included at least one urban settlement within the expected home range in the European region (Zanni et al. 2023). The increasing interactions with man have led to an increment in anthropogenic origin mortality (David Mech and Luigi 2006, Musto et al. 2021). This is reflected in the collection of carcasses for this study, which are often difficult to detect because specimens have been victims of illegal killing (Musto et al. 2021). In fact, out of the total of twenty specimens, only 15% died of natural causes (intraspecific aggression, cachexia) not imputable to humans.

Hair was the chosen matrix as it presents multiple advantages because its sampling may be considered one of the more appropriate solutions for post-mortem hormonal dosages. Although this is a preliminary and opportunistic study that has been conducted on dead specimens, the possible future

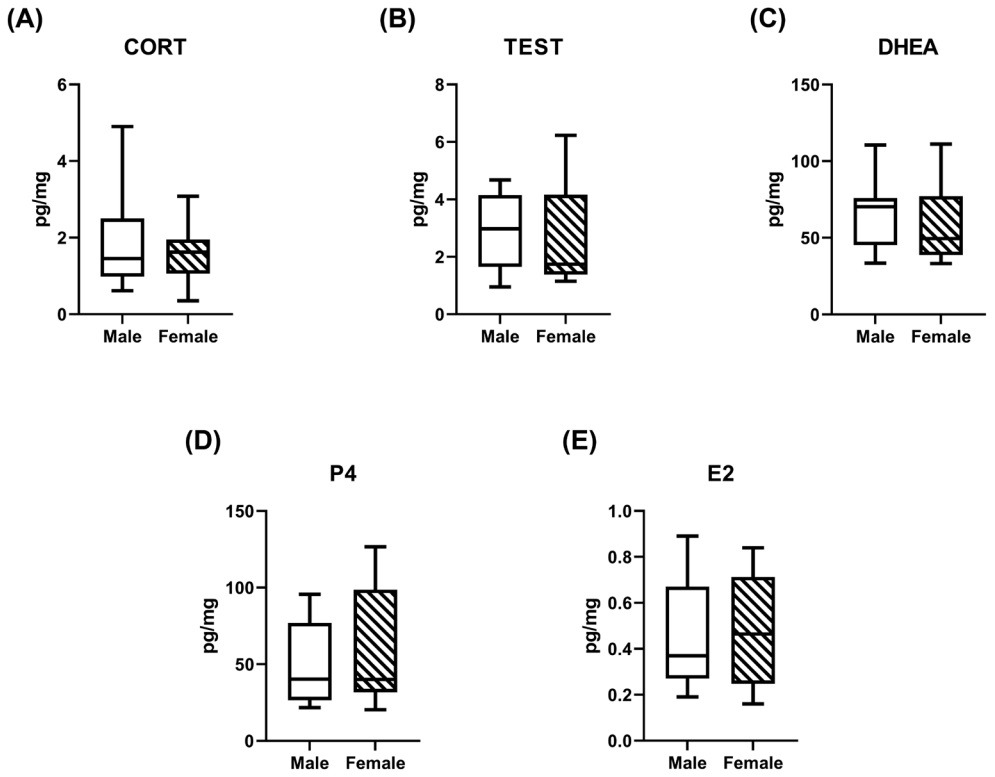

Figure 2. Concentration expressed in pg/mg of each hormone object of the study comparing by sex, using the Mann–Whitney non-parametric test: (A) cortisol - CORT, (B) testosterone - TEST, (C) DHEA, (D) progesterone - P4, (E) oestradiol - E2.

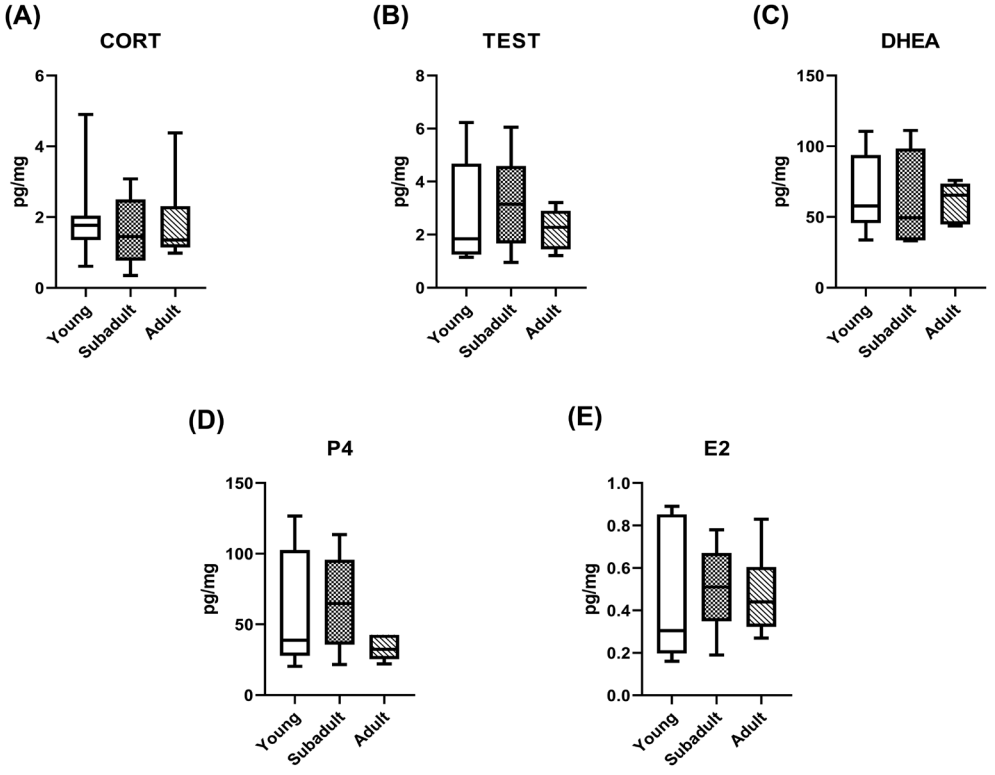

Figure 3. Concentration expressed in pg/mg of each hormone object of the study comparing by age, using the Kruskal–Wallis non-parametric test: (A) cortisol - CORT, (B) testosterone - TEST, (C) DHEA, (D) progesterone - P4, (E) oestradiol - E2.

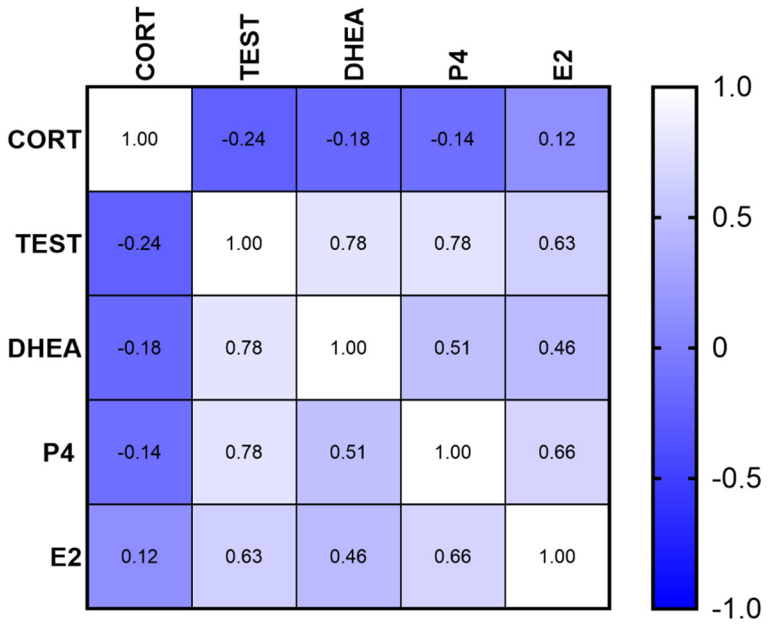

Figure 4. Spearman rank correlation coefficients (ρ) table for all the analysed parameters.

application with a living collection requires a methodology validation. The most common matrices in hormonal dosages are blood and saliva collection, which require containment actions during living sample collection. The other non-invasive matrices are faeces and urine, but faecal samples are rich in many metabolites, while urine provides a measure of secretion of hormones over a range of 12–24 hours (Ataallahi et al. 2022). Moreover, both have shorter storage requirement times, whereas hair can be stored at room temperature. Each matrix may serve its own purpose, and hair can be one of the most stable and reliable when the goal is to assess the influence of the environment on wildlife biology over a longer time span. Indeed, in the last two decades this matrix has become extremely popular in wild species (Caslini et al. 2016, Ventrella et al. 2020), and in wolf (Bryan et al. 2015, Pereira et al. 2022, Roffler et al. 2022), due to its utility in long-term evaluation of HPG axis activity. Furthermore, the use of hair could promote studies on demography (population size, reproduction, mortality), ecology (distribution, habitat use), health status of the population itself and genetic determination of species.

This study aimed at demonstrating the feasibility of hair sampling and hormone quantification methods in the Apennine wolf *Canis lupus italicus* and, at a preliminary stage, to understand if there were differences among age and sex classes. As for the first objective, the results confirm the efficacy of hair as a non-invasive matrix for hormonal dosage in wolf using radioimmunoassay. The in-house antibodies showed high performance except for the progesterone one, which showed significant cross-reactions with other progestans. No statistically significant differences were observed between individuals, either categorized by sex or age, probably because of the small sample size, resulting in a low frequency of adult individuals (35%) and a high frequency of sexually immature individuals (65%). Nonetheless, the same lack of statistical differences for cortisol between wolves divided per sex are reported in other studies (Pereira et al. 2022, Roffler et al. 2022).

Cortisol levels in animals are influenced by temperature and physiological states. In red deer, lower cortisol values are observed during warmer months, with an increase in late pregnancy (Ventrella et al. 2020). Similarly, roe deer males experience elevated cortisol due to stress from territorial fights in spring (Ventrella et al. 2018), as do wolves in physical conflict during the mating season (Eggermann et al. 2013). Hair cortisol concentration in this species, in fact, peaks in winter due to increased social instability during the mating season, while the lowest levels occur in May when competition and instability decrease (Pereira et al. 2022). Moreover, another study of 2015 stated that higher levels of stress and reproductive hormones likely reflect different environmental conditions, including human-caused mortality in wolf (Bryan et al. 2015). Our results are similar to the ones detected in previous studies conducted on wolves using the same matrix (Roffler et al. 2022), somewhat proving the consistency of the method. The Spearman's rank correlation analysis showed that cortisol was the only hormone, out of the analysed ones, not correlating to others. This finding may be imputable to the fact that, within the steroidogenic pathway, it is the only glucocorticoid, while the other chosen analytes are either androgens or estrogens, more deeply connected to the reproductive physiology.

The second hormone was testosterone, which has a seasonal trend in seasonal breeder animals with the highest peaks occurring in the blood during reproductive activity (Kozioł and Koziorowski 2013). Another decisive impact on testosterone levels is played by age of individuals, where increasing concentrations are expected when sampling occurs in animals

of reproductive age and even more in the period leading up to mating. These age- and season-related fluctuations are also clearly shown in studies involving boars with radioimmunology quantification (Macchi et al. 2010, Aniballi et al. 2023). Our results, instead, do not show higher testosterone levels in adults. It is nonetheless important to highlight that the age categorization performed in this study led to very small groups, with the added confounding effect represented by the inclusion of both sexes. Indeed, consistent with what seen in boars and roe deer, differences in testosterone levels between males and females have also been highlighted through hair matrix in domestic dogs, where testosterone was higher in uncastrated males compared to females and neutered males (Calamari et al. 2020). Despite the lack of statistical significance, once again probably imputable to the relatively low sample size, the female animals analysed in this study also showed lower mean values than males.

Our progesterone and oestrogen concentrations are somewhat hard to analyse too, due to the lack of background data and physiological in-depth investigations. Our P4 data fall within the range concentration already proposed by others (Roffler et al. 2022), strengthening the validity of the obtained values. In a previous study conducted on wolf, progesterone and testosterone were positively correlated, so that the authors hypothesized a correlation with reproductive activity too, probably due to social disturbances for anthropogenic reasons (Roffler et al. 2022). These data are also supported by another study in which authors found higher progesterone levels in tundra–taiga wolves, especially females. The authors correlated a higher human presence in the environment with an increased concentration of progesterone in female specimens (Bryan et al. 2015). Additionally, other studies have highlighted differences in progesterone levels linked to different stages of pregnancy using the same matrix and quantification technique, but in different wild species (Ventrella et al. 2020). Our results show a strong positive correlation of both P4 and E2 with testosterone, in complete alignment with the above-mentioned existing literature. A milder positive correlation was also noted with DHEA and between P4 and E2 themselves. Being DHEA a testosterone precursor, such correlation may be reflecting the one to testosterone, stronger yet positive.

No other considerations can be made for DHEA, given that we do not have consistent data to compare with in literature. However, our results did not show any significant variations among sex and ages. Since the literature highlighted a negative correlation between DHEA and aging (Zhou and Glowacki 2018), further investigation is needed to deepen our knowledge. As expected, in the present study it was strongly positively correlated to testosterone, being its precursor.

To conclude, this preliminary and opportunistic study conducted on the Apennine wolf allowed us to understand the feasibility of the steroid quantification technique through radioimmunoassay in hair samples collected post-mortem. The results hereby shown are consistent and could be used to propose further studies, with a larger and better distributed sample population in terms of sex and age, to better understand the reproductive cycle and physiological status of Apennine wolves, as well as to evaluate the relationship with the surrounding environment, providing new information on the physiological response to chronic stressors such as increased anthropogenic pressure.

Acknowledgements – We thank the Provincial Police, the Local Health Authority (ASL) and the Forest Police of each province included in this study and the Canislupus Italia Association for providing assistance in the recovery of wolf carcasses.
Funding – The work was supported by RFO from the University of Bologna.

Author contributions

Ilaria Troisio: Formal analysis (equal); Writing – original draft (equal). **Carmela Musto**: Conceptualization (equal); Writing – review and editing (equal). **Nicola Acquisti Casi**: Methodology (equal); Writing – original draft (equal). **Nadia Govoni**: Methodology (equal); Writing – review and editing (equal). **Giuseppe Merialdi**: Methodology (equal); Resources (equal). **Domenico Ventrella**: Formal analysis (equal); Writing – review and editing (equal). **Alberto Elmi**: Conceptualization (equal); Formal analysis (equal); Project administration (equal). **Mauro Delogu**: Resources (equal); Supervision (equal). **Maria Laura Bacci**: Resources (equal); Supervision (equal).

Data availability statement

Data are available from the AMSActa Institutional Research Repository of the University of Bologna: https://amsacta.unibo.it/id/eprint/7786 (Troisio et al. 2025).

References

Abraham, G. E. 1974. Radioimmunoassay of steroids in biological fluids. – Clin. Biochem. 7: 193–201.
Aniballi, C., Elmi, A., Govoni, N., Bulla, T., Canelli, E., Casalini, A., Bacci, M. L. and Ventrella, D. 2023. Influence of age and seasonality on boar seminal plasma steroids quantification: a preliminary study. – Vet. World 16: 2150–2157.
Ataallahi, M., Nejad, J. G. and Park, K.-H. 2022. Selection of appropriate biomatrices for studies of chronic stress in animals: a review. – J. Anim. Sci. Technol. 64: 621–639.
Bacci, M. L., Nannoni, E., Govoni, N., Scorrano, F., Zannoni, A., Forni, M., Martelli, G. and Sardi, L. 2014. Hair cortisol determination in sows in two consecutive reproductive cycles. – Reprod. Biol. 14: 218–223.
Boitani, L. 1984. Genetic considerations on wolf conservation in Italy. – Boll. Zool. 51: 367–373.
Boitani, L. 1992. Wolf research and conservation in Italy. – Biol. Conserv. 61: 125–132.
Boitani, L. 2000. Action Plan for the conservation of the wolves (*Canis lupus*) in Europe. – Nat. Environ. Ser. No. 113, Council of Europe Publishing.
Boumba, V. A., Ziavrou, K. S. and Vougiouklakis, T. 2006. Hair as a biological indicator of drug use, drug abuse or chronic

exposure to environmental toxicants. – Int. J. Toxicol. 25: 143–163.
Brasington, T., Hadley, J., Stahler, D., Stahler, E. and Cassidy, K. 2023. A visual guide to wolf dentition and age determination: for researchers and wildlife professionals. – Wildl. Biol.: www.researchgate.net/publication/374921532.
Breitenmoser, U. 1998. Large predators in the Alps: the fall and rise of man's competitors. – Biol. Conserv. 83: 279–289.
Bryan, H. M., Smits, J. E. G., Koren, L., Paquet, P. C., Wynne-Edwards, K. E. and Musiani, M. 2015. Heavily hunted wolves have higher stress and reproductive steroids than wolves with lower hunting pressure. – Funct. Ecol. 29: 347–356.
Calamari, C. V., Viau, P., Nichi, M., Martins, G. S., Sobral, G., Mangueira Dias, J. H. and Alvarenga de Oliveira, C. 2020. Hair as an alternative noninvasive matrix: sources of variation in testosterone levels. – Domest. Anim. Endocrinol. 72: 106477.
Caslini, C., Comin, A., Peric, T., Prandi, A., Pedrotti, L. and Mattiello, S. 2016. Use of hair cortisol analysis for comparing population status in wild red deer (*Cervus elaphus*) living in areas with different characteristics. – Eur. J. Wildl. Res. 62: 713–723.
David Mech, L. and Boitani, L. 2006. Wolves : behavior, ecology, and conservation. – Univ. Chicago Press.
Dini, F. M., Musto, C., De Nigris, V. M., Bellinello, E., Sampieri, M., Merialdi, G., Barca, L., Delogu, M. and Galuppi, R. 2024. Sero-epidemiological investigation on *Toxoplasma gondii* infection in Apennine wolf (*Canis lupus italicus*) and wild boar (*Sus scrofa*) in Italy. – B.M.C. Vet. Res. 20: 62.
Eggermann, J., Theuerkauf, J., Pirga, B., Milanowski, A. and Gula, R. 2013. Stress-hormone levels of wolves in relation to breeding season, pack size, human activity, and prey density. – Ann. Zool. Fenn. 50: 170–175.
Elmi, A., Galligioni, V., Govoni, N., Bertocchi, M., Aniballi, C., Bacci, M. L., Sánchez-Morgado, J. M. and Ventrella, D. 2020. Quantification of hair corticosterone, DHEA and testosterone as a potential tool for welfare assessment in male laboratory mice. – Animals 10: 2408.
Fabbri, E., Miquel, C., Lucchini, V., Santini, A., Caniglia, R., Duchamp, C., Weber, J.-M., Lequette, B., Marucco, F., Boitani, L., Fumagalli, L., Taberlet, P. and Randi, E. 2007. From the Apennines to the Alps: colonization genetics of the naturally expanding Italian wolf (*Canis lupus*) population. – Mol. Ecol. 16: 1661–1671.
Fuentes, N. and Silveyra, P. 2019. Estrogen receptor signaling mechanisms. – Adv. Protein Chem. Struct. Biol. 116: 135–170.
Galaverni, M., Caniglia, R., Fabbri, E., Milanesi, P. and Randi, E. 2016. One, no one, or one hundred thousand: how many wolves are there currently in Italy? – Mamm. Res. 61: 13–24.
Ghassemi Nejad, J., Ghaffari, M. H., Ataallahi, M., Jo, J.-H. and Lee, H.-G. 2022. Stress concepts and applications in various matrices with a focus on hair cortisol and analytical methods. – Animals 12: 3096.
Knezevic, E., Nenic, K., Milanovic, V. and Knezevic, N. N. 2023. The role of cortisol in chronic stress, neurodegenerative diseases, and psychological disorders. – Cells 12: 2726.
Kolatorova, L., Vitku, J., Suchopar, J., Hill, M. and Parizek, A. 2022. Progesterone: a steroid with wide range of effects in physiology as well as human medicine. – Int. J. Mol. Sci. 23: 7989.
Kozioł, K. and Koziorowski, M. 2013. Ormoni steroidei nel plasma sanguigno periferico e recettori degli androgeni nei testicoli e nell'epididimo del maschio di capriolo (*Capreolus capreolus*) durante la stagione riproduttiva. – Small Rumin. Res. 115: 86–93.
ISPRA Ist. Super. Prot. E Ric. – Ambient Press.
Macchi, E., Cucuzza, A. S., Badino, P., Odore, R., Re, F., Bevilacqua, L. and Malfatti, A. 2010. Seasonality of reproduction in wild boar (*Sus scrofa*) assessed by fecal and plasmatic steroids. – Theriogenology 73: 1230–1237.
Mech, L. D. 1981. The wolf: the ecology and behavior of an endangered species. – Univ. Minnesota Press.
Montana, L., Caniglia, R., Galaverni, M., Fabbri, E. and Randi, E. 2017. A new mitochondrial haplotype confirms the distinctiveness of the Italian wolf (*Canis lupus*) population. – Mamm. Biol. 84: 30–34.
Musto, C., Cerri, J., Galaverni, M., Caniglia, R., Fabbri, E., Apollonio, M., Mucci, N., Bonilauri, P., Maioli, G., Fontana, M. C., Gelmini, L., Prosperi, A., Rossi, A., Garbarino, C., Fiorentini, L., Ciuti, F., Berzi, D., Merialdi, G. and Delogu, M. 2021. Men and wolves: anthropogenic causes are an important driver of wolf mortality in human-dominated landscapes in Italy. – Global Ecol. Conserv. 32: e01892.
Nenezic, N., Kostic, S., Strac, D. S., Grunauer, M., Nenezic, D., Radosavljevic, M., Jancic, J. and Samardzic, J. 2023. Dehydroepiandrosterone (DHEA): pharmacological effects and potential therapeutic application. – Mini Rev. Med. Chem. 23: 941–952.
Norman, A. W. and Litwack, G. 1987. Hormones. – Academic Press.
Nowak, R. M. and Federoff, N. E. 2002. The systematic status of the Italian wolf *Canis lupus*. – Acta Theriol. 47: 333–338.
Oettel, M. and Mukhopadhyay, A. K. 2004. Progesterone: the forgotten hormone in men? – Aging Male 7: 236–257.
Olvera-Maneu, S., Carbajal, A., Gardela, J. and Lopez-Bejar, M. 2021. Hair cortisol, testosterone, dehydroepiandrosterone sulfate and their ratios in stallions as a retrospective measure of hypothalamic–pituitary–adrenal and hypothalamic–pituitary–gonadal axes activity: exploring the influence of seasonality. – Animals 11: 2202.
Pereira, P., Fandos Esteruelas, N., Nakamura, M., Rio-Maior, H., Krofel, M., Di Blasio, A., Zoppi, S., Robetto, S., Llaneza, L., García, E., Oleaga, Á., López-Bao, J. V., Fayos Martinez, M., Stavenow, J., Ågren, E. O., Álvares, F. and Santos, N. 2022. Hair cortisol concentration reflects the life cycle and management of grey wolves across four European populations. – Sci. Rep. 12: 5697.
Ralph, C. R. and Tilbrook, A. J. 2016. Invited review: the usefulness of measuring glucocorticoids for assessing animal welfare. – J. Anim. Sci. 94: 457–470.
Ripple, W. J., Estes, J. A., Beschta, R. L., Wilmers, C. C., Ritchie, E. G., Hebblewhite, M., Berger, J., Elmhagen, B., Letnic, M., Nelson, M. P., Schmitz, O. J., Smith, D. W., Wallach, A. D. and Wirsing, A. J. 2014. Status and ecological effects of the world's largest carnivores. – Science 343: 1241484.
Roffler, G. H., Karpovich, S., Charapata, P. and Keogh, M. J. 2022. Validation and measurement of physiological stress and reproductive hormones in wolf hair and claws. – Wildl. Soc. Bull. 46: e1330.
Russell, E., Koren, G., Rieder, M. and Van Uum, S. 2012. Hair cortisol as a biological marker of chronic stress: current status, future directions and unanswered questions. – Psychoneuroendocrinology 37: 589–601.
Stalder, T. and Kirschbaum, C. 2012. Analysis of cortisol in hair – state of the art and future directions. – Brain Behav. Immun. 26: 1019–1029.

Szewczyk, M., Nowak, S., Niedźwiecka, N., Hulva, P., Špinkytė-Bačkaitienė, R., Demjanovičová, K., Bolfíková, B. Č., Antal, V., Fenchuk, V., Figura, M., Tomczak, P., Stachyra, P., Stępniak, K. M., Zwijacz-Kozica, T. and Mysłajek, R. W. 2019. Dynamic range expansion leads to establishment of a new, genetically distinct wolf population in central Europe. – Sci. Rep. 9: 19003.

Troisio, I., Musto, C., Casi, N. A., Govoni, N., Merialdi, G., Alberto Elmi, D. V., Delogu, M. and Bacci, M. L. 2025. Data from: Quantification of steroid hormones in free-ranging Apennine wolf *Canis lupus italicus* hair samples collected post-mortem. – AMSActa Institutional Research Repository of the University of Bologna: https://amsacta.unibo.it/id/eprint/7786.

Ventrella, D., Elmi, A., Barone, F., Carnevali, G., Govoni, N. and Bacci, M. L. 2018. Hair testosterone and cortisol concentrations in pre- and post-rut roe deer bucks: correlations with blood levels and testicular morphometric parameters. – Animals 8: 113.

Ventrella, D., Elmi, A., Bertocchi, M., Aniballi, C., Parmeggiani, A., Govoni, N. and Bacci, M. L. 2020. Progesterone and cortisol levels in blood and hair of wild pregnant red deer (*Cervus elaphus*) hinds. – Animals 10: 143.

Vrtačnik, P., Ostanek, B., Mencej-Bedrač, S. and Marc, J. 2014. The many faces of estrogen signaling. – Biochem. Med. 24: 329–342.

Zanni, M., Brogi, R., Merli, E. and Apollonio, M. 2023. The wolf and the city: insights on wolves' conservation in the Anthropocene. – Anim. Conserv. 26: 766–780.

Zhou, S. and Glowacki, J. 2018. Dehydroepiandrosterone and bone. – Vitam. Horm. 108: 251–271.